

1. Report No. FHWATX78-177-4		2. Government Accession No.		3. Recipient's Catalog No.	
4. Title and Subtitle LABORATORY STUDY OF THE EFFECT OF NONUNIFORM FOUNDATION SUPPORT ON CONTINUOUSLY REINFORCED CONCRETE PAVEMENTS				5. Report Date August 1977	
				6. Performing Organization Code	
7. Author(s) Enrique Jimenez, B. Frank McCullough, and W. Ronald Hudson				8. Performing Organization Report No. Research Report 177-4	
9. Performing Organization Name and Address Center for Highway Research The University of Texas at Austin Austin, Texas 78712				10. Work Unit No.	
				11. Contract or Grant No. Research Study 3-8-75-177	
				13. Type of Report and Period Covered Interim	
12. Sponsoring Agency Name and Address Texas State Department of Highways and Public Transportation; Transportation Planning Division P. O. Box 5051 Austin, Texas 78763				14. Sponsoring Agency Code	
				15. Supplementary Notes Study conducted in cooperation with the U. S. Department of Transportation, Federal Highway Administration. Research Study Title: "Development and Implementation of the Design, Construction, and Rehabilitation of Rigid Pavements"	
16. Abstract <p>Design of continuously reinforced concrete pavements is a procedure that involves numerous complex variables. To accomplish the evaluation of these variables, several steps must be taken, such as observations of the effects of environmental factors and the behavior of soil supports that affect the pavement performance during its service life. Different steps to evaluate the pavement behavior must be followed in an effort to design pavements with longer good service condition life. The laboratory is one of the principal means the designer has for developing relationships for pavement behavior in the field. A precursory laboratory experiment concerning CRC pavement performance was performed under NCHRP Research Project 1-15 with fully supported slabs.</p> <p>This report presents a study of loss of support of small dimension laboratory slabs. The purpose of the experiment is to compare and observe the behavior of experimental laboratory slabs with voids beneath them of various dimensions and to compare these slabs with uniformly supported slabs previously tested under NCHRP 1-15. A theoretical approach is included in the experiment in an effort to model all the laboratory inputs and outputs that can give solutions close to the ones obtained through the experimental physical test.</p> <p>At the end, both the theoretical solutions and the laboratory observations are analyzed and their accuracy is defined. Finally, observations, conclusions, and recommendations are presented in an effort to implement the study solutions within the design of CRC pavements.</p>					
17. Key Words voids, slab modelling, discrete element stress analysis, deflection criterion, fatigue, pavement thickness, pavement design, load repetitions, CRCP			18. Distribution Statement No restrictions. This document is available to the public through the National Technical Information Service, Springfield, Virginia 22161.		
19. Security Classif. (of this report) Unclassified		20. Security Classif. (of this page) Unclassified		21. No. of Pages 103	22. Price

LABORATORY STUDY OF THE EFFECT OF NONUNIFORM FOUNDATION SUPPORT
ON CONTINUOUSLY REINFORCED CONCRETE PAVEMENTS

by

Enrique Jimenez
B. Frank McCullough
W. Ronald Hudson

Research Report Number 177-4

Development and Implementation of the Design, Construction,
and Rehabilitation of Rigid Pavements

Research Project 3-8-75-177

conducted for

Texas
State Department of Highways and Public Transportation

in cooperation with the
U. S. Department of Transportation
Federal Highway Administration

by the

CENTER FOR HIGHWAY RESEARCH
THE UNIVERSITY OF TEXAS AT AUSTIN

August 1977

The contents of this report reflect the views of the authors, who are responsible for the facts and the accuracy of the data presented herein. The contents do not necessarily reflect the official views or policies of the Federal Highway Administration. This report does not constitute a standard, specification, or regulation.

PREFACE

This report summarizes the results of an experiment to study the effects of subbase or subgrade support loss on slab deflection, distress manifestation, and load transfer. This is a follow-up experiment to the analysis of laboratory slab behavior under NCHRP Research Project 1-15 and the results of that project were used as the primary basis for this research.

The project is supervised by Dr. W. R. Hudson, Professor of Civil Engineering, and Dr. B. F. McCullough, Associate Professor of Civil Engineering, and is being conducted at the Center for Highway Research, The University of Texas at Austin, as part of the Cooperative Highway Research Program sponsored by the State Department of Highways and Public Transportation and the Federal Highway Administration.

Special appreciation is also due to Pieter Strauss, Jim Long, and Larry Olson for their friendly help concerning this laboratory experiment.

Enrique Jimenez
B. Frank McCullough
W. Ronald Hudson

Austin, Texas
August 1977

LIST OF REPORTS

Report No. 177-1, "Drying Shrinkage and Temperature Drop Stress in Jointed Reinforced Concrete Pavement," by Felipe R. Vallejo, B. Frank McCullough, and W. Ronald Hudson, describes the development of a computerized system capable of analysis and design of a concrete pavement slab for drying shrinkage and temperature drop.

Report No. 177-2, "A Sensitivity Analysis of Continuously Reinforced Concrete Pavement Model CRCP-1 for Highways," by Chypin Chiang, B. Frank McCullough, and W. Ronald Hudson, describes the overall importance of this model, the relative importance of the input variables of the model and recommendations for efficient use of the computer program.

Report No. 177-3, "A Study of the Performance of the Mays Ride Meter," by Yi Chin Hu, Hugh J. Williamson, B. Frank McCullough, and W. Ronald Hudson, discusses the accuracy of measurements made by the Mays Ride Meter and their relationship to roughness measurements made with the Surface Dynamics Profilometer.

Report No. 177-4, "Laboratory Study of the Effect of Nonuniform Foundation Support on CRC Pavements," by Enrique Jimenez, W. Ronald Hudson, and B. Frank McCullough, describes the laboratory tests of CRC slab models with voids beneath them. Deflection, crack width, load transfer, spalling, and cracking are considered. Also used is the Slab 49 computer program that models the CRC laboratory slab as a theoretical approach. The physical laboratory results and the theoretical solutions are compared and analyzed and the accuracy is determined.

ABSTRACT

Design of continuously reinforced concrete pavements is a procedure that involves numerous complex variables. To accomplish the evaluation of these variables, several steps must be taken, such as observations of the effects of environmental factors and the behavior of soil supports that affect the pavement performance during its service life. Different steps to evaluate the pavement behavior must be followed in an effort to design pavements with longer good service condition life. The laboratory is one of the principal means the designer has for developing relationships for pavement behavior in the field. A precursory laboratory experiment concerning CRC pavement performance was performed under NCHRP Research Project 1-15. In that experiment, small dimension slabs were tested using the field practices of the State Department of Highways and Public Transportation in the construction of CRC pavements. However, the precursory study was done with fully supported slabs. One of the most important variables that affects CRC pavement performance is the loss of support under the slab, specifically when voids are created beneath the pavement due to swelling clay or subbase settlement.

This report presents a study of loss of support of small dimension laboratory slabs. The purpose of the experiment is to compare and observe the behavior of experimental laboratory slabs with voids beneath them of various dimensions and to compare these slabs with uniformly supported slabs previously tested under NCHRP 1-15. A theoretical approach is included in the experiment in an effort to model all the laboratory inputs and outputs that can give solutions close to the ones obtained through the experimental physical test.

At the end, both the theoretical solutions and the laboratory observations are analyzed and their accuracy is defined. Finally, observations, conclusions, and recommendations are presented in an effort to implement the study solutions within the design of CRC pavements.

KEY WORDS: voids, slab modelling, discrete element stress analysis, deflection criterion, fatigue, pavement thickness, pavement design, load repetitions, CRCP, portland cement concrete pavements

SUMMARY

This report presents the results of a laboratory and a computer simulation study to investigate the effect on pavement performance of voids beneath a portland cement concrete slab. Limitless studies of in-service pavements have found that voids beneath the slabs severely reduced the performance life. The intent of this study was to demonstrate the possibility of using pavement thickness to offset the effect of the voids. A computer simulation shows that the performance of laboratory pavements under repetitive loading and various void sizes can be simulated using the discrete-element theory. These results are then used to demonstrate the possibility of using load cracking and maximum deflection as criteria for establishing a pavement thickness design. The report demonstrates the need for incorporating into the present pavement thickness design procedures, a method of considering voids beneath the pavement, and the probability of occurrence.

IMPLEMENTATION STATEMENT

The definition of the critical condition created by the combined effects of environmental stresses (temperature and moisture variations) and traffic load stresses is essential for predicting failure conditions in concrete pavement. Mathematical models used must simulate actual field conditions as defined by environment, traffic and support soil variations such as voids beneath the pavement.

By using the SLAB program, the stress distribution in a full size slab can be predicted at various ages as the average crack spacing progresses from a wide value of approximately 25 feet to less than 2 feet. In addition, variable support conditions can be considered. These data can be used to establish the critical condition from a wheel load standpoint. Furthermore, the wheel load stress data for various crack patterns can be superimposed on stresses predicted from the CRCP-1 due to volume change effects of temperature and shrinkage. Thus, a crack pattern due to the coupled effect of wheel loads on the pavement and volume change stresses developed from temperature and shrinkage can be predicted along with crack width and steel stresses. This realistic simulation of in-service conditions permits an optimum design for pavement thickness, steel percentage, and other factors to be determined considering control criteria of crack width, crack spacing, steel stress, and concrete strength.

TABLE OF CONTENTS

PREFACE	iii
LIST OF REPORTS	iv
ABSTRACT AND KEY WORDS	v
SUMMARY	vi
IMPLEMENTATION STATEMENT	vii
CHAPTER 1. INTRODUCTION	
Objectives	3
The Scope of the Study	3
Outline of Report	3
CHAPTER 2. ANALYSIS AND LABORATORY PROCEDURES	
Nature of the Problem	5
Simulation of Field Conditions	7
Adoption of Experimental Techniques	7
SLAB 49 Computer Program	9
CHAPTER 3. ANALYTICAL STUDY	
Void Selection	13
Solutions of the Computation Experimental Design	16
Summary	20
CHAPTER 4. LABORATORY STUDY	
The Laboratory Slab Background	22
Slab Type and Configuration	22
Slab Preparation	22
Final Inspection of the Slab	25
Slab Placement	26
Quality Control	26
Curing the Slab	27
Laboratory Experimental Slab Observations	30
General Laboratory Slab Observations	32
Slab Model 177-1	34
Slab Model 177-2	37
Slab Model 177-3	42
Comparison of Observations on Slabs	45

CHAPTER 5. ANALYSIS OF THE EXPERIMENT

The Experimental Parameters	46
Slab Deterioration Predictions	49
Crack Development with Load Applications	55

CHAPTER 6. INTERPRETATION AND APPLICATION OF RESULTS

Cracking Criteria	58
Deflection Criteria	60
Design Applications	62
Summary	62

CHAPTER 7. OBSERVATIONS, CONCLUSIONS AND RECOMMENDATIONS

Observations	64
Conclusions	64
Recommendations	65

REFERENCES	66
----------------------	----

APPENDICES

Appendix 1. Data for Laboratory Slab Model L-5	68
Appendix 2. Computer Output for the Slab Model 177-2	70

THE AUTHORS	93
-----------------------	----

CHAPTER 1. INTRODUCTION

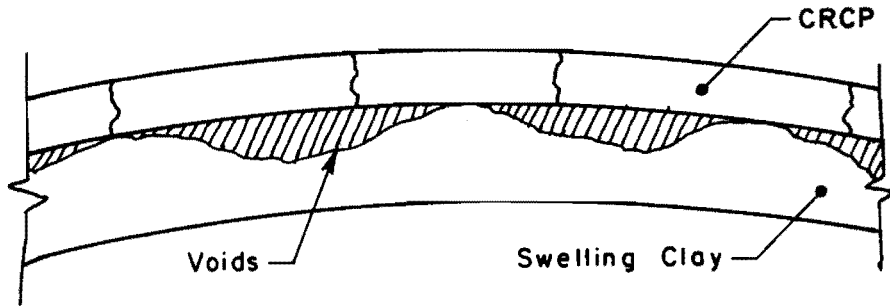
Highway and airport continuously reinforced concrete pavements (CRCP) are structures supported on specially prepared subgrades or subbases.

In the past, all CRCP design procedures separated the determination percent of steel reinforcement and pavement thickness into independent functions. The procedure developed as a result of the NCHRP Research Project 1-15 makes the same fundamental assumption. In this recent development, computations of average crack width, average crack spacing, the state of stress, and the distress manifestations are checked against the "limit criteria" also developed as part of the study.

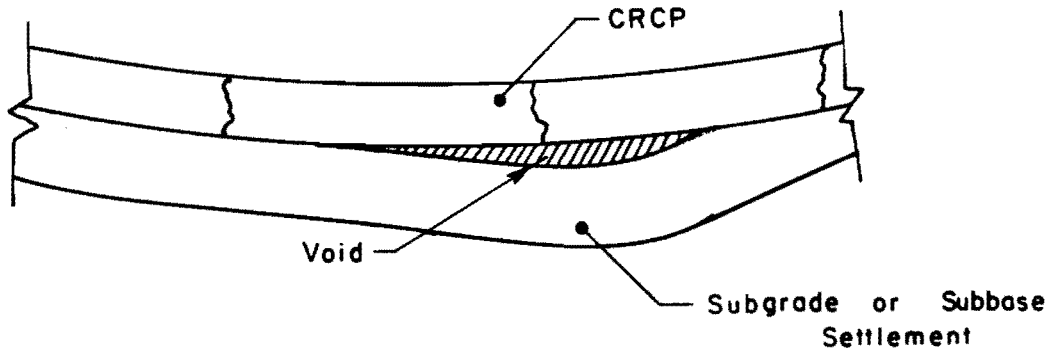
Thickness designs for continuously reinforced concrete pavements basically assume uniform support; however, in the field support is lost due to various soil conditions, such as swelling, settlement, and densification, as illustrated in Fig 1.1. The variation of soil support depends on the construction site and material characteristics. Since these support variations affect the CRC pavement life, it is important to understand how they increase or decrease the pavement distress, in order to be able to predict future pavement performance affected by these soil support variations.

Field observations indicate that pavements tend to bridge nonuniform support, whereas the subbase layers conform to the underlying soil movements (Fig 1.1). However, these pavements eventually collapse under repeated traffic loading since the CRC slabs are not designed to provide bridging action. It has been hypothesized that designers could allow for these conditions by increasing the slab thickness and percent of steel reinforcement to provide an adequate bridging action of the CRC slab above the nonuniform soil support.

In the previous studies (NCHRP 1-15), special laboratory equipment was used for studying the effects of several variables on the performance of small dimension CRC slabs under repeated load applications. That study involved the repeated laboratory testing of small dimension continuously reinforced slabs on a uniform rubber subgrade, with a modulus of subgrade



(a) swelling clay



(b) Settlement

Fig 1.1. Void creation under CRC pavements due to (a) swelling clay and (b) settlement.

reaction equal to 255 pci. The same equipment was used to study the effect of voids beneath the CRC slab model, using the same slab model dimensions, load magnitude, load frequency, load amount, crack width, and concrete properties.

Objectives

The principal objective of the study is to investigate the effect of voids on the performance of CRCP and the use of increased pavement thickness when voids are anticipated. A secondary objective is to model the observations using SLAB 49 so that laboratory tests can be extrapolated to consider diverse conditions to give theoretical solutions.

Comparisons between theoretical solutions and the laboratory observations permit an evaluation of the effect of nonuniform foundation support under these laboratory slabs on concrete pavement distress. A successful prediction of a laboratory slab distress with a computer program will permit simulation of full support and nonuniform support under in-service pavements.

The Scope of the Study

The scope of the experiment was as follows:

- (1) A theoretical analysis of seven small dimension slabs was conducted to investigate the effect of loss of support to help design the size and shape of the void for use in the laboratory study.
- (2) A series of three small dimension slabs was tested with two levels of subgrade support loss and two thickness levels in order to observe the effect of repeated loads on performance.
- (3) The laboratory slab model behavior including the crack pattern development with repeated load was modeled with the SLAB 49 computer program.
- (4) The results for the unsupported slabs were compared with the results for the fully supported slabs tested in the previous study (Ref 1).

Outline of Report

This precursory study was conducted to examine the potential effect of small dimension tests in determining the effect of loss of support. It is not a complete factorial analysis, but rather a step by step experiment which

includes designing each subsequent slab based on the results of tests of the slab. In the report, recommendations and suggestions are outlined for future studies of this type.

Chapter 2 outlines the analysis and laboratory results that cover the observed problem in the field, simulation of the problem in the laboratory, the summation of previous experimental observations concerning fully supported slabs, and the theoretical approach using the SLAB 49.

Chapter 3 presents the selection of slab dimensions and characteristics to simulate most of the field conditions for CRC pavements within the State of Texas. The void size selection obtained through the SLAB 49 computer solutions, is also presented.

Chapter 4 outlines the laboratory experiment and the laboratory observations.

Chapter 5 presents the analysis of the experiment. The objectives of this analysis are discussed and the experiment parameters are outlined, as is the comparison of the experimental calculated and measured data.

Chapter 6 presents the conclusions and future recommendations for the same type of experiment as well as for improvement in CRC pavement design.

CHAPTER 2. ANALYSIS AND LABORATORY PROCEDURES

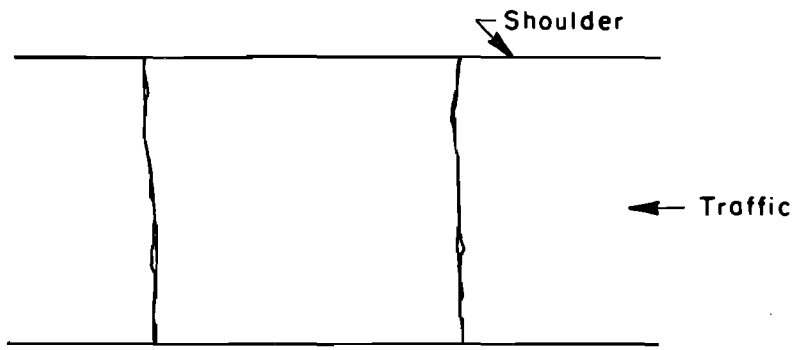
This chapter discusses the nature of the problem as observed in the field, how this field problem is simulated in the laboratory, how previous laboratory experience from the NCHRP 1-15 study are used, and the theoretical approach using the SLAB 49 computer program and its solutions.

Nature of the Problem

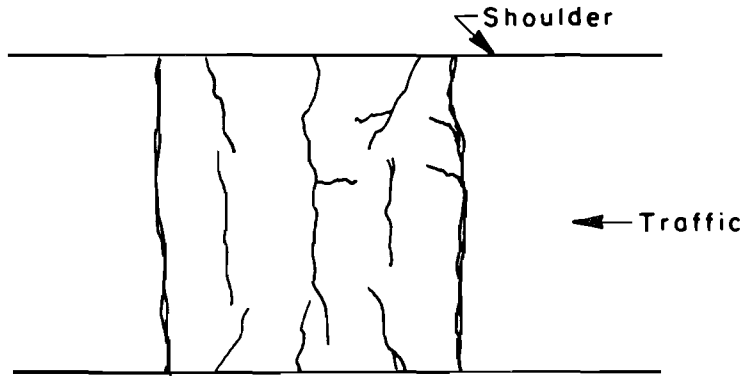
CRC pavements are designed to provide longitudinal reinforcement adequate to keep the crack tightly closed and to provide pavement thickness adequate for the traffic wheel loads. One of the important assumptions in design for CRC pavements is good support conditions. This emphasizes the need for observing and evaluating actual conditions as a guide to preventive maintenance in an effort to prevent future pavement distress. This study is concerned with pavement performance as affected by voids beneath the pavement and with general observations that help define where and how distress occurs when the voids are present under the pavement. Several observations of both the top and bottom of the CRC pavements on Texas highways show some of the distress occurring in the pavement is due to loss of support under the pavement.

Figure 2.1 shows in schematic form the usual sequence of the distress occurrence in the field. The distress occurrence rate depends on the traffic frequency, load magnitude, and environmental conditions (temperature changes, rain, snow, etc.). In addition, the soil support characteristics (swelling, settlement, densification, etc.) will influence the distress occurrence rate.

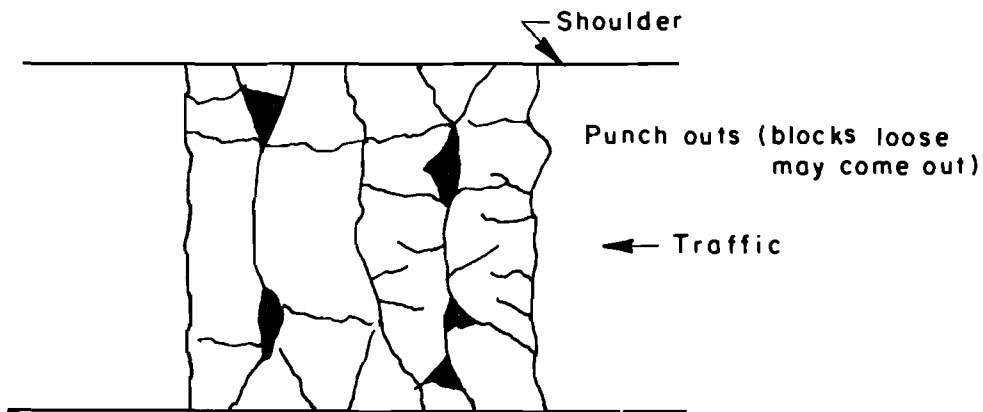
Figure 2.1a shows normal transverse cracks in CRC pavement prior to the wheel load applications. Figure 2.1b shows the crack pattern after 2×10^6 equivalent 18-kip single axle load applications. The repetitive wheel loads (fatigue) initiate new transverse cracking as well as develop longitudinal cracking.



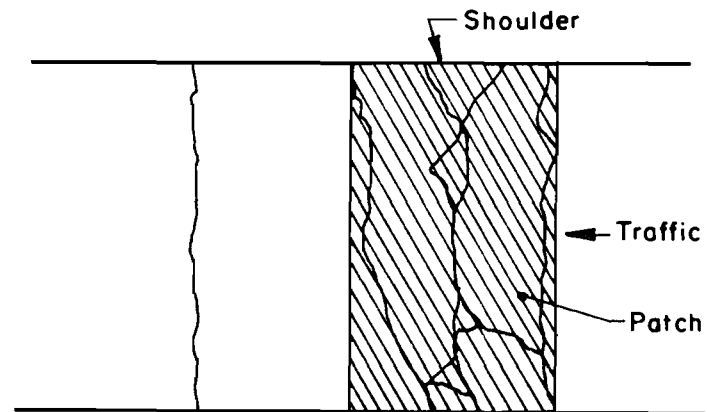
(a) New pavement section, zero load applications.



(b) Pavement distress after 2×10^6 load applications.



(c) Pavement distress after 4×10^6 load applications.



(d) Patch on top of deteriorated batch.

Fig 2.1. CRC pavement section at four different fatigue stages.

Figure 2.1c shows the crack development after 4×10^6 equivalent 18^k single axle load applications. In the figure, note how transverse and longitudinal crack developments lead to punch outs and consequently to loose concrete blocks that eventually come out. This type of deterioration results from a short fatigue life due to higher slab stresses when voids are present beneath the CRC pavements (Fig 1.1).

Figure 2.1d shows how the distress is corrected by repairing the CRC pavement by patching. Usually, patching is used to increase the CRC pavement life service.

Figure 2.2 is a sequence of pictures of a CRC pavement on a Texas highway that presents the same characteristics shown in Fig 2.1a, b, c, and d.

Simulation of Field Conditions

A common laboratory approach to simulate field conditions is through use of small dimension specimens that represent most of the field conditions. Small dimension slabs can adequately represent a field pavement section in the laboratory if proper modeling techniques are used. The equipment used for testing model slabs in a previous laboratory experiment (Ref 1) was used in this study.

The in-service CRC pavement has external and internal loading effects that must be simulated in the laboratory.

The laboratory equipment was designed to consider these factors in an effort to simulate field conditions, such as volume changes of concrete and steel (by the pulling action mechanism) and the resulting crack width, and crack development effects.

Adoption of Experimental Techniques

The procedures used in this study for preparing the slab, crack initiation, loading sequence, etc. are identical to those used in the NCHRP 1-15 study. The reader is referred to the report of that research (Ref 1) for a detailed description of the testing procedures. This approach permitted a one to one comparison of results from the two experiments.

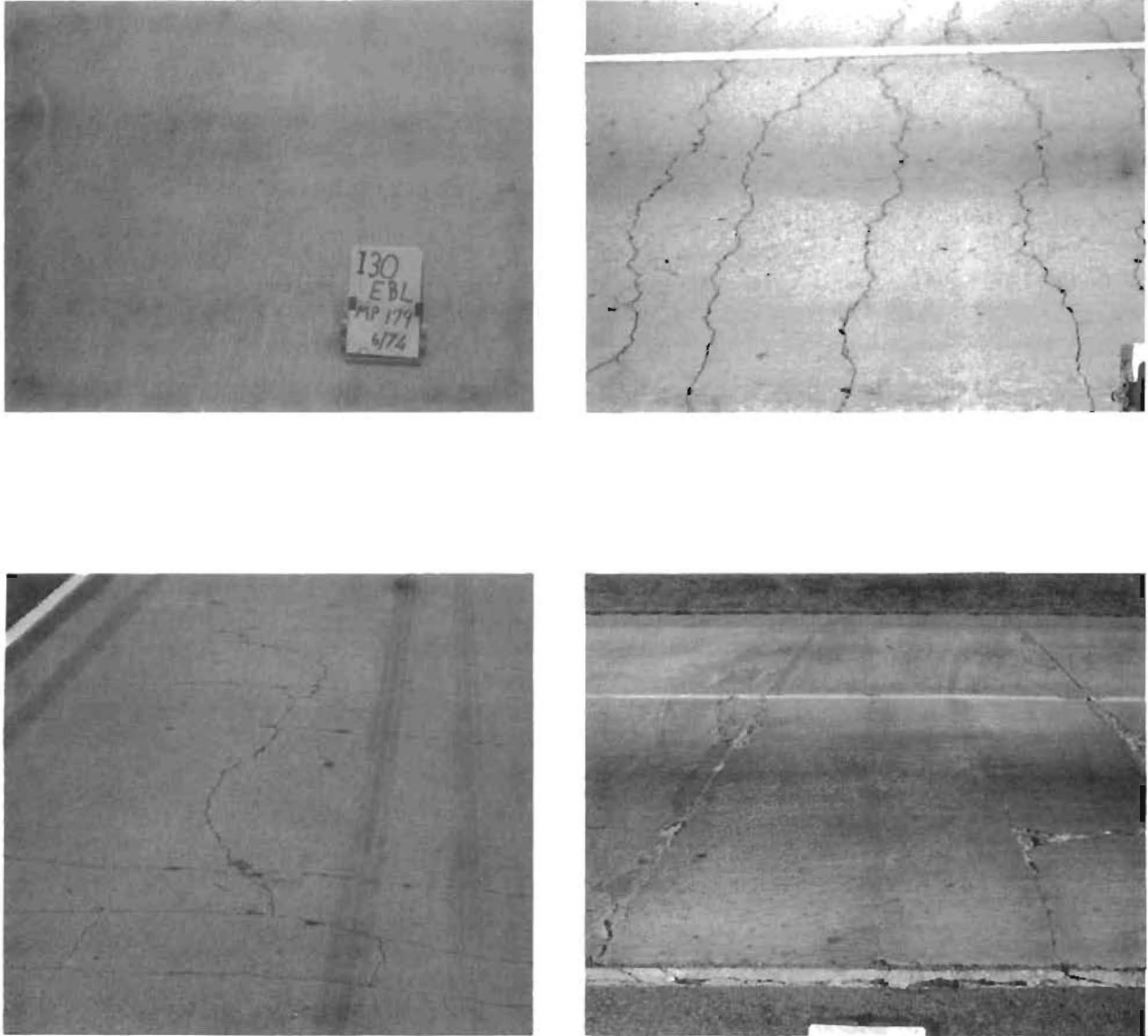


Fig 2.2. Sequence of CRC pavements distress that leads to a very severe pavement disintegration.

Observations of small dimension slabs with full support from the laboratory experiment from the NCHRP 1-15 study were used in the present experiment to compare how slabs behave when voids appear beneath them. To develop a void under the laboratory slab for simulating loss of support under the CRC pavement, part of the top rubber layer was removed.

Since it was preferable to reproduce most of the usual Texas design conditions, such as percent steel, steel location, and construction techniques, Slab No. L-5 from the NCHRP 1-15 experiment was used as the control slab. Table 2.1 presents the essential design features of the control slab. As may be seen, these components are similar to those used in most of the CRCP constructed in Texas from 1959 to 1974.

SLAB 49 Computer Program

In order to evaluate the expected behavior of small dimension slabs, the analysis was made using the SLAB 49 computer program, developed by Hudson, Matlock, et al (Refs 2, 3, 4, 5, and 6). This program is a discrete element analytical technique which solves a physical model of the slab consisting of rigid bars connected by elastic blocks and supported on appropriate springs to represent the foundation (Fig 2.2).

The method allows for nonlinear input, discontinuities in the slab and the subgrade, and varying support in the subgrade. The model also allows for axial loads in the slab similar to those imposed by continuous reinforcement.

With the SLAB 49 computer program, it is possible knowing the physical properties of the slab and the subgrade to directly model the small dimension slab and solve for the expected deflection and stresses. It is difficult to directly determine the support modulus of the rubber subgrade, but it is possible to adjust the overall results with actual measured deflections in the laboratory. The results from the previous laboratory experiment were inconsistent for two different thicknesses of the rubber subgrade. It was evident during the laboratory testing of the CRCP slab models that there was very little difference in subgrade support as offered by the 3 and 6-inch thicknesses of rubber mat. Since the predicted results can be adjusted using the actual measured laboratory data for deflections versus the K-value (support value), one can predict with greater accuracy this data as a function

TABLE 2.1. COMPARISON BETWEEN THE STATE DEPARTMENT OF HIGHWAYS AND PUBLIC TRANSPORTATION CONTINUOUSLY REINFORCED CONCRETE PAVEMENT DESIGN AND THE LABORATORY SMALL DIMENSION CONTINUOUSLY REINFORCED CONCRETE SLAB.

Area of Comparison	SDHPT	CFHR Laboratory
Percent steel reinforcement	0.50 - 0.56 percent	0.55 percent
Reinforcement depth	Mid-depth	Mid-depth
Type of steel	Deformed Bars	Deformed Bars
Bar size	No. 5	No. 4
Bar spacing	7.5 inches	7.0 inches
Bond area/concrete volume	$Q = \frac{15.36}{5760} = .002667$	$Q = \frac{7.20}{2688} = .002679$
Load	0,000 lb/wheel load	2250 lb/wheel load
Stress at bottom of slab	$\sigma = 421.9$	$\sigma = 421.9$
Thickness	8 inches	4 inches
Mix Design	(1) Type I cement 5 1/2 sacks/cu yd (2) 1-inch maximum size aggregate (3) 2 to 5-inch slump (4) 3 to 6 percent air	(1) Type I cement 5 1/2 sacks/cu yd (2) 3/4-inch maximum size aggregate (3) 2 to 5-inch slump (4) 3 to 6 percent air

of slab thickness (Fig 2.3). The comparison of both the measured and the calculated deflections permits a K-value to be derived that may be used in the SLAB 49 computer program.

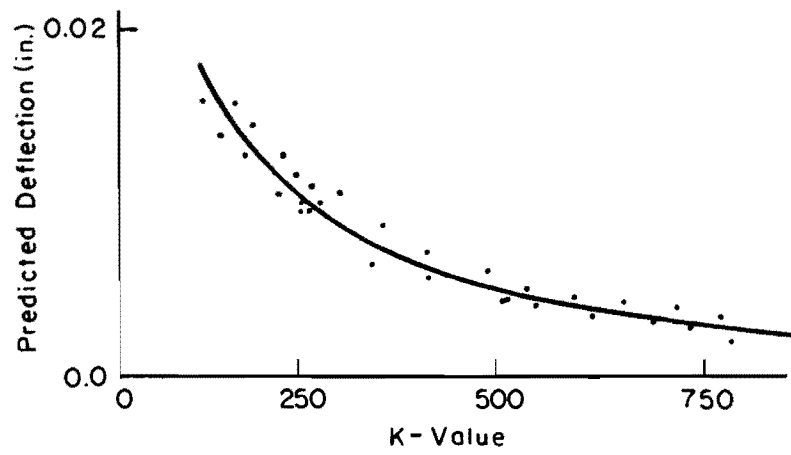


Fig 2.3 Relationship between slab deflection and K-value.

CHAPTER 3. ANALYTICAL STUDY

This chapter covers the analytical study of the slab characteristics, such as percent of steel reinforcement, thickness, position of the steel, and crack width. From field observations, it was noted that the voids creating the highest distress were near the transverse cracks at the middle of the lane or near the shoulders (Fig 3.1). The findings of the computer analysis are presented and discussed in the objective of selecting and defining void location and size that represent the field conditions creating the highest distress in the CRC Pavements.

Void Selection

Computation Experiment. Seven different cases were selected to study during the computation experiment to ascertain which case creates the critical field conditions, such as higher deflection and stresses. Figure 3.2 represents six different void positions and sizes that can be found under CRC pavements in the field. Their introduction into the study through the SLAB 49 computer program will help to determine the void size and location that create the highest deflections and stresses, specifically, the ones in the laboratory study which behave as nearly as possible as to those in the field.

As discussed in Chapter 1, voids under the slab are created by several soil support conditions (settlement, swelling, etc.). Furthermore, infiltration of water into the edges at the shoulders can create a pumping situation that leads to a void and consequently higher distress in that particular area.

If voids begin to develop beneath the pavement, higher deflection and stresses (tensile) develop, producing higher distress in the pavement slab. The decision was made to select from the computer solutions the case which presented the highest deflection and stresses and to use its void characteristics during the laboratory slab experiment.

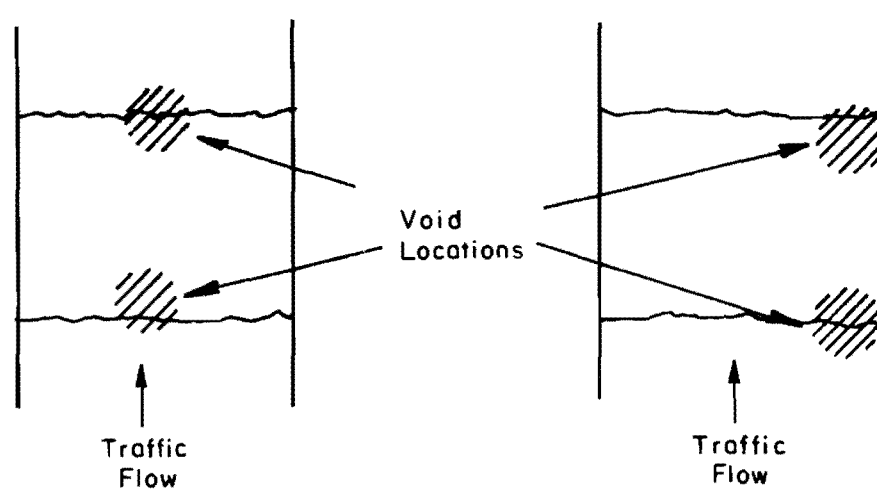


Fig 3.1 Selected voids used during the experiment according to field criteria.

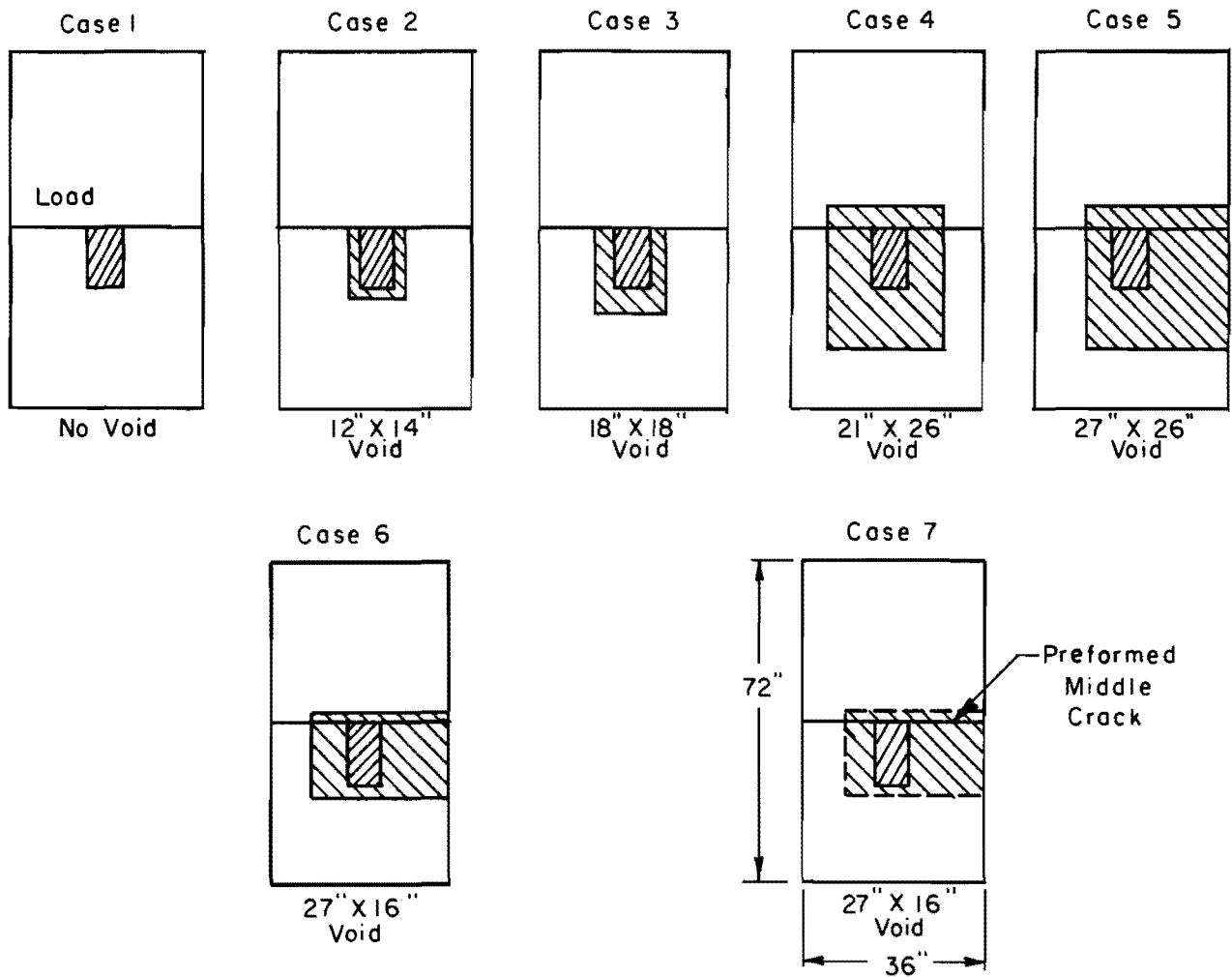


Fig 3.2. Void sizes studied with the computer program to decide which one will be used for the laboratory slab models. Cases 1, 2, 3, 4, 5, and 6 used four-inch slab-thicknesses, Case 7 used a 2-inch slab thickness.

Analysis of Data. After running the SLAB 49 computer program, an analysis of the output for the seven different cases (Fig 3.2) resulted in the following observations:

- (1) The first case, the full support under the slab, was retained since it simulated the control laboratory slab L-5 from the previous experiment (Ref 1).
- (2) The second and third case, introduction of 12×14 -inch and 18×18 -inch void sizes beneath the middle of the slab and under the load area, were discarded because the deflection and stress profiles were similar to those of the fully supported slab.
- (3) In cases four, five, six, and seven, drastic differences in deflections and stresses appeared in the solutions, compared to those in the first three cases, when void sizes of 21×26 -inch, 27×26 -inch, 16×27 -inch, and 16×27 -inch were introduced and they were retained respectively.

Cases 4, 5, and 6 introduced greater void sizes and the deflection and stresses were also greater. When the void was moved near the edge, higher deflections and stresses were developed than with the voids in the middle of the slab. In cases 6 and 7, no change was made in void size nor position; the change is in the slab thickness. Reviewing all solutions, the deflections and stresses in the last four cases were the largest. Since comparison of one of the most critical conditions, pumping at the edges, is what it is worth, the solutions from cases 5, 6, and 7, for which the voids are at the edge, were selected (Fig 3.3).

Solutions of the Computation Experimental Design (Slab 49 Computer Program)

Observations derived from the void size analysis using the solutions from the SLAB 49 computer program led to the following findings:

- (1) The slab deflections are directly influenced by the void size (Fig 3.4).
- (2) If the slab thickness is increased, the deflections will decrease (Figs 3.4 and 3.5).
- (3) The slab stresses decreased when the slab thickness increased (Fig 3.5).

In Fig 3.4, the deflection increases due to increase in void size. The slab dimension is 36 inches by 72 inches (2592 in^2), the low void dimension represents 16.71 percent of the total area ($16 \times 27 \text{ in}$), and the high void dimension represents 27.10 percent of the total area (26×27). The

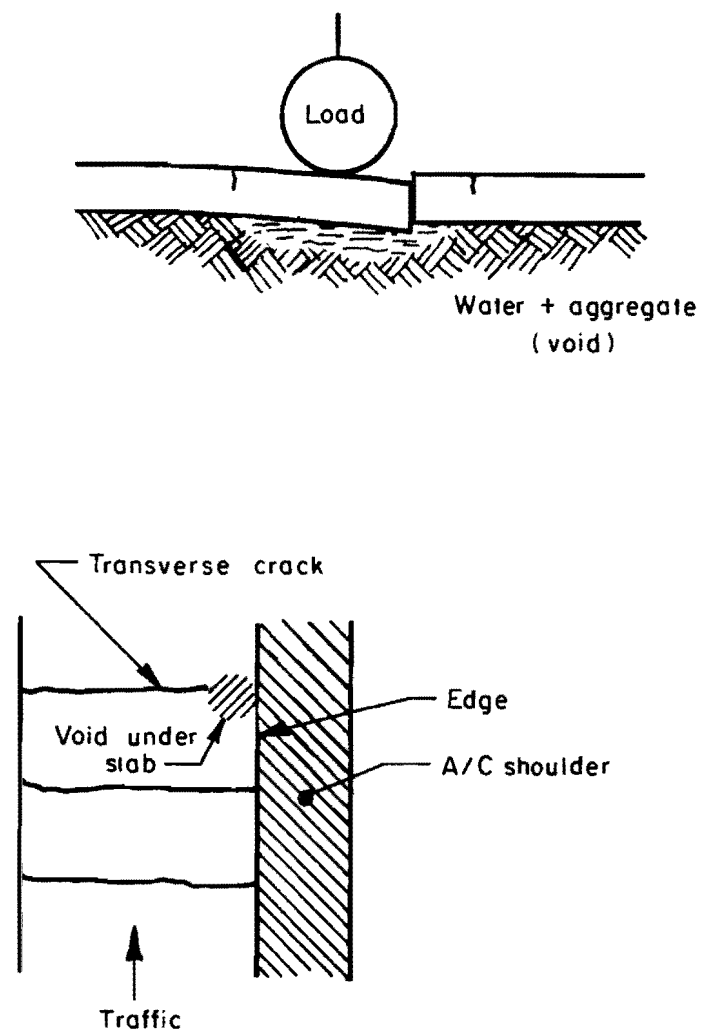


Fig 3.3 Representation of void created by pumping situation at the edges of the CRC pavements.

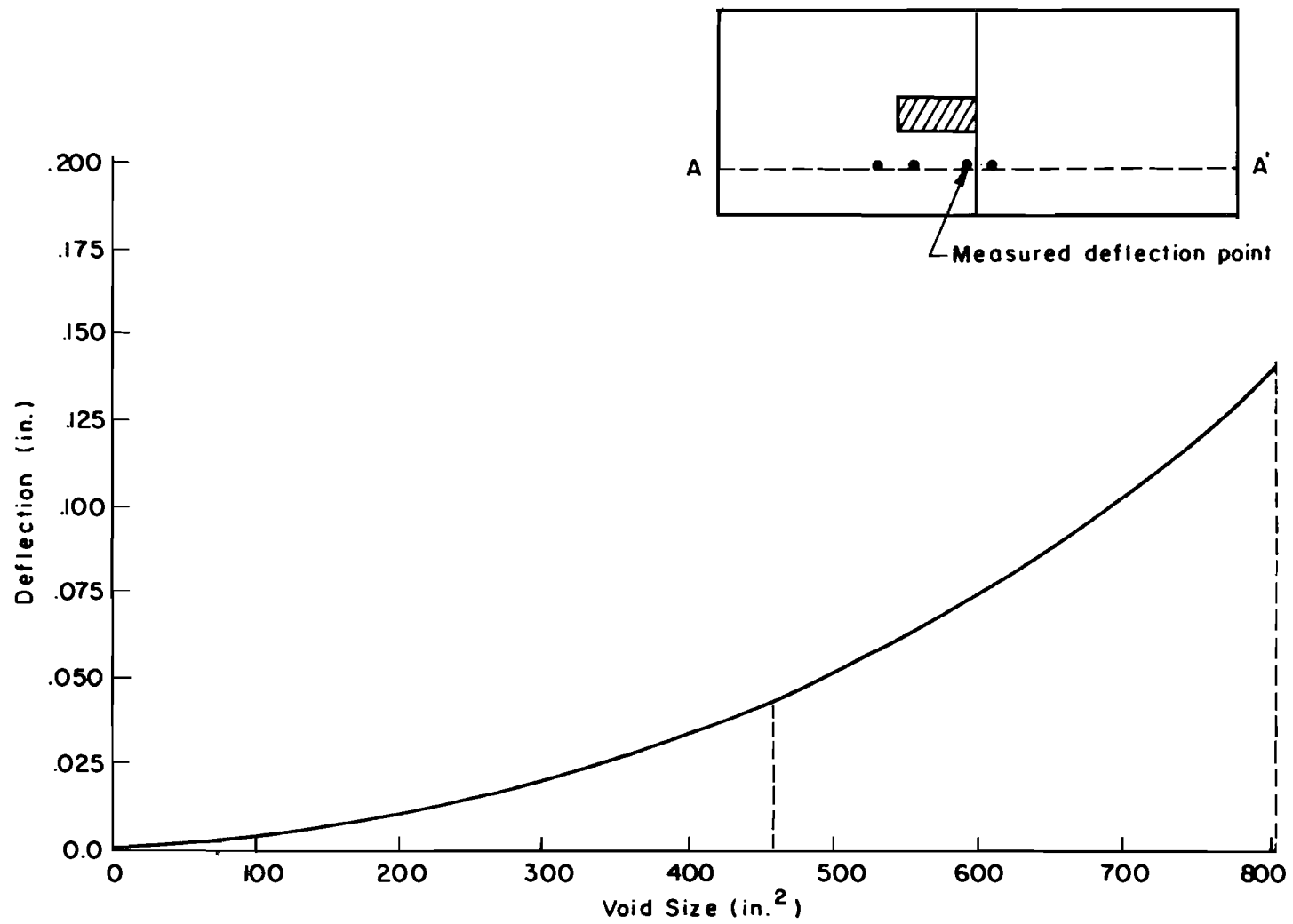


Fig 3.4. Increase in slab deflection at the measured deflection point for the 4-inch slab thickness (calculated deflection).

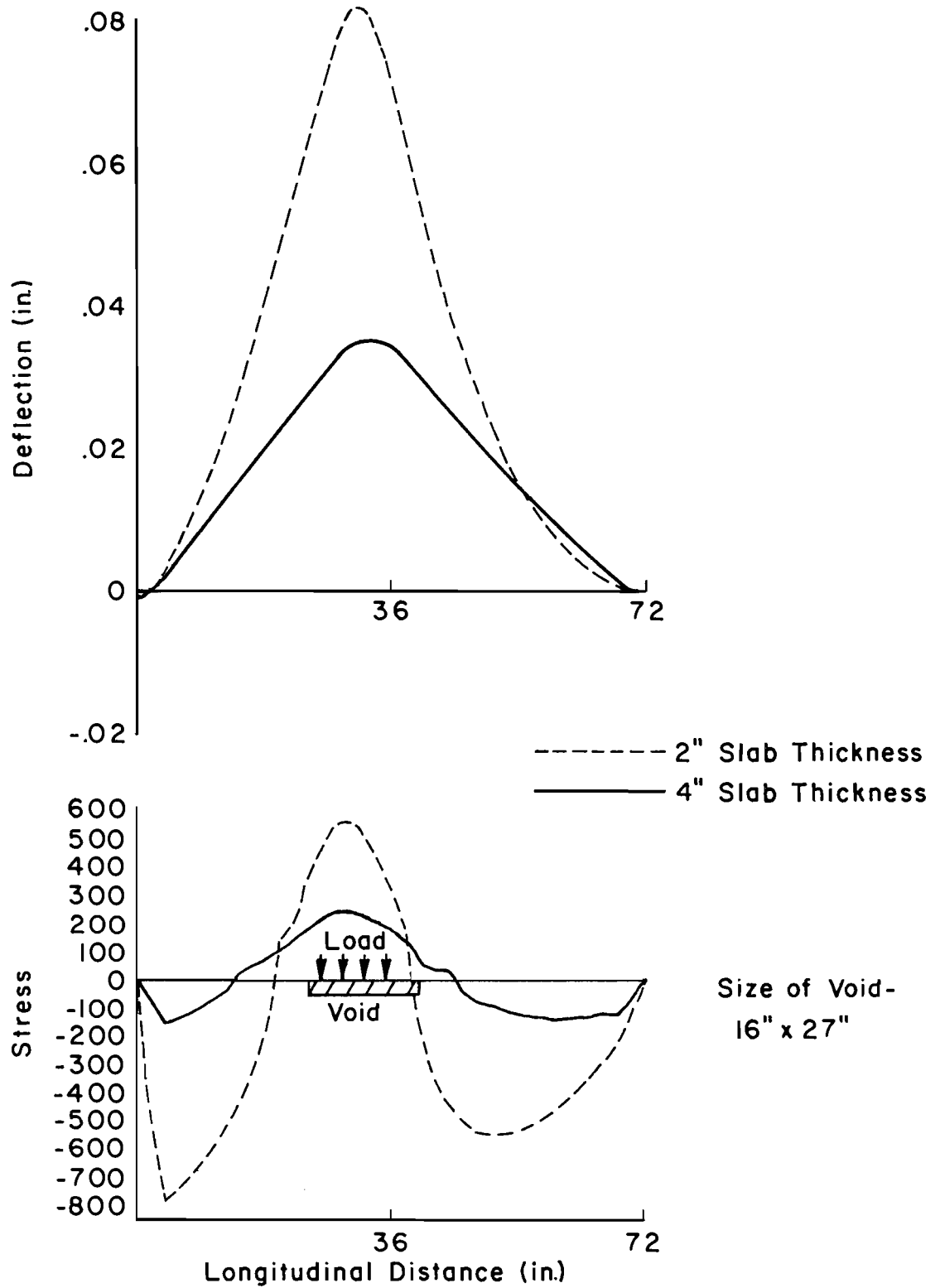


Fig 3.5. Longitudinal slab deflection stress for 2-inch and 4-inch slab thicknesses.

deflection for the fully supported slab was .0155 in., for the low void was .0267 in., and for the high void was .0324 in. Figure 3.5 presents a comparison of the longitudinal stress and deflection profile for the 2-inch and 4-inch slabs. The signs for the stress profile are for the bottom of the slab, with (-) being tension and (+) being compression. The top of the slab would have equal stress but with opposite signs. Note that the maximum stress occurs outside the void and with the 2-inch thickness. The maximum tensile stress occurs in the top of the slab.

From this observation, one can point out that the deflection will increase as the percent of void area increases. However, if the slab thickness is increased, it is possible to decrease the slab deflection and consequently the stresses will decrease. The designer must be aware of all these factors or possibilities in order to decide the most adequate thickness design of the CRC pavement to control these factors.

Summary

Theoretically, from these experiments, it was found that deflection and stress increase when a void is present under the slab. In addition, deflection and stress increased when the slab thickness was reduced. Cases 5 and 6 proved to have the most significant deflections and stresses in the 4-inch-thick slab. However, case 7, where the slab thickness was reduced to 2 inches showed the earliest distress at an early stage for all three cases (5, 6, and 7).

Figures 3.6 shows the factorial experiment design used for both the 2-inch and 4-inch slab model thicknesses.

Slab Thickness	Void Size		
	No Void	Low Void	High Void
2"	—	X	—
4"	⊗ (1-15)	X	X

- ⊗ Previous experiment
 X This experiment

Fig 3.6 Experimental factorial design used for both 2-inch and 4-inch slab model thickness.

CHAPTER 4. LABORATORY STUDY

This chapter presents the laboratory slab study as it was conducted. Included are the background on slab type, configuration, and mix design; the slab preparation and inspection prior to its testing phase; the slab testing operation and procedures; and the observations made during the laboratory tests.

The Laboratory Slab Background

The comparison of laboratory slab behavior with the field observations calls for a systematic, logical approach in an effort to develop comprehensive and rational improvement in CRC pavement design. All types of pavements are complicated physical systems that involve a combination of several important variables that interact in a complex way and are difficult to simulate in the laboratory.

However, our theoretical study and our laboratory slab design approximated most field conditions, such as construction techniques, concrete mix design specifications, percent of steel reinforcement, soil support (rubber mat), and volume changes (pulling action mechanism).

Slab Type and Configuration

The laboratory test slab is a small dimension version of CRC field pavement slabs and measures 36 inches by 72 inches. The model slabs were 4 inches thick (177-1 and 177-2) and 2 inches thick (177-3). The slab's size was chosen using discrete element analysis techniques so as to approximate two-dimensional bending models which still fit into the laboratory space requirements. The slab dimension in the previous experiment (Ref No. 1) was the same as the one used in this laboratory experiment.

Slab Preparation

In forming the slab model, several steps must be followed in order to insure low variance and high quality results.

Forms. In forming up the CRCP slabs, stiff reusable metal forms were used. Prior to placing the concrete, these forms were cleaned, snugly fitted together with connecting bolts, carefully aligned, and covered with conventional oil. Following 24 hours of curing, these forms were carefully removed so as to allow for easy formation of the transverse crack.

Bond Breaker. To reduce friction between the rubber subgrade and the concrete slab, a bond breaker was used in the laboratory investigation. The thin polyethylene sheet that was used as a bond breaker was placed over the entire rubber subgrade prior to the forming of the slab. To keep the polyethylene in place and to minimize wrinkling, the sheet was securely taped to the metal forms.

Metal Strip. Following placement of the bond breaker and the metal forms, a strip of 20 gauge metal was positioned across or along the width of the bottom of the slab at mid-length. This strip of metal was 40 inches in length and either one inch in height (for slabs 4 inches thick) or one-half-inch (for slabs 2 inches thick). Its purpose was to create a weak section, and thus to preform the transverse crack at the desired point across the middle of the slab. The metal strip was securely held in place in slots in the metal forms.

Longitudinal Reinforcement. In this laboratory experiment, the amount of steel reinforcement was 0.55 percent for both the 4-inch and the 2-inch slab thickness. Four deformed number four bars were used for the 4-inch slab, while four deformed number three bars were used for the 2-inch slab (Fig 4.1)

Depth of Reinforcement. Only mid-depth reinforcement was used in this study, for both the 4 and the 2-inch slab thicknesses.

Pulling Bars. In addition to the longitudinal reinforcement, the slab model in the laboratory study contained four pulling bars. These pulling bars were part of the overall pulling mechanism used to simulate volumetric forces on the slab as described in Ref 1, Appendix C.

The pulling bars consisted of four grade 60, number 6, deformed reinforcing bars for the 4-inch slab and four number five for the 2-inch slab. Each of these bars was bent into a U-shape with an inside diameter of 5 1/4

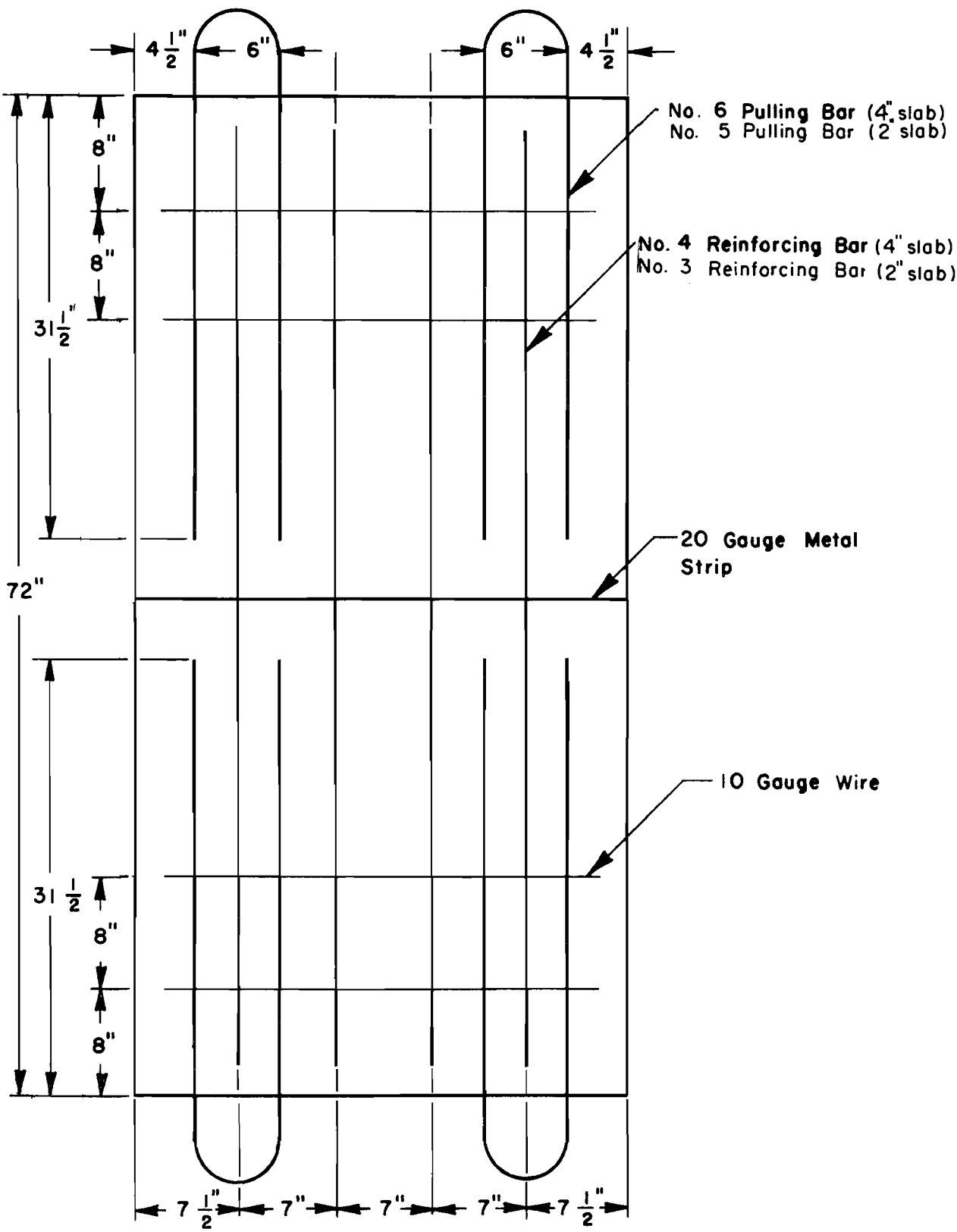


Fig 4.1 Steel layout for .55 percent reinforced slabs.

inches. Two lengths of pulling bars were used. One type had legs 46 inches long, while the other type had legs 41 inches long. This difference in length was necessary to fit the pulling mechanism.

The pulling bars were positioned at the mid-depth of the slab with steel chairs. Each of the four pulling bars extended 31 1/2 inches into the slab. By extending the pulling bars this distance into the slab, the bond length necessary to avoid slippage was attained and the bars were still 4 1/2 inches short of the middle of the slab, thus preventing interference with stiffness characteristics at the crack. The first 6 inches that each leg of each pulling bar extended into the slab was covered with polyethylene. This bond breaker was used to permit the movement to initiate at the crack, which simulates field conditions.

Transverse Wire. In order to provide for a more uniform pull action across the laboratory slabs and to further avoid bar slippage, a 64-inch-long section of 10 gauge wire was looped around the pulling bars. The wire was secured with tie wire to the pulling bars only.

Final Inspection of the Slab

Following the steel placement, and prior to concrete placement, a careful inspection of each slab was made. This inspection was made to insure compliance with experimental specifications and to eliminate as much slab-to-slab variation as possible. Alignment of the pulling bars, pulling mechanism, and the slab itself, was very important. Therefore all alignments were carefully rechecked prior to slab placement. The general slab layout was inspected to see that it met specifications as to position and depth of all slab components. All components were also checked for proper clearances to insure good concrete placement. As a last step, all the tie wire and other connections were inspected along with a general overall check to insure good concrete placement and checked to insure elimination of all foreign material from the slab. Following the final slab inspection, photographs and drawings were made to document the exact position of all slab components.

Slab Placement

Since the concrete placement procedures during construction may affect performance, emphasis during laboratory slab operation was placed on using proper construction techniques representative of good field practice and on limiting slab-to-slab variation.

The concrete was ordered from a commercial supplier. Prior to placing the concrete in the slab, various quality control tests and inspections of the mix were made. If the delivered concrete met all specifications, it was carefully placed into the slab form to full depth, taking great care not to disturb any of the slab components. The concrete was carefully vibrated in all areas with a spud type vibrator to insure good consolidation throughout the slab without causing segregation. After the concrete was placed, the slab was struck-off to the proper level with a hand screed and hand troweled to produce a smooth, even surface.

Quality Control

To insure high quality concrete, a number of quality control steps were taken following the arrival of the concrete from the commercial supplier and prior to placing the concrete:

- (1) An inspection of the batch ticket was made to insure proper mix contents.
- (2) A general visual inspection of the concrete was made to insure proper mixing of the ingredients, cleanliness, proper type and size of aggregate, etc.
- (3) A number of slump tests were performed on the concrete to insure proper water-cement ratio.
- (4) A number of Rollometer tests were performed to insure proper air content.

Failure of the delivered concrete to pass the above quality control inspections resulted in a rejection of the particular concrete batch. At the time each laboratory slab was placed, compression cylinder test and flexural beam specimens were molded to provide seven-day strength evaluations. Following seven days of proper curing, these specimens were tested appropriately and the average value for each test was then recorded.

Table 4.1 shows the results of all the quality control tests performed on the concrete for each laboratory slab. The values are the average results for each type of quality control test (4 or more tests).

Curing the Slab

Following concrete placement and initial set, a curing compound was applied to the concrete surface. A hydrocide resin-base curing compound manufactured by Sohneborn Building Products was used exclusively. The compound was carefully applied with a hand brush and allowed to dry and form a membrane. After the membrane had formed, conventional wet curing mats were placed over the slab. Wet mat curing continued for seven days, at which time the mats were removed and testing of the slabs began.

Testing Operation. One of the most important aspects of the laboratory study of CRC pavements was the development of a realistic means by which to simulate the horizontal loading of the test slabs (i.e., horizontal stresses caused by concrete shrinkage and temperature fluctuations). To simulate these horizontal forces, a pulling mechanism and an experimental procedure were developed and are in the previous experiments (Ref 1, Appendix C). The same pulling mechanism was used in this study.

To obtain and correlate the laboratory study concerning deflection, load transfer, crack width, void size and location, and crack and spalling development, the following experimental procedure was followed:

- (1) After 24 hours of proper curing, the pulling mechanism was used to form the middle crack.
- (2) After 7 days of curing of the slab, the void under the slab was created by pulling out the pre-cut piece of rubber mat under the slab (a void of 27 X 14 inches across the crack, along the edge, as shown in Fig 4.2).
- (3) The loading plates were positioned on the slab according to the procedure outlined in Ref 1, Appendix C, and shown in Fig 4.2,
- (4) Using the pulling mechanism and the Barry strain gauge, the transverse middle crack was opened to the 0.01-inch crack width level, the experimental crack width during the first two million load applications.

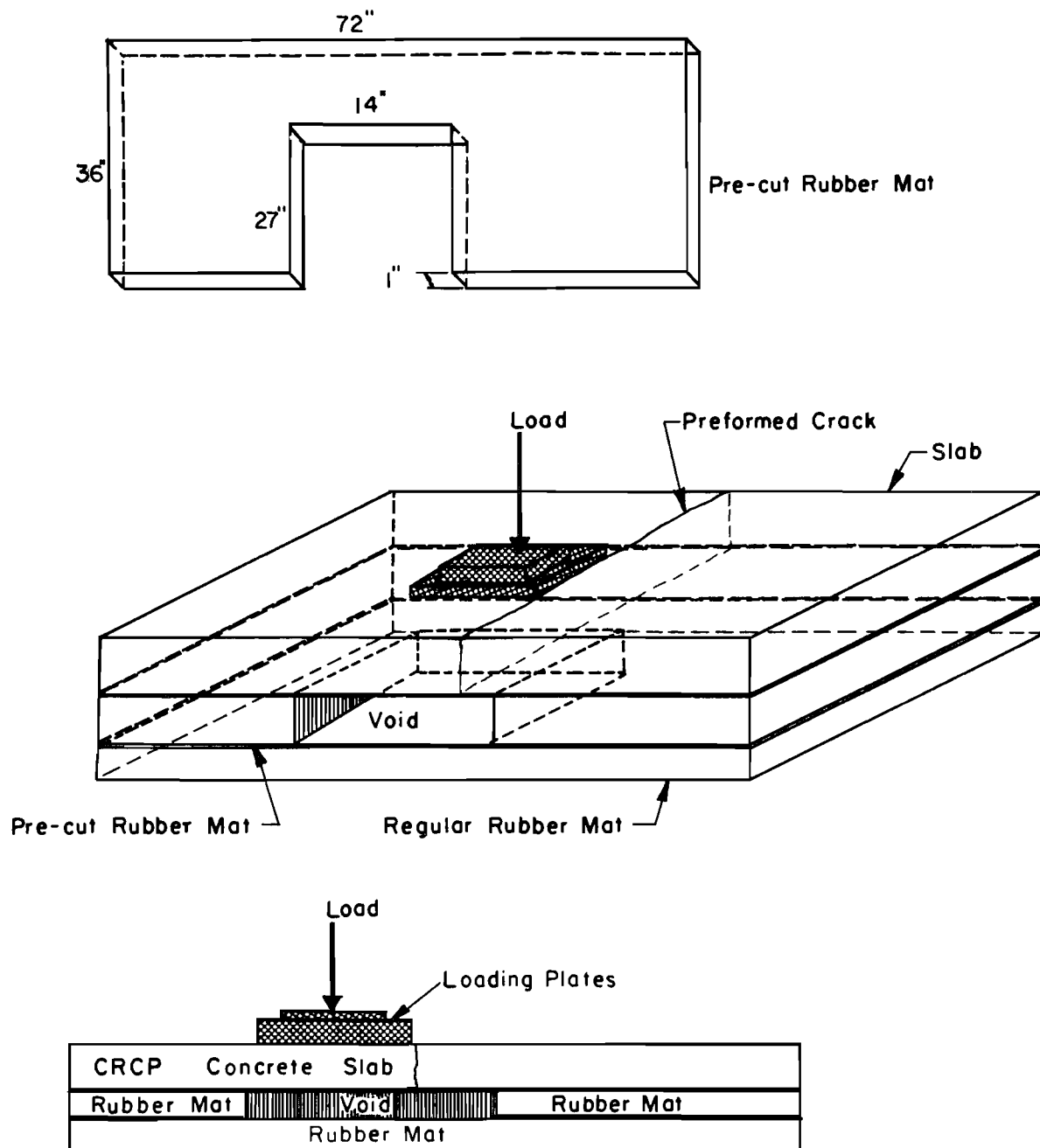


Fig 4.2 Procedures for creating the void under the slab.

TABLE 4.1. RESULTS OF LABORATORY QUALITY CONTROL TESTS

<u>Slab</u>	<u>Slump Test (inches)</u>	<u>Air Entrained (percent)</u>	<u>Seven-Day Compressive Strength(psi)</u>	<u>Seven-Day Flexural Strength(psi)</u>
L-5	2 3/4	4.0	3510	543
177-1	4	3.5	3888	577
177-2	4	2.3	4187	563
177-3	2 1/4	1.5	2856	481

- (5) All of the stations or points were checked very carefully and recorded prior to the pulling mechanism operation to insure that the determination of the 0.01-inch of crack width is reached without any difference in all of the stations.
- (6) The MTS System, oscillograph, LVDT's, voltmeter, and amplifiers were turned on and allowed to warmup for a minimum of 15 minutes, then the calibration of the system was carefully checked.
- (7) The hold-down beams were positioned and bolted down to fingertip tightness.
- (8) The LVDT's were carefully positioned, and, in this instance, the position was changed to the opposite side of the load; this change was made for the following reasons:
 - (a) because the deflection of the slab measured from the new LVDT position will be more sensitive to the size of the void than the old position, and
 - (b) to correlate with the increments that are in the computer program and then obtain more accurate data within the experiment (Fig 4.3).
- (9) The oscillograph and MTS System were zeroed, and specific care was taken when LVDT's were calibrated.
- (10) Vertical loading of the slab was initiated, and 500 to 5000 pounds at five cycles per second level was reached.
- (11) A complete review of all the System was done and the loading counter was initiated and notes were taken of the initial reading.
- (12) The vertical loading of the slab was continued for 111 hours and 12 minutes to complete two million load repetitions on the load counter. Regular inspection of the system was made to insure that the equipment was working under optimum conditions and also to make notes of the crack development on the oscillograph chart to insure that all data correlate with the time of the slab testing behavior.
- (13) After the 0.01-inch crack width level test was completed, the system was stopped completely and the crack development was carefully reviewed and colored in accordance with the coloring code. Black and white color pictures were taken with the objective of differentiating the crack developments at the 0.04-inch level of crack width.
- (14) Steps 4 through 12 were then repeated, with the load transfer investigation of each slab being finished at the completion of the testing at the 0.04-inch level of crack width.

Laboratory Experimental Slab Observations

As previously discussed, this experiment attempted to define the behavior of CRC pavements when support is lost under the pavement. The observations

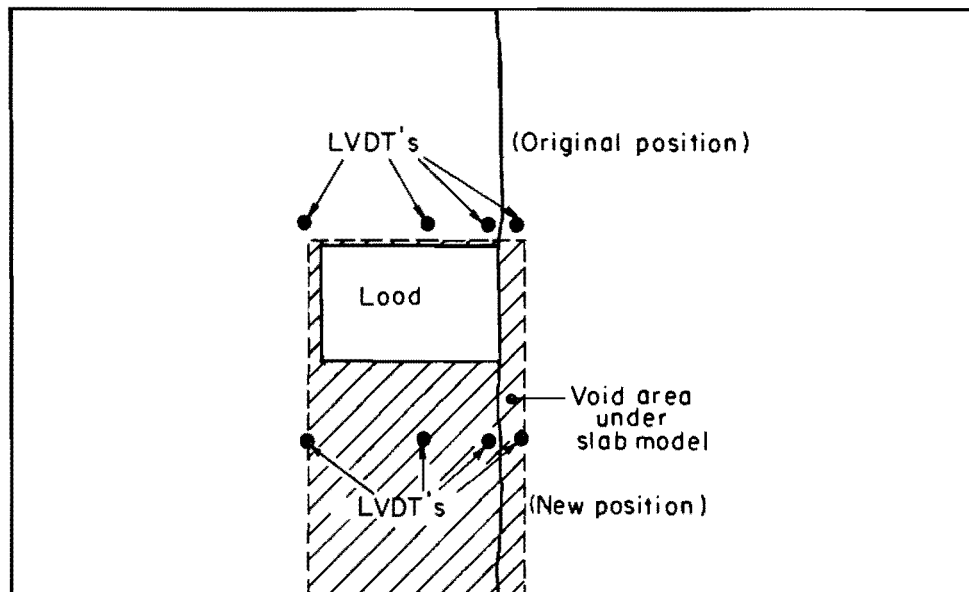


Fig 4.3 Modified position of LVDT's for slab Models 177-2 and 177-3.

during the laboratory slab experiment are very important since this is the best way to define and compare how the CRC slab behaves when the conditions vary (i.e. how deflection is affected by thickness variation).

Appendix 1 presents the cracking and deflection information for the control slab L-5 from Ref 1. The data are presented in the same format as used for this experiment, which provides a basis for comparison.

General Laboratory Slab Observations

The following observations and results were systematically recorded during the experiment:

- (1) Deflections in the slab due to repetitive load applications (dynamics load) over a specified period of time and number of applications (fatigue) were observed and measured.
- (2) Slab distress such as cracking and spalling development due to repetitive load applications were recorded at two different crack width levels and for the bottom of the slab at the end of testing.
- (3) Load transfer characteristics between slab segments were recorded during testing to give design information for maximum permissible crack width.
- (4) The change to a thinner slab (2-inch) provided data on load transfer, load carrying capacity, and distress index as affected by slab thickness.
- (5) Slab distress and deflection variations due to a void under the slab (loss of support) were recorded.

Table 4.2 provides a summary of the maximum deflection and distress at the end of each testing period for each test slab. This will be referred to in the subsequent discussions of the individual slabs.

Notice that the deflection measurement obtained for the voided slabs (177-1 and 177-2) are even smaller than that of the fully supported slab (L-5) recorded in NCHRP 1-15 report. This leads us to believe that either the construction of the experimental slabs or the operation procedure used fails to reproduce the L-5 slab constructed in the NCHRP 1-15 project. For this reason, the results obtained from the L-5 slab reported in NCHRP 1-15 project will be precluded as a control for the fully support condition and instead, the computed results predicted by the discrete element program will be used as a control to compare with the other voided slabs.

TABLE 4.2 CRACK DEVELOPMENT AND MAXIMUM DEFLECTIONS
MEASURED DURING PHASE I AND PHASE II TESTING

Slab Model	Support	Thickness (inches)	Crack Development Length (inches)			Deflection (inches)
			Top	Bottom	Total	
<u>PHASE I (2×10^6 load applications)</u>						
L-5	Full	4	**	*	*	.05***
177-1	High void	4	95	*	*	0.041
177-2	Low void	4	65	*	*	0.033
177-3	Low void	2	430	*	*	0.090
<u>PHASE II (4×10^6 load applications)</u>						
L-5	Full	4	**	**	207	.062***
177-1	High void	4	302	235	537	0.063
177-2	Low void	4	80	76	156	0.051
177-3	Low void	2	535	449	984	0.180

* Measurements not available for bottom of the slab until end of Phase II testing.

** Unavailable data

*** Notice this deflection is even higher than the deflection measured from the voided slabs, the explanations were given in the previous page.

Slab Model 177-1

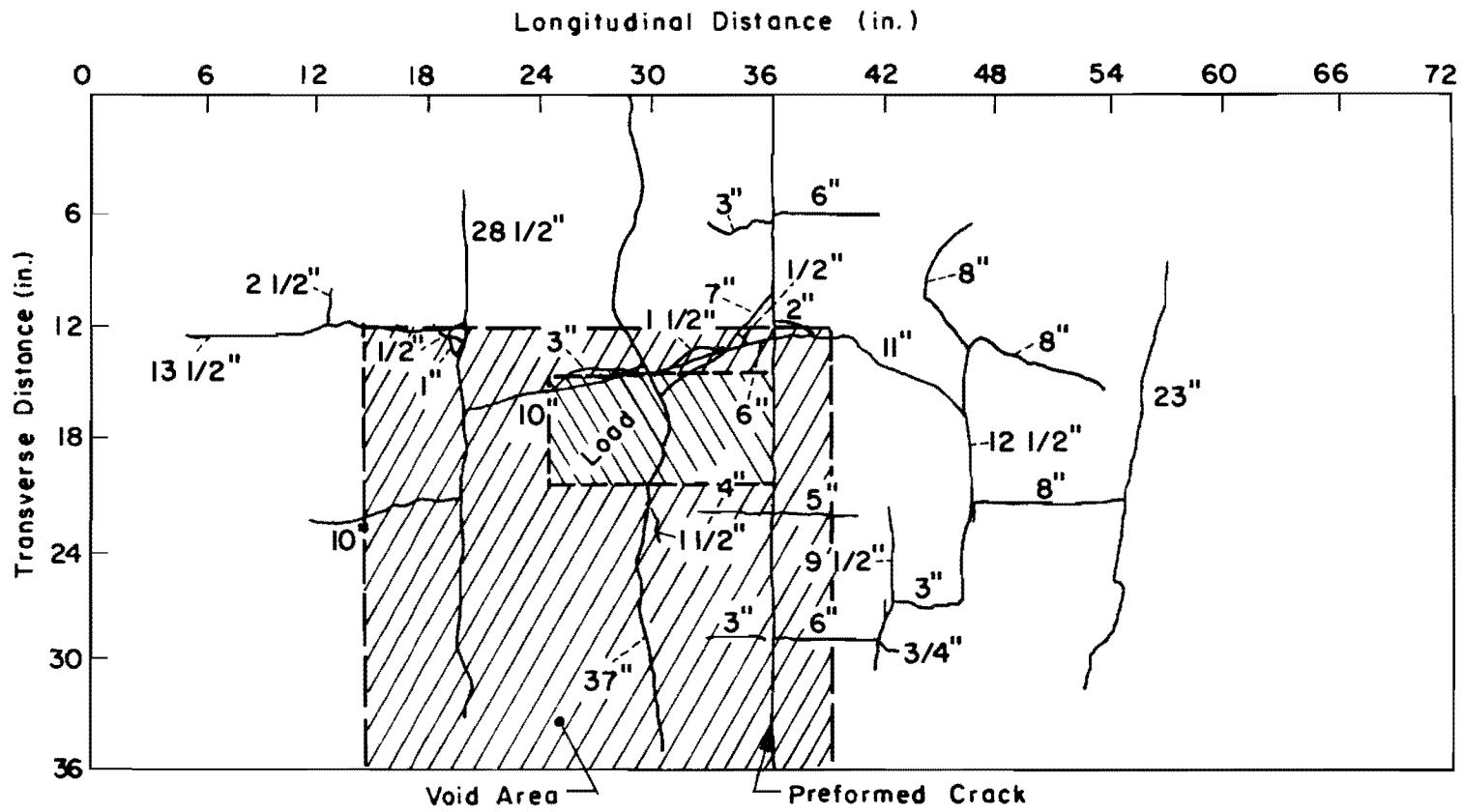
Slab Model 177-1 experienced very little distress on top of the slab during the first phase of the experiment (crack width level of 0.01 inch). The larger void under the slab was used during this experiment (26 X 27- inches near the edge and across the crack). During the first testing phase, i.e. the first two million applications, the deflection data showed only a small increase of the measured deflection and very little distress. However, the deflections and distress increases were greater than those measured in the control experiments (Slab L-5, Ref 1) due to the void under the slab.

After the preformed crack was opened to the second crack width level (0.04-inch), it was observed that no new cracks were formed during the process of opening the crack width level.

During the second testing phase, it was observed that in the void area, the deflection and cracking increased considerably near the preformed crack. Eighty percent of the crack development for this experimental slab model occurred after the middle crack was opened from the 0.01-inch to the 0.04-inch crack width level. After the second test phase, the repeated loading was stopped and the slab was lifted to observe the bottom face. A detailed survey was made to detect the cracking development on top and under the slab.

During the experiment, the deflection increased after the crack width level was opened from 0.01-inch to 0.04-inch and the crack development increased considerably. From this experiment, an analysis of the data leads to the following observations:

- (1) As expected from previous experiments (Ref 1), the slab deflection increased near the crack, but it was much greater this time because of the void under the slab.
- (2) The crack development in the slab was greater when the slab was tested at 0.04-inch of crack width level.
- (3) The total crack development pattern appeared more severe near the void area; this gave a clear indication of the support loss beneath the slab (Figs 4.4 and 4.5).
- (4) A transverse crack developed across the bottom of the slab (Fig 4.5), in which is the area of maximum tensile strength (Fig 3.5). The crack is only partially reflected in the top of the slab, but would show through after a period of time.



* Numbers shown are length of crack in inches.

Fig 4.5. 177-1 Laboratory slab model crack development at the bottom.

- (5) Longitudinal cracks have started in the bottom of the slab between the preformed crack and the bottom transverse crack discussed in item 4 above. The longitudinal cracks are partially reflected in the top but would possibly be more so if the testing had continued. These longitudinal cracks would eventually lead to punch outs, as has been observed in the field.
- (6) The transverse cracks across the top of the slab (Fig 4.4) in the area away from the preformed crack and the load area have developed across the width. Using Fig 3.5 as a reference, the area of cracking shows up in the maximum tensile stress area in the top of the slab. In this case, the transverse crack is only partially reflected in the bottom of the slab at the end of testing.

Slab Model 177-2

With the second slab experiment, there was considerable reduction of the void area (50 percent reduction). All the steps previously discussed for the slab model 177-1 were followed again for the two different crack width levels (0.01-inch and 0.04-inch) and the two different phases of load applications. In this experiment, it was observed that the variation of deflection was very small and, also, that the distress development showed a very small crack at the top of the slab during the first level of crack width and first set of 2×10^6 applications.

After the crack width was opened from 0.01-inch to 0.04-inch, a very small crack developed at the top and at the bottom of the slab (Figs 4.6 and 4.7). The measured deflection also increased with the 0.04-inch crack width level. Again, the distress increased at the higher crack width level. The following observations are applicable to this slab:

- (1) The deflection of this slab model was lower than with slab 177-1, indicating that the void area can reduce or increase the deflection, depending on its size or location.
- (2) The distress behavior of this slab was much lower than the slab 177-1. The large influence of deflections on the fatigue life of the pavement was successfully demonstrated through this experiment, as has been the case previously (Ref 1).
- (3) Additional transverse cracking occurred in the area of maximum tensile stress in the top (Fig 4.8) and in the bottom (Fig 4.9). This was also the case with slab 177-1.
- (4) Cracking around the void is substantially less than was the case for 177-1, i.e., a reduced void area has substantially reduced cracking.

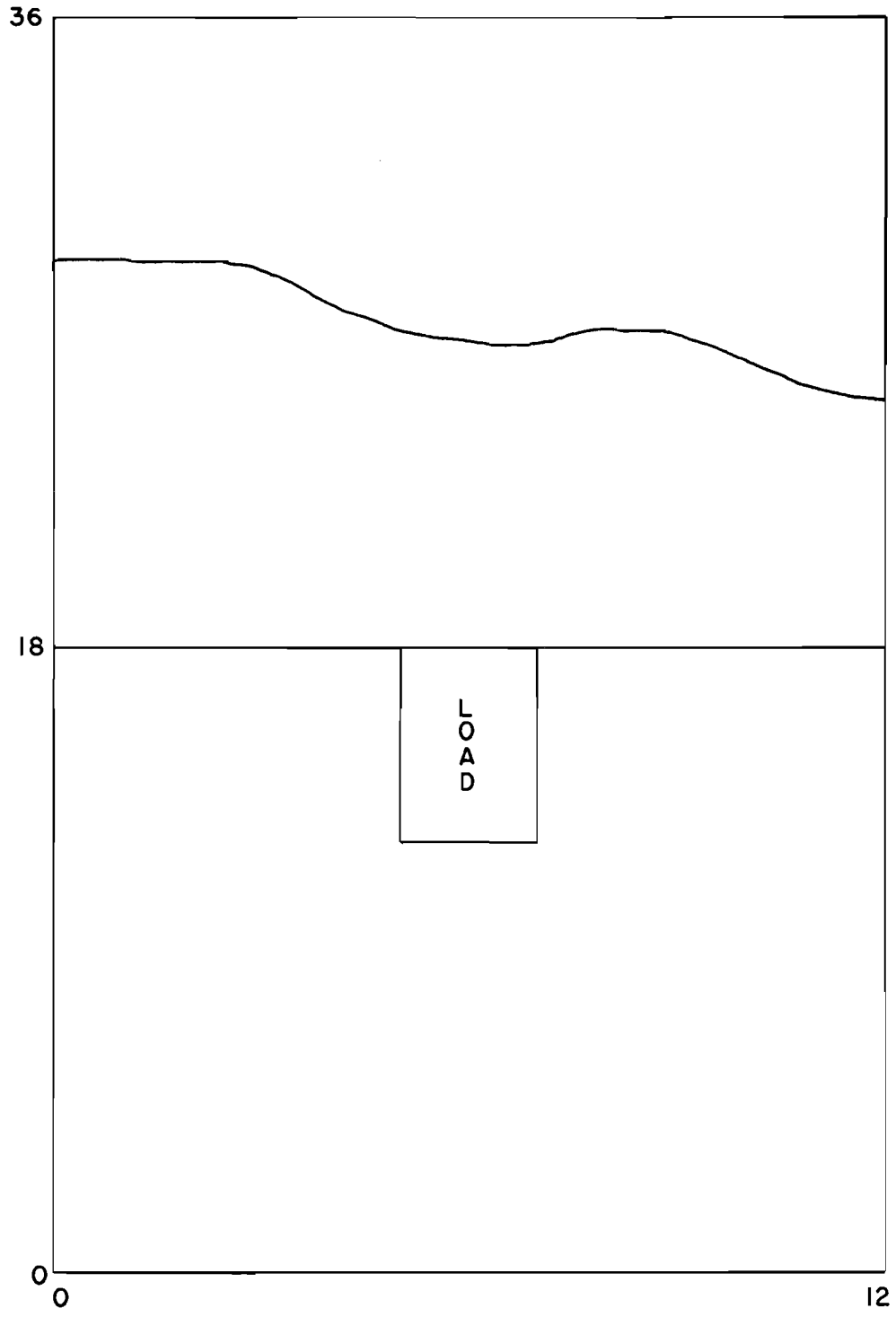


Fig 4.6. Laboratory slab model 177-2 total crack development at the top.

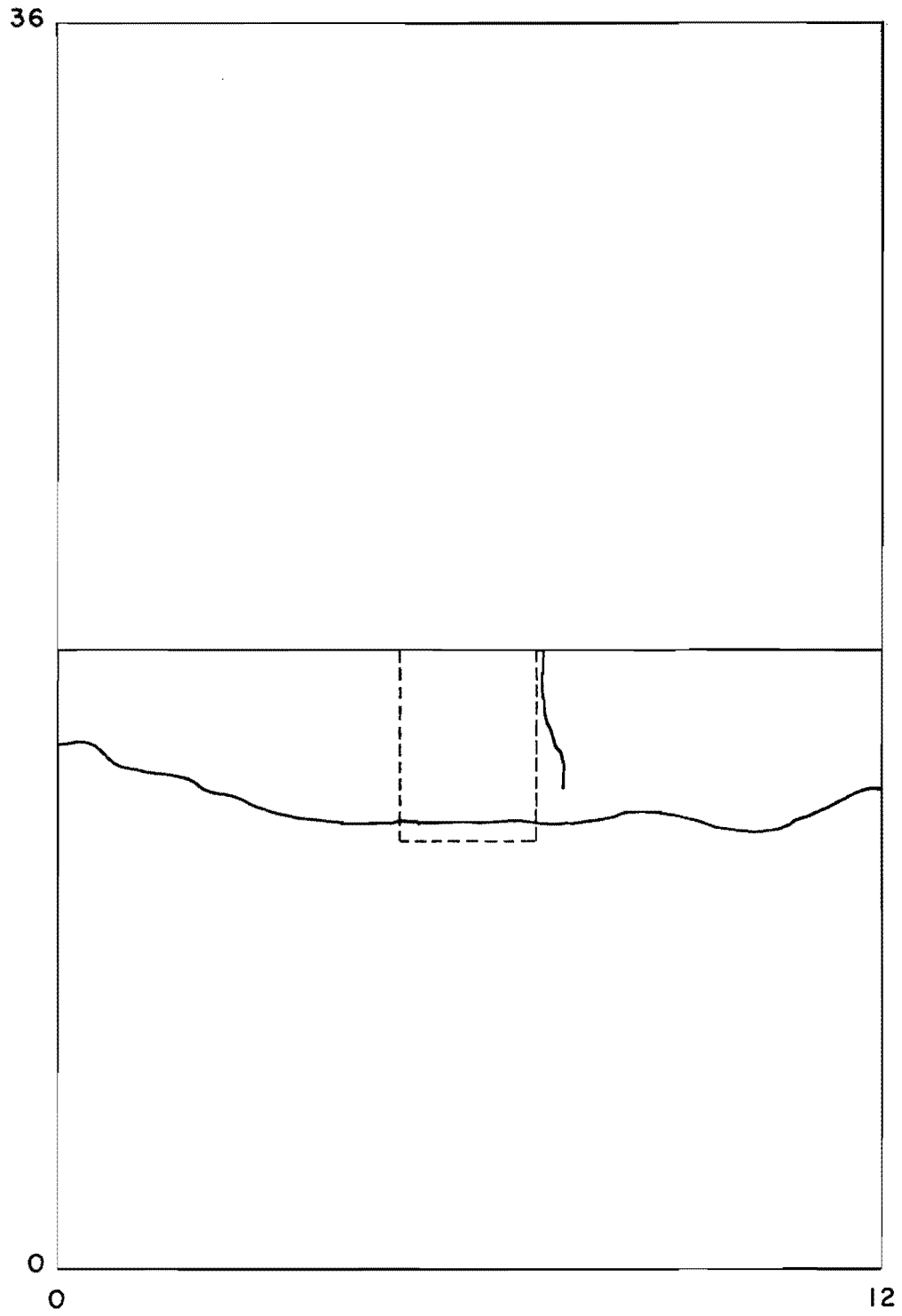


Fig 4.7. Laboratory slab model 177-2 total crack development at the bottom.

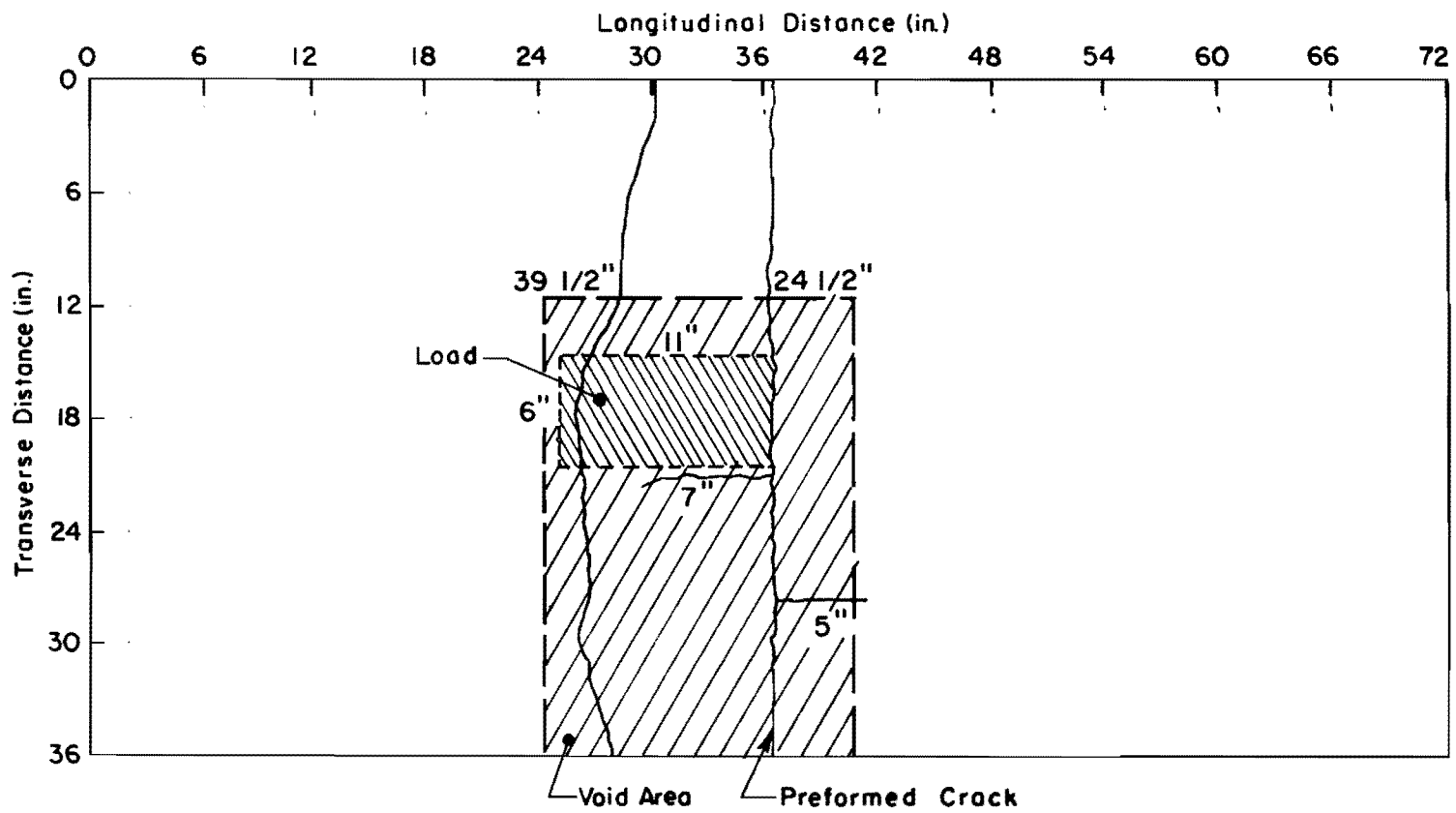


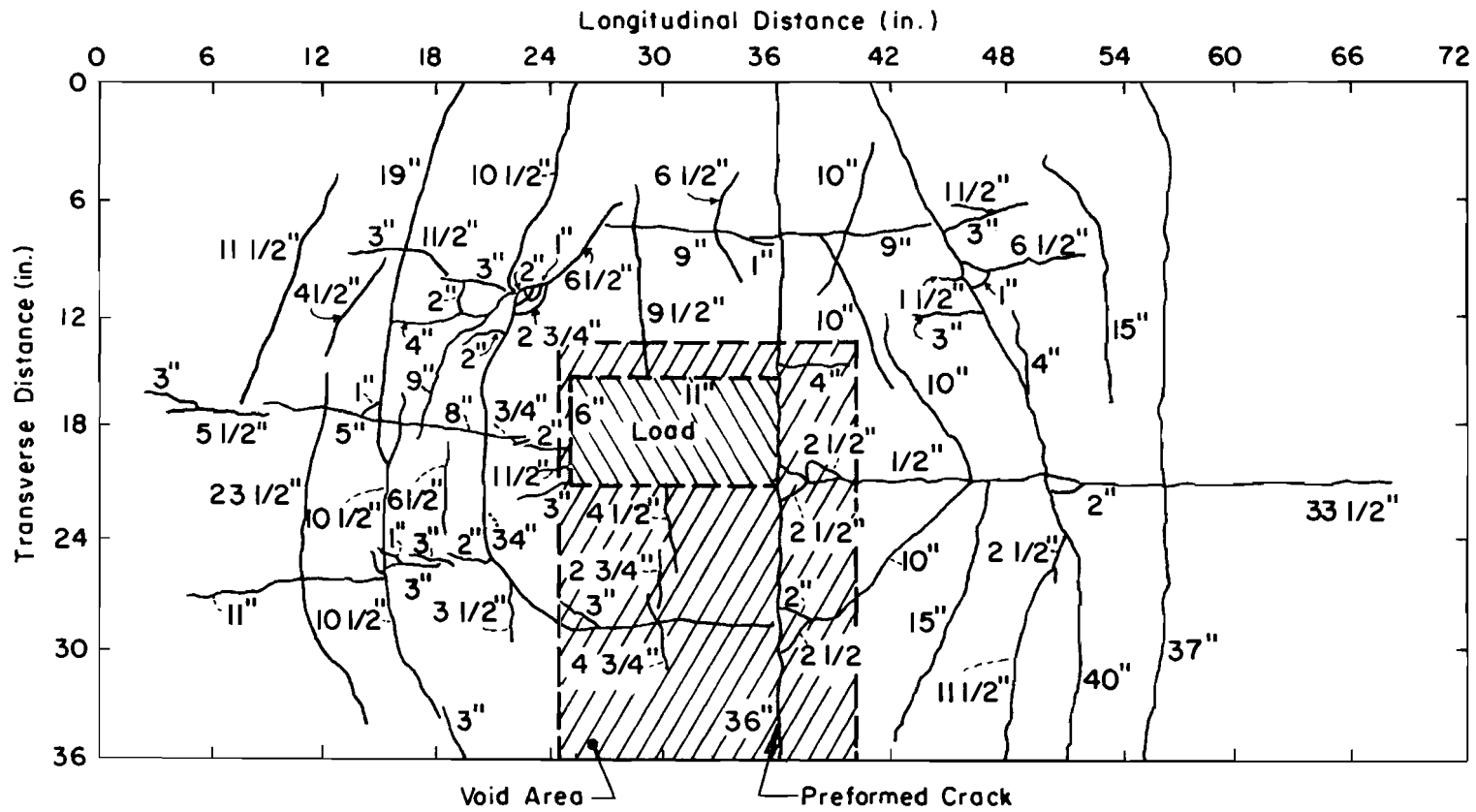
Fig 4.9. 177-2 Laboratory slab model crack development at the bottom.

- (5) The longitudinal cracking between the preformed crack and the transverse crack (Fig 4.9) has commenced, but it is substantially less than at the end of the testing for slab 177-1, illustrating the effect of void area on the stresses in cracking and resulting cracking in the slab.

Slab Model 177-3

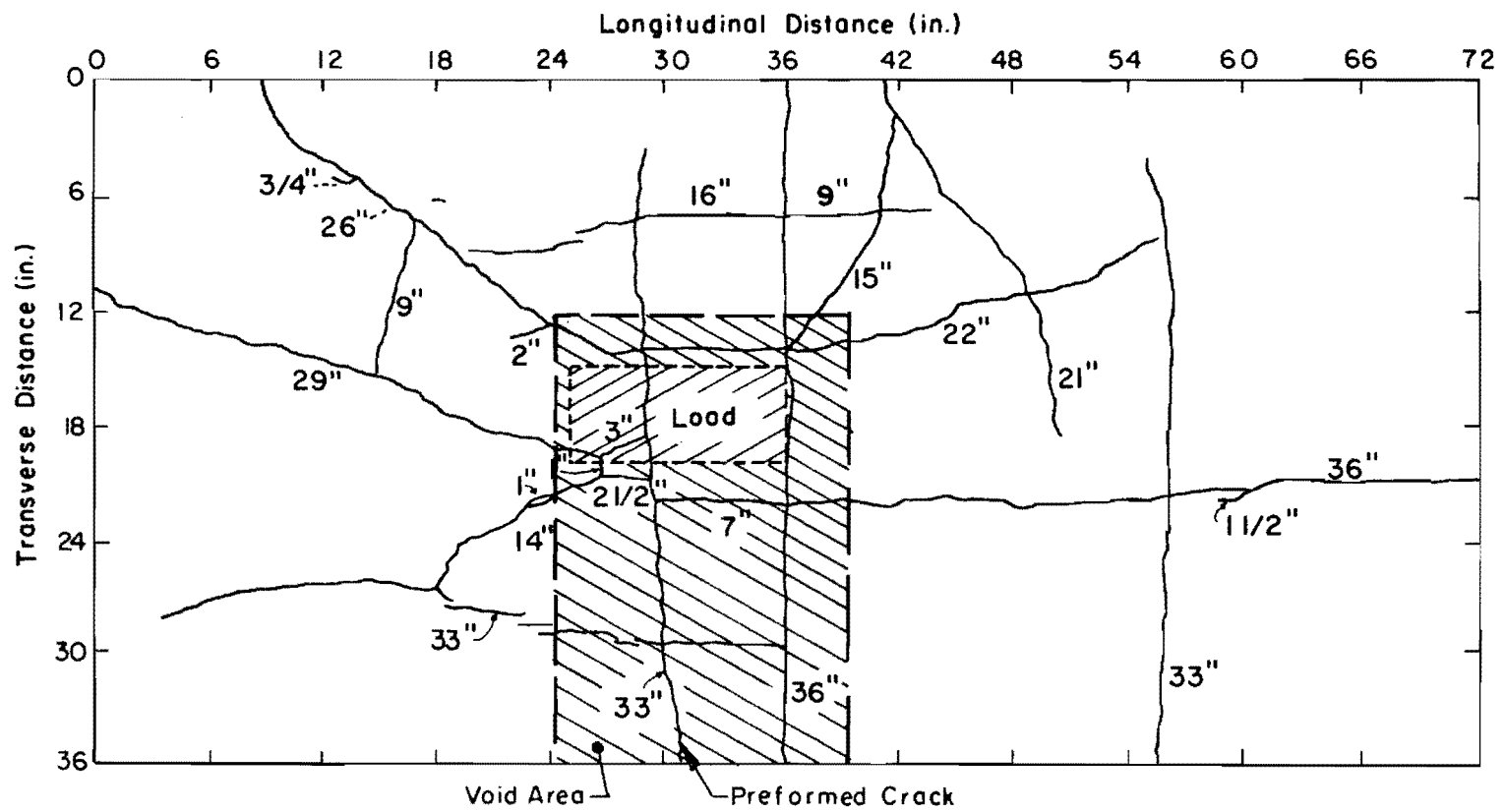
The third experimental slab (where the slab thickness was reduced from 4 inches to 2 inches) experienced the most significant changes of all the experiments. The objective of this slab experiment was to observe the influence of thickness on distress and deflection. All the steps used in the previous experiments (Slabs 177-1 and 177-2) were followed. The analysis of data for this experiment led to the following observations:

- (1) More distress and higher deflections were observed during the first part of the experiment, (2×10^6 load applications at 0.01-inch crack width level) than in previous experiments.
- (2) During the process of opening the crack width level from 0.01-inch to 0.04 inch, the slab developed cracks.
- (3) The distress behavior which took place after the completion of the second part of the experiment (2×10^6 load applications at 0.04-inch crack width level, was much greater than that which occurred during the previous experiments (Slab models 177-1 and 177-2). There was also a permanent deformation of the slab. From this last observation, it is pointed out that the fatigue life of the slab is greatly influenced by the thickness reduction (from 4-inch to 2-inch slab thickness).
- (4) Note the circular pattern of cracking that occurs around the void. This is very similar to the pattern developed in the field where a breakup occurs. With traffic movement, the small blocks are generally "whipped out" to leave a small area that must be filled with asphalt as a temporary measure.
- (5) The longitudinal cracking is much more extensive in this case than in the previous slabs. In Fig 4.10 and 4.11, the longitudinal cracking covers the entire length of the slab.
- (6) Although this slab was tested with a smaller void than 177-1, the breakup is greater than with the larger void, which demonstrates the effect of thickness.



* Numbers shown are length of crack in inches.

Fig 4.10 177-3 Laboratory slab model crack development at the top.



*Numbers shown are length of crack in inches.

Fig 4.11. 177-3 Laboratory slab model crack development at the bottom.

Comparison of Observations on Slabs

A comparison of the data from the experimental slabs from this project leads to the following pertinent observations:

- (1) Cracking increases with load applications. The sequence of occurrence of the cracks definitely points to the factor of load amplitude. The cracks generally start in an area of maximum tension and progress to the other area of the slab. In numerous instances, the cracks only partially extended from top to bottom or vice versa. These observations meant previous observations have indicated that transverse cracking spacing is reduced with load applications.
- (2) An increase in void area beneath a slab leads to additional slab distress and breakup. A comparison of the results from slab 177-1 with 177-2 shows that the larger void results in more distress. The cracking pattern developed around the void simulates that observed under field conditions. Limited field studies have found voids beneath slabs experiencing a breakup pattern very similar to the small-scale slab used in this experiment.
- (3) The slab thickness has a large influence on the rate of distress development. In this experiment, a reduction of thickness from 4 to 2 inches had a significant influence on the rate of deterioration in terms of load applications. This emphasizes that additional thickness may help correct problem areas to reduce distress in areas where voids are anticipated beneath the slab.
- (4) Deflection increases with load applications and is greater with the larger void sizes.
- (5) In observing the crack development on all the slabs, it appears that the slab acts as a unit initially. First, transverse cracks appear. This results in the slab acting as a small segment transversely, which eventually results in longitudinal cracking development. In the field, this generally leads to small blocks of concrete that can easily be "whipped out" by traffic. This points out the need for taking this into account when designing concrete pavements.

In summary, this experiment demonstrates the effect of void size and thickness on distress development. The sequence of breakup leads to the obvious conclusion that the designer should attempt to simulate this analytical model. If this can be accomplished, then the results can be reflected in a design equation.

CHAPTER 5. ANALYSIS OF THE EXPERIMENT

This chapter presents the analysis of the laboratory results, including both the calculated and the measured data. As was previously discussed, the objective of this study is to determine how accurately the small dimension slab performance can be predicted when it is subjected to a vertical repeated load (dynamic load) with a void under the slab.

The Experimental Parameters

The experiment compared the parameters that were selected as the most important in an effort to obtain realistic results that can be compared with field observations. These parameters are as follows:

- (1) Support
 - (a) fully supported
 - (b) void under the slab
- (2) Level of void
 - (a) high void (27 X 26 sq in)
 - (b) low void (27 X 16 sq in)
- (3) Thickness
 - (a) thick slab (4 inches)
 - (b) thin slab (2 inches)
- (4) Deflections
 - (a) measured
 - (b) calculated
- (5) Slab Performance
 - (a) calculated stress level (max)
 - (b) measured distress

Support. The state of slab stress and strain was theoretically calculated using a K-value of 225 psi for the fully supported slab (L-5) and zero for void conditions. During the previous NCHRP experiment, the K-value for the slab model with poor support was determined to be 225 psi using plate load tests. As stated earlier in Chapter 4, the deflection measurement obtained from the slab L-5 in NCHRP 1-15 project for the fully supported condition cannot be used to compare with the voided slabs in this project. The comparison, therefore, can only be made between the calculated non-void slab deflection and the calculated voided slab deflections. The results in Table 5.1 shows twice as much computed deflection for the 27 × 26 square inch voided slabs as compared to the deflection for the fully supported slab.

Level of Voids. Two levels of voids (high and low) were tested under the slab models and the results, discussed in the previous chapter, showed that the greater the void area, the greater the slab model distress. In our theoretical solutions, where the inputs are the two different levels of void (high and low), as used in the experimental slab model, the results showed that increasing the void size will increase the stresses. This means that higher tensile stresses in the computer solutions will predict greater distress in the CRC slab.

Thickness. The effect of the slab thicknesses can be found by comparing the theoretical analysis between the slab 177-2 and the slab 177-3. While both slabs have the same void size, slab 177-2 is twice the thickness of slab 177-3. Table 5.1 shows the computed deflection for slab 177-2 to be 2 1/2 times less than that for slab 177-3. By examining the experimental slab results, both 177-1 and 177-2 experienced less deterioration than slab 177-3.

Calculated and Measured Deflection. In the theoretical calculations, a reduction in bending stiffness is used to model the cracks (Ref 11 and Appendix 2). Only the deflections that correspond to the performed crack were recorded.

For the first level of 0.01 inch crack width, the measured deflection and the computed deflection were shown in columns A and D of Table 5.1. The trend of increase or decrease of the measured deflection for different slab thicknesses and void sizes are consistent with the computed deflection.

TABLE 5.1. PRINCIPAL RESULTS FROM THEORETICAL AND MEASURED VARIABLES USED WITHIN THE OVERALL EXPERIMENT DURING PHASE I WITH 2×10^6 LOAD APPLICATIONS

Slab Model	Support	Thick-ness (inches)	Column A	Column B	Column C	Column D
			Calculated Deflection for K = 255 pci (inches)	Calculated Deflection \times 30% for K = 255 pci (inches)	Calculated Deflection for K = 150 pci (inches)	Measured Deflection (inches)
L-5	Full	4	.0155	.0202		
177-1	High Void	4	.0324	.0420	.041	.041
177-2	Low Void	4	.0267	.0347	.035	.033
177-3	Low Void	2	.0654	.0850	.082	.09

$$1 \text{ pci} = 2.714 \times 10^5 \text{ N/M}^3$$

$$1 \text{ inch} = 2.54 \text{ cm}$$

The SLAB 177-1 with a 27×26 square inches void has a measured deflection of 0.041 inches as compared to the 0.0324 inch deflection computed. If we increase the computed deflections by 30 percent for all three slabs (177-1, 177-2 and 177-3) as shown in column B of Table 5.1, the measured and the computed deflections are very close, indicating an underprediction of the deflections due to an assigned input variable above or below the true value. As pointed out earlier, the subgrade support value, K, was obtained through loading a square-inches circular plate directly over the rubber support and calculating the load versus deflection ratio as opposed to the loading of the tested slabs in this experiment in which the load was transmitted to the rubber support through a 72×36 square-inches rectangular slab. The originally assigned K value of 225 pci, therefore, may not be a realistic value to use. The difficulty in securing a proper K value had long been recognized. Among others, the size and the shape of the loaded medium can affect the value of K. The primary objective of this experiment, however, is not to investigate the proper value for K but to test the effect of voids in CRC pavement systems. For this reason, the K value was adjusted until the measured deflection for one of the tested slabs (177-1) is comparable with the computed deflection. Then, the same K value was used for the other two slabs (177-2 and 177-3). Column C of Table 5.1 shows the computed deflection using a subgrade modulus of 150 pci. The results match quite well with the measured deflections in column D of Table 5.1.

Figure 5.1 gives the comparison of the maximum deflection for both the calculated deflection using a K value of 150 pci and the measured deflections along the axis (A - A') in the slab model 177-2. The measured deflection dropped off much more rapidly across the crack, indicating that a greater loss of load transfer is experienced than is modeled.

Slab Deterioration Predictions

In this section, a comparison is made between the predicted stresses and the crack development. In the first section the calculated stress levels along a longitudinal line of a slab are computed for various stages of the

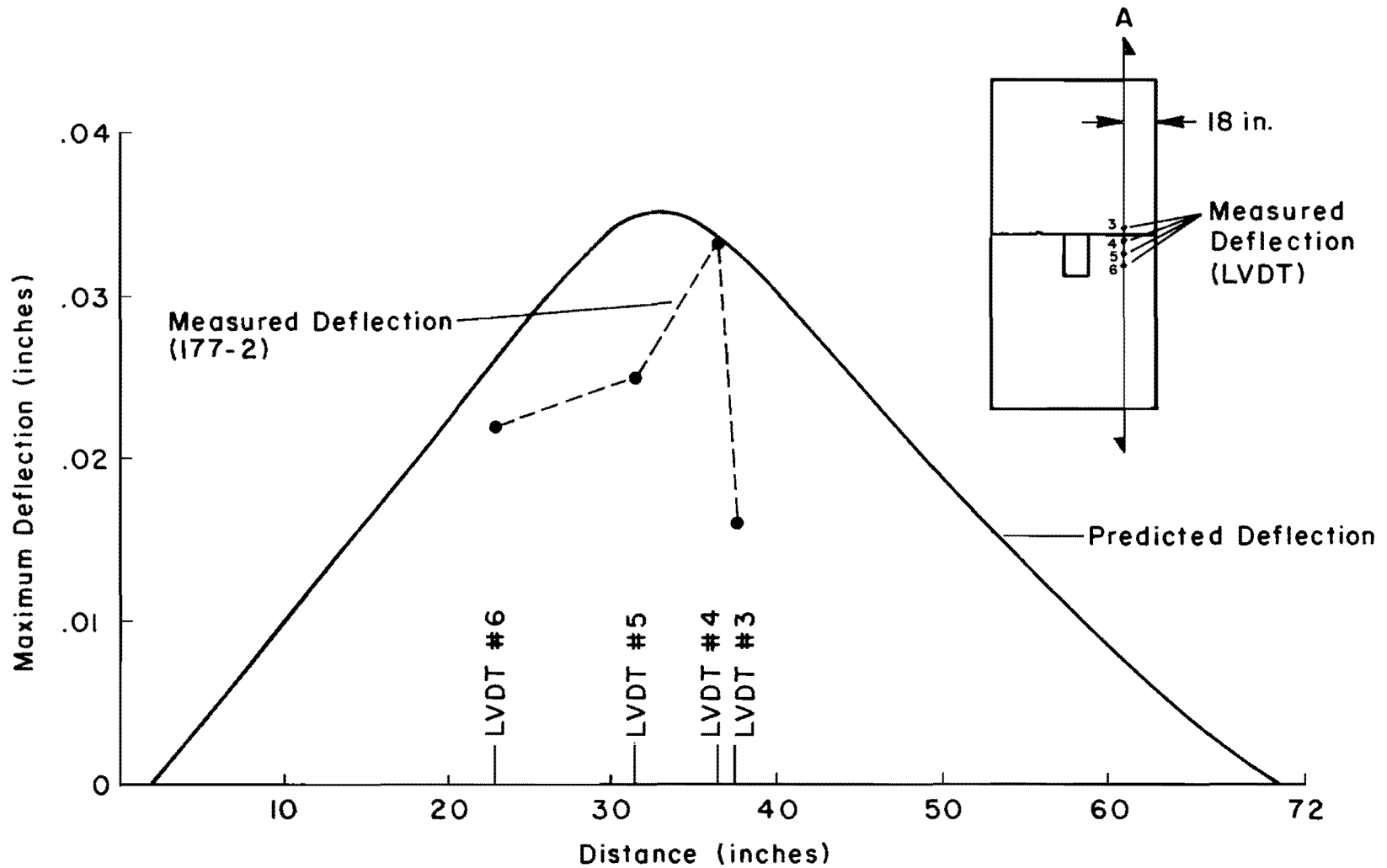


Fig 5.1. Comparison of calculated and measured deflection expressed as a percentage of the maximum value along the Axis A - A'.

crack development. In the second section, the calculated stress contours are compared with the slab crack pattern. For the first case, a comparison is made for all three slabs and, for the latter case, a comparison is made only for the laboratory slab model 177-2.

Calculated Stress Level and its Comparison with Principal Crack Development. Using the slab program, the presence of a discontinuity such as a crack or void can be simulated. Since it was apparent that the primary transverse cracks had a sequential order of development, an attempt was made to model these consecutively in using the slab program. Therefore an output of stress and deflection was obtained with the addition of each new crack. In Figs 5.2, 5.3, and 5.4 the longitudinal stress pattern is shown for each sequence of crack development for slabs 177-1, 177-2, and 177-3. These are computed along an axis A - A' which is over the void area, and along the line of the measured deflection. For each slab, a layout of the sequential order of the cracking as can best be determined from laboratory observations is shown. In some cases, it was difficult to ascertain at what point the bottom crack came into the slab. In several cases, an estimate of the sequential order was made. In all cases the first crack shown in the slab is the performed crack.

Modeling of the cracks were done by the procedure described in Ref 11 in which a certain percentage of the bending stiffness was removed from the cracked area for the simulation of the crack. Notice that the stresses predicted by the SLAB program are reasonable in magnitude for the first crack (the performed crack). However, for the second, the third and the fourth crack, the stresses predicted are enormously high, indicating that for the cracks that are closely spaced, the procedure described in Ref 11 may not be applicable.

Referring to Fig 5.2, the solid line shows the predicted stress distribution along the longitudinal axis with all of the first crack, the performed crack, in the slab. Note the high compression at the bottom of the slab between station 22 and station 30. This high compression on the bottom fibre, or high tensile stress on the top fibre of the slab, resulted crack number 2 and later crack number 4 to develop. Also, the high tensile stress at the bottom between stations 2 and 9 causes crack number 3 to form within this area.

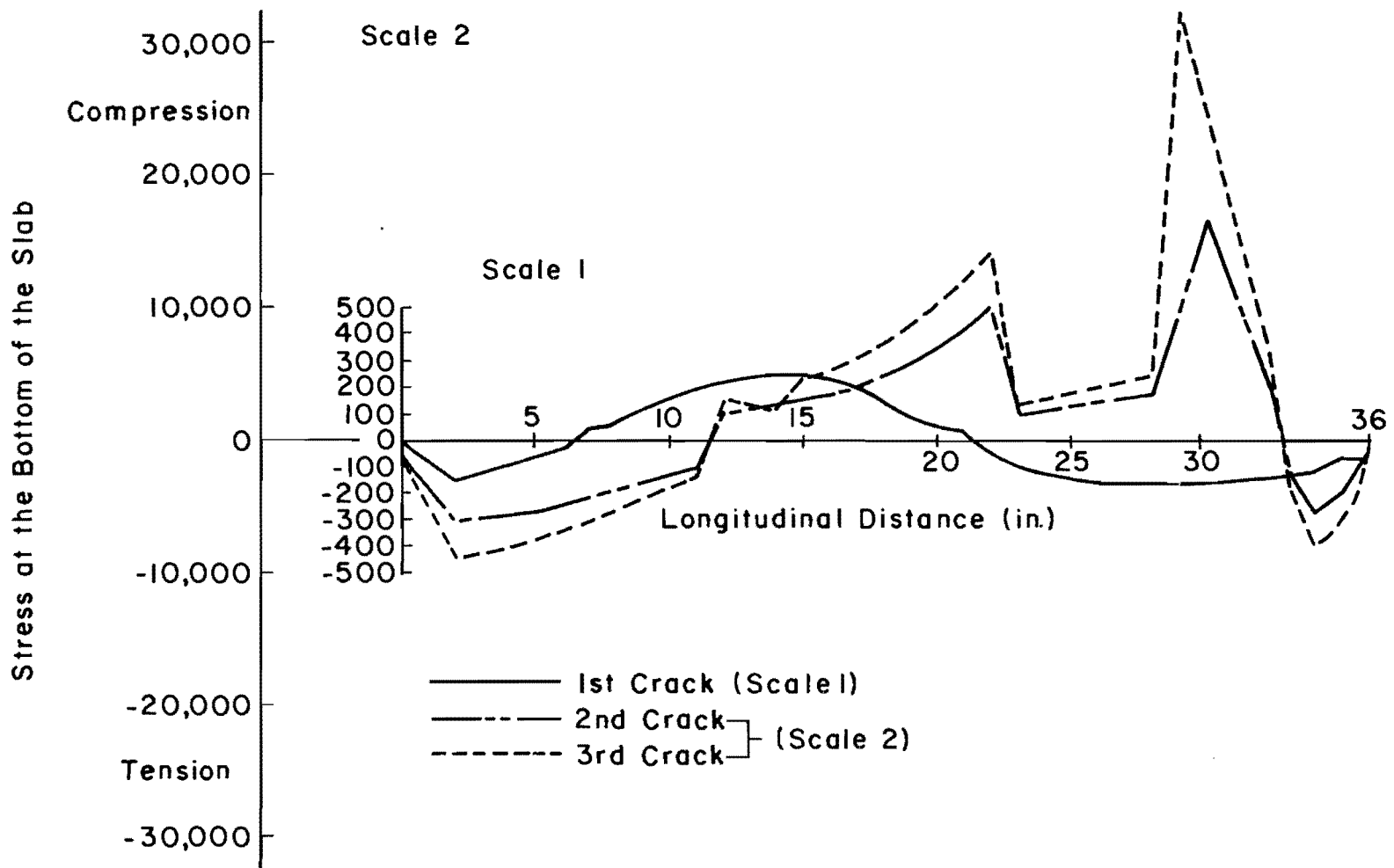


Fig 5.2. Slab model 177-1 calculated stress level according to the most important crack development.

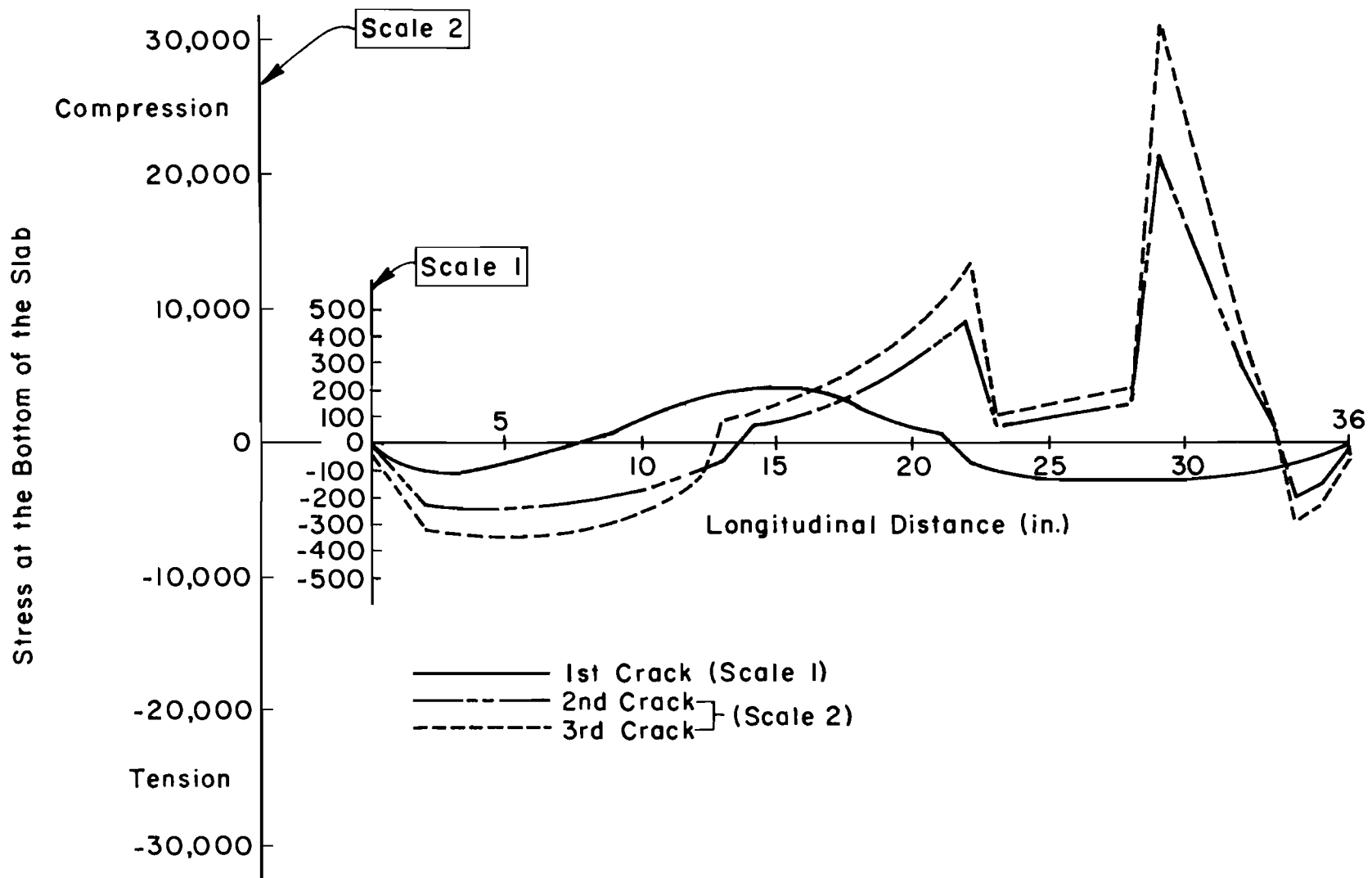


Fig 5.3. Slab model 177-2 calculated stress level for various levels of crack development for the more important cracks.

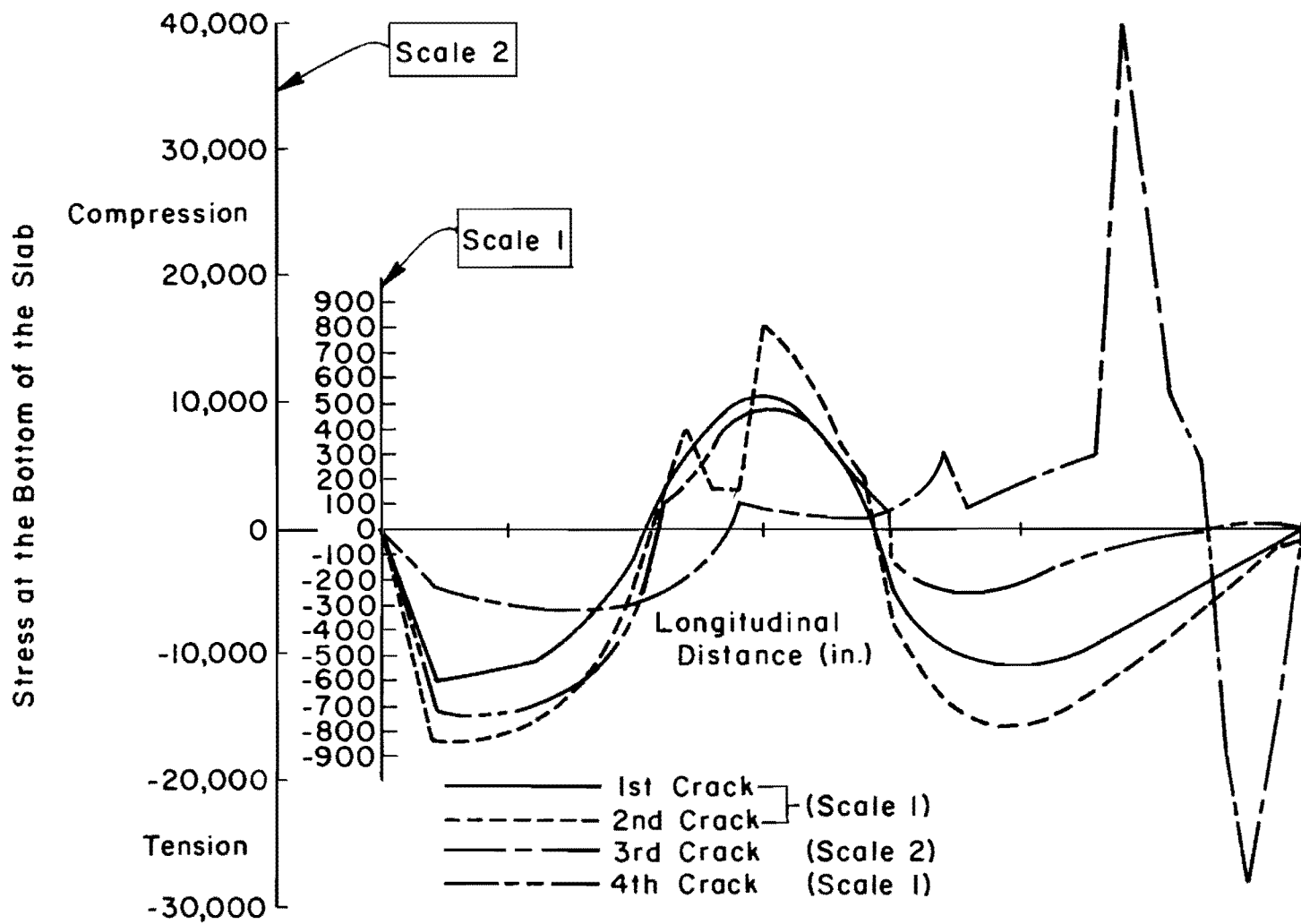


Fig 5.4. Slab model 177-3 calculated stress level for various levels of crack development for the more important cracks.

The crack development in slab 177-2 is very similar to the one previously described, only in this case, the fourth transverse crack did not form. There is a slight differential in stress distribution, but the results are very similar.

Using slab 177-3 stress distribution as shown in Fig 5.4, a slightly different sequence of events occurred. The second crack, in this case, occurred at station 15. Notice that the stress distributions on the loaded side of the preformed transverse crack are in high compression after the occurrence of both the first and second cracks. This causes the third transverse crack to occur in this area, starting from the top down. The fourth transverse crack occurs between station 12 and 13. This corresponds with the build-up of stresses that are occurring in this area.

Compression of Stress Contours With Crack Development. Using the output from the SLAB program, a stress profile can be plotted for both the top and the bottom of the slab. In this case, only the tensile stress at the bottom are shown since these are critical from the standpoint of cracking.

Figure 5.5 shows the predicted maximum tensile stress contours at the bottom of the slab 177-2, and it overlays the crack pattern at the bottom of the slab shown in Fig 4.9. Note that the high tensile stress in the bottom reflects the crack that occurs directly under the load. Furthermore, note the effect of the void; high tensile stresses are also at the edge of the slab in the area from 30 to 40 inches from the lower left-hand corner. On several of the slabs, where transverse cracking occurred on the load side of the preformed crack it appears that two cracks may have developed.

Crack Development with Load Applications

During the experiment, the number of applications was measured when the principal crack occurred and Table 5.2 gives the results. From the results, it can be pointed out that the earlier crack development occurred when the thickness was reduced, i.e., slab model 177-3 developed its first principal crack earlier than slab model 177-2. From these results it can be hypothesized that increases in thickness will prolong the life of CRC slabs and may be used as a method to account for conditions where voids may occur beneath the slab.

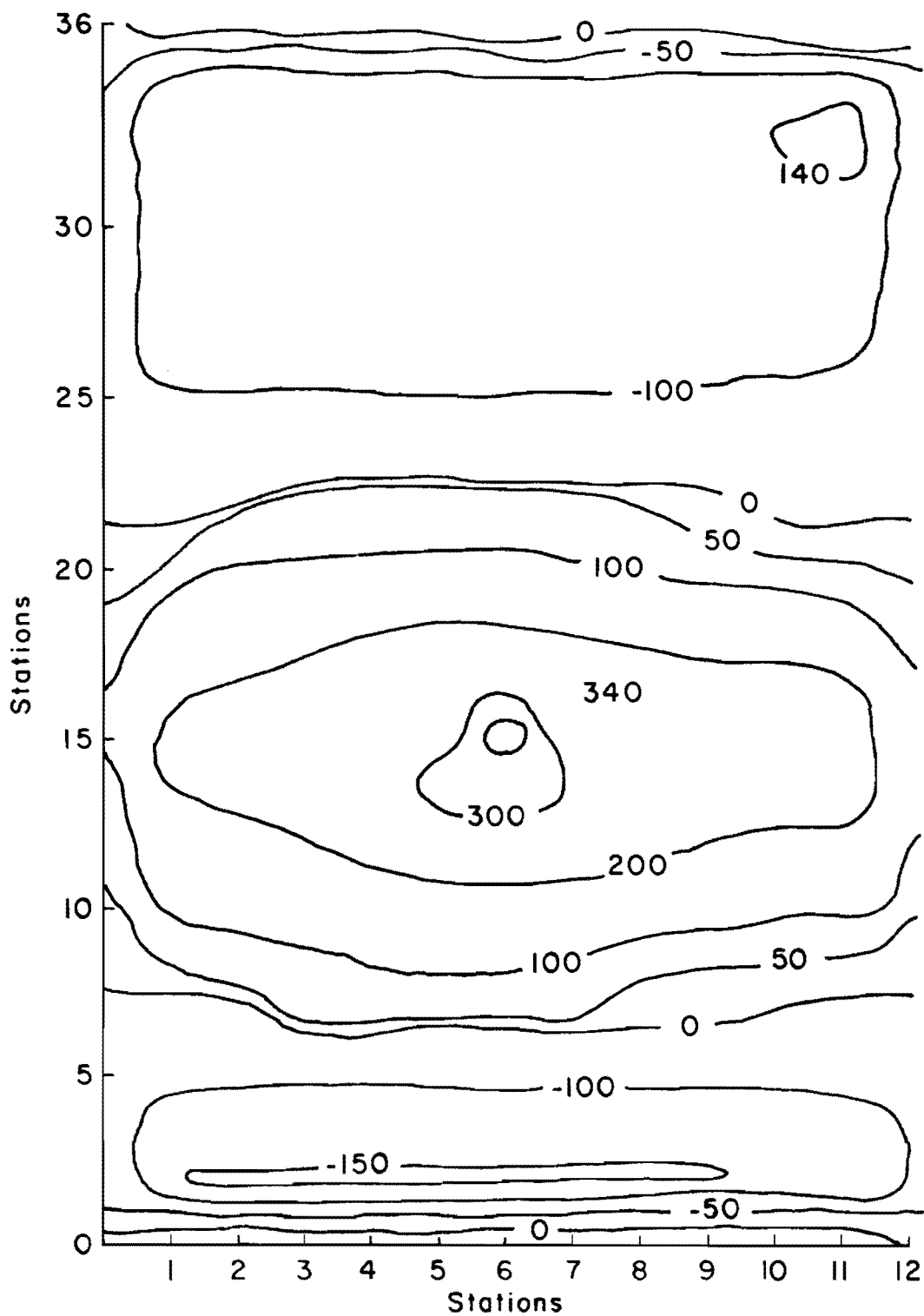


Fig 5.5. Predicted maximum stress contours at the bottom of the slab model 177-2.

TABLE 5.2. NUMBER OF LOAD APPLICATIONS APPLIED WHEN THE LARGEST AND DEEPEST CRACK OCCURS, AND ITS CONSECUTIVE APPEARANCE ORDER IN EACH LABORATORY SLAB MODEL.

Slab Model	1st crack (middle crack)	Number of applications ($\pm 50,000$)			
		2nd crack	3rd crack	4th crack	5th crack
177-1	0	950,000	2,350,000	3,900,000	
177-2	0	1,550,000			
177-3	0	120,000	1,250,000	2,150,000	2,950,000

CHAPTER 6. INTERPRETATION AND APPLICATION OF RESULTS

Various performance studies of in-service CRC pavements have shown small areas of concrete breakout with increasing traffic applications. Many of these breakouts coincide with voids beneath the pavement created by loss of material beneath the pavement due to water erosion or by soil movements, i.e., swell or settlement. In either case, a small void is created beneath the pavement and that eventually leads to an increased rate of pavement distress.

In the previous chapters, test results on scale model slabs revealed that voids beneath the portland cement pavement increased the rate of failure. The larger the void area beneath the pavement, the greater the rate of deterioration. These factors were also found to be applicable to the deflection of the slab, i.e., deflection increased with voids and decreased with the slab thickness.

In addition, it was shown that the points of cracking could be predicted by using the discrete-element program to predict stress concentrations in the slabs. The stress concentrations coincided with the points where cracking initiated. Furthermore, higher stress levels, and thus a greater rate of failure, were predicted with voids. Since the discrete-element method can be used to simulate the performance of the pavement slabs, design charts can be developed that take into account the effect of voids.

Considering the above, the purpose of this chapter is to demonstrate the feasibility of using test results such as presented in this report to develop design criteria. These design criteria may be then applied in design charts of procedures. In the following paragraphs, criteria for reducing the rate of load cracking, deflection criteria, and design chart applications are discussed.

Cracking Criteria

Figure 6.1 shows cracking as a function of the maximum slab deflection. These data were developed from the test slabs after four million applications

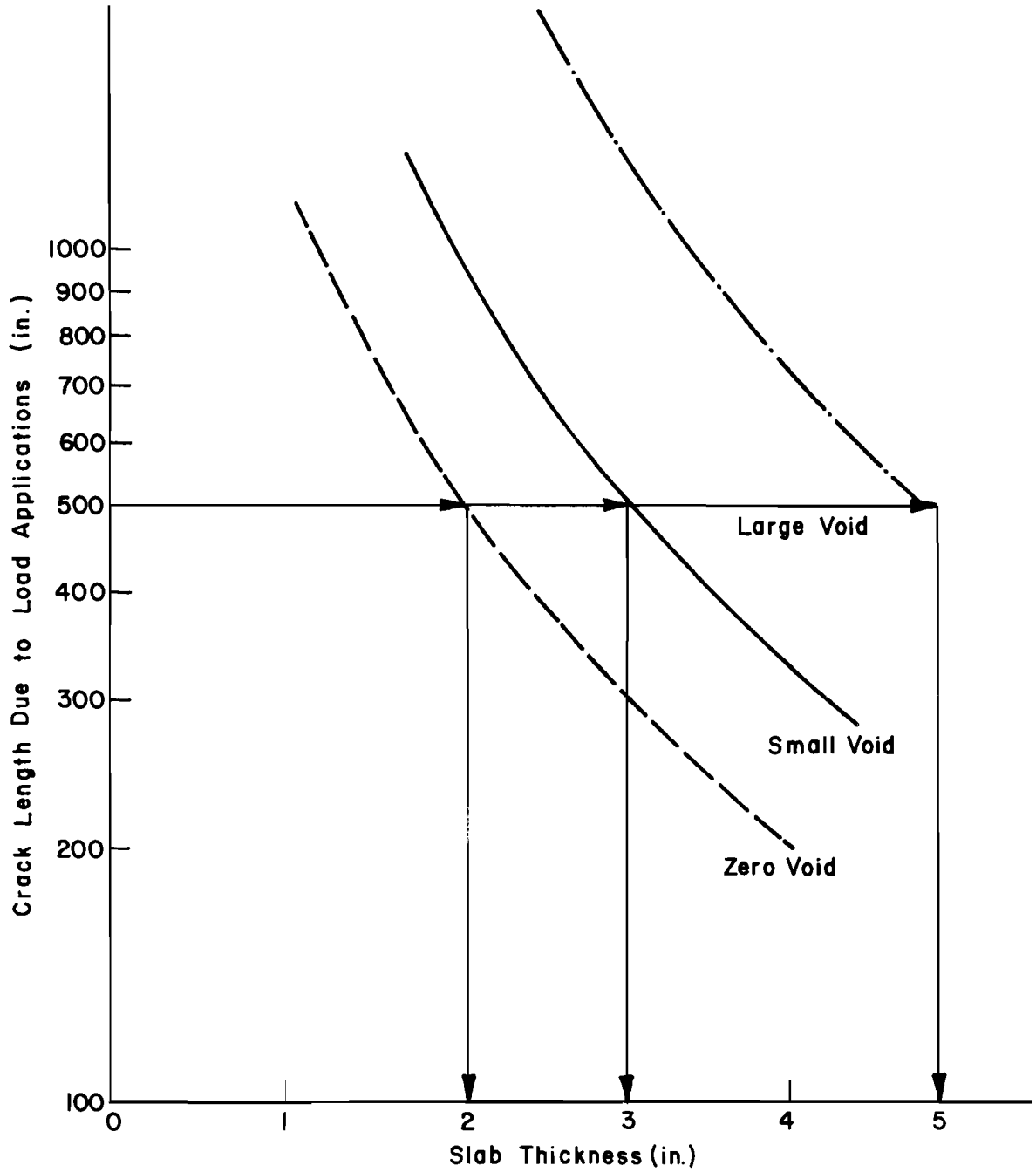


Fig 6.1. Illustrates the effect of slab thickness and void size on load cracking.

of equivalent 18-kip axle loads. The graph shows that as the pavement thickness increases, the linear length of load cracking after four million applications decreases. In addition, it shows that the larger a void beneath a pavement, the greater the rate of cracking for a given pavement thickness. The condition of zero void on the graph represents full pavement support, whereas small and large void conditions represent the conditions previously reported in the text. If we establish limit criteria of additional cracking due to load, for example, 500 linear inches of cracking beyond the initial volume change cracking, the required thicknesses can be determined. Note on the graph that, if the value 500 inches is projected horizontally to the various void lines, three different thicknesses are derived. These data are presented in Fig 6.1, which shows a thickness of 2 inches would be adequate for a zero void condition, whereas, for the severe condition of a large void beneath the pavement, 5 inches would be required for the pavement to last four million load applications. Thus, if voids are anticipated under the pavement due to any soil movement or subbase erosion, a thicker slab must be used. Applying these results to a subbase design, for example, one where a fully non-erosive subbase is used, shows that possibly a zero void condition exists, and thus a thinner concrete slab can be used. However, if an erosive subbase is used, or erosion is anticipated, a thicker slab must be used to obtain the same pavement life.

Also, if an area of high swelling clays is considered, the probability of voids beneath the pavement would be very high. Thus, a design curve with some degree of voids in the pavement should be used. In the past, it was assumed that a pavement had full support during its lifetime, but this may not be the case for in-service pavements. For example, recent studies by Machado et al found high swelling clay areas do have a much higher rate of pavement failures than non-swelling areas.

Deflection Criteria

Figure 6.2 shows maximum slab deflection as a function of pavement thickness for several support conditions. These graphs were also developed from the test results presented earlier. In this case, as was the case for cracking, the maximum deflection decreases as the slab thickness increases. Also, the deflection increases as the void size increases.

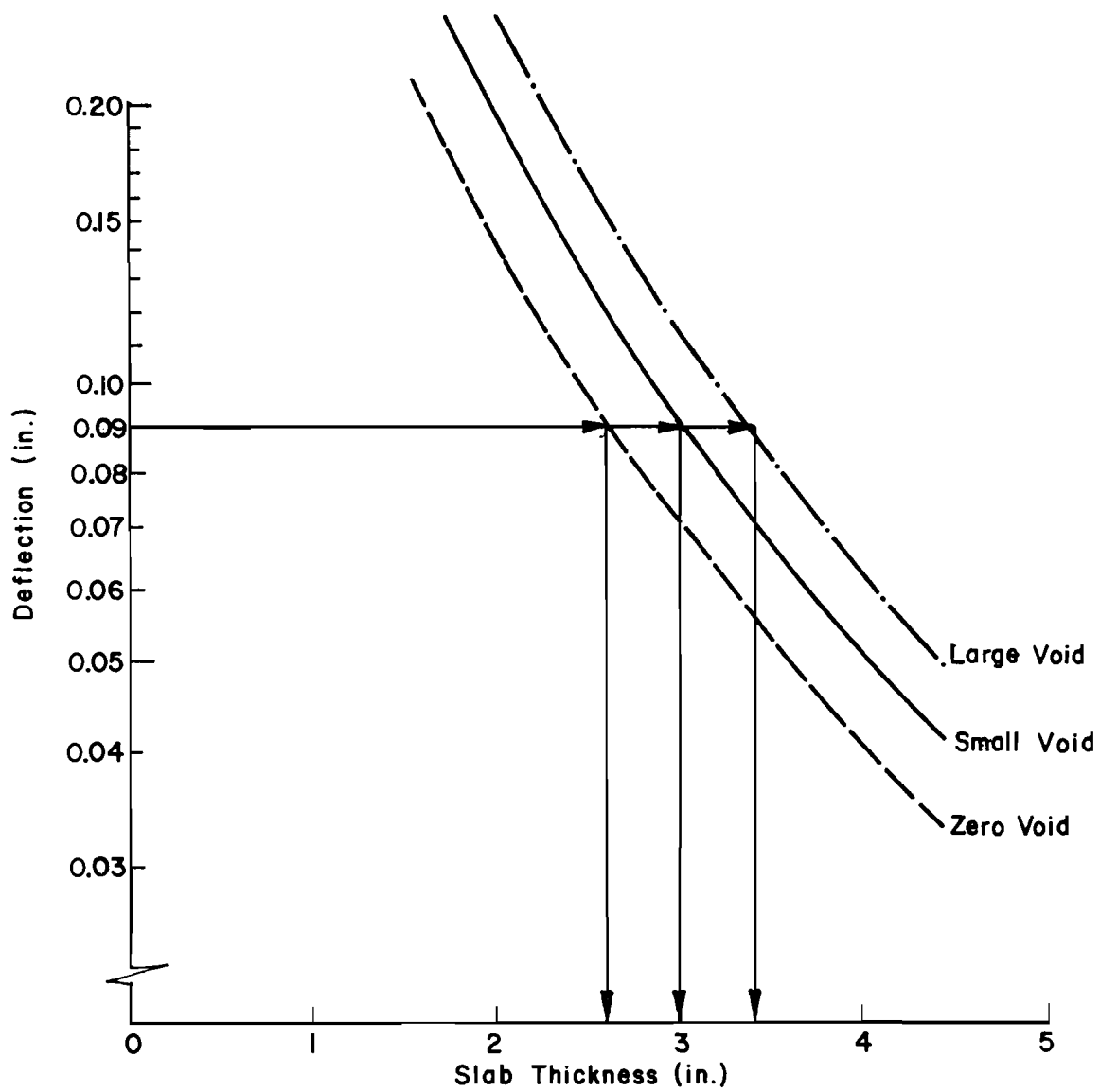


Fig 6.2. Illustrates the effect of slab thickness and void size on deflection.

If we were to establish a maximum allowable deflection in the slab, for example 0.09 inch, then we could enter the graph and project horizontally across to the various void conditions and arrive at the required slab thickness. These data are plotted in Fig 6.2, which shows that 2.6 inches of pavement thickness is required to zero voids, whereas, if large voids are anticipated under the pavement, 3.4 inches is required.

The interpretations developed in the previous sections for cracking criteria are also applicable here to deflection criteria. Thus, it is again emphasized that a pavement thickness should reflect the probability of voids developing beneath the pavement in order to design for an analysis period.

Design Applications

Figure 6.3 is a conceptual graph showing stress as a function of void areas for various pavement thicknesses. Using discrete-element theory as previously demonstrated in this report, a graph similar to that shown can readily be developed. Field studies of failure areas may be used to develop void area criteria. Thus, a designer could anticipate the relative void size that might be expected beneath the pavement during the life of the facility. These sizes may be related to different soil types, subbase types, or pavement grade line. Thus, enter an allowable stress value based on a fatigue equation, and the anticipated void area in the pavement into the graph, then the thickness required can be obtained. The designer may then want to investigate possible trade-offs in use of water ponding on a project to reduce the amount of, or probability of, voids beneath the slab. The other alternative would be to anticipate that the voids are going to exist and design for them. The designer could then investigate the cost trade-offs of these two alternatives and make a decision appropriately.

Summary

The data and concepts presented in this chapter demonstrate the need for revising design procedures to reflect real-world conditions that are experienced by in-service pavements. Design models and a limited criteria have been developed on the basis of laboratory studies. Thus, future data should be developed to revise the procedures as outlined in this chapter.

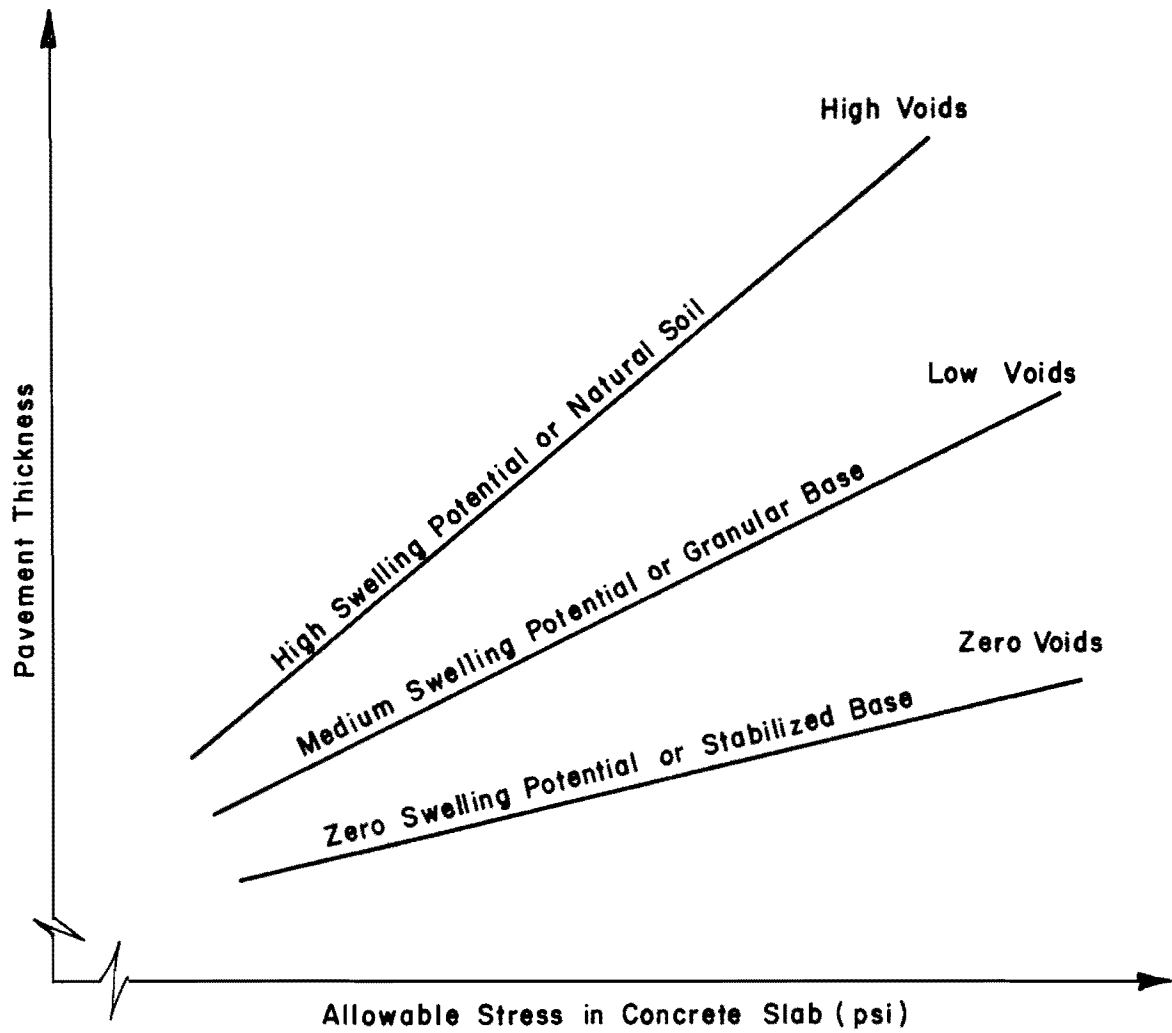


Fig 6.3. Conceptual pavement thickness design chart accounting for potential void conditions.

CHAPTER 7. OBSERVATIONS, CONCLUSIONS AND RECOMMENDATIONS

Observations

As previously discussed, the objective of the experiment was to observe the effect of nonuniform foundation support on CRC pavements and to simulate this condition in a laboratory study. Furthermore, the experiment itself is based on the results of actual laboratory slab models and the comparison with the theoretical solutions obtained through the SLAB 49 analysis computer program.

The slab model experiment results can be described as follows:

- (1) The deflections are affected when voids appear under the slab, and they also become greater as the void increases in size.
- (2) The deflections decrease when the thickness of the slab increases.
- (3) The crack development is greatly affected by the middle crack width level. Higher crack development occurred when the slabs were tested at a 0.04-inch crack width level.
- (4) To model cracks in rigid pavements, the procedure recommended in Ref 11 can be used to reduce the bending stiffness along the crack. For closely spaced cracks, however, such procedure seems to give erroneous results.

Conclusions

A discrete element analytical technique such as the SLAB 49 computer program, provides solutions to analyze and predict the CRC slab model performance. It has been observed during the experiment that slabs with smaller void size have less deterioration than slabs with bigger void. It was also observed that thinner slabs (2 inches thick) showed earlier deterioration when subjected to repeated load than thicker slabs (4 inches thick).

It can be concluded that both the theoretical solutions and the experimental laboratory results from the study of CRC pavements will assist in predicting pavement behavior when CRC pavements are subjected to repeated load. Also it can be concluded that the laboratory study will assist in future CRC pavement designs and evaluations.

Recommendations

The effect of voids can be incorporated into the design procedure. In addition, the sequence of cracking should also be considered in formulating the stresses for use in design. For example, using the SLAB program, the stress distribution in a full size slab could be predicted for various stages as the average crack spacing progresses from a wide value of approximately 15 feet to less than 2 feet. In addition, a random type crack spacing could also be investigated. These data could be used to establish the critical condition from a wheel load standpoint. Furthermore, the wheel load stress data for various crack patterns could be superimposed on stresses predicted from the CRCP-1 due to volume change effects of temperature and shrinkage. Thus, a crack pattern due to the coupled effect of wheel loads on the pavement and volume change stresses due to temperature and shrinkage could be predicted along with crack width and concrete stresses. An optimum design for pavement thickness, steels, and other factors could be predicted considering control criteria of crack width, steel stress, and concrete stress.

In areas where the probability of voids beneath a slab is high, a thicker slab should be used. Certainly this limited experiment has demonstrated that increased thickness would significantly reduce the deterioration that occurs with wheel load repetitions.

This study has opened up many potential areas of design that should be pursued fully; furthermore, additional lab studies may be used to evaluate the effectiveness of mud jacking and/or other techniques to restore the subbase support. Other effects on the slab life could be demonstrated.

REFERENCES

1. McCullough, B. F., Adnan Abou-Ayyash, W. R. Hudson, and J. P. Randall, "Design of Continuously Reinforced Concrete Pavements for Highways," National Cooperative Highway Research Program Project 1-15, Center for Highway Research, The University of Texas at Austin, August 1975.
2. W. R. Hudson, and Hudson Matlock, "Discontinuous Orthotropic Plates and Pavement Slabs," Research Report 56-6, Center for Highway Research, The University of Texas, Austin, May 1966.
3. Van Til, C. J., B. A. Vallerga, and R. G. Hicks, "Evaluation of AASHTO Interim Guides for Design of Pavement Structures," National Cooperative Highway Research Report 128, Highway Research Board, 1972.
4. Carey, W. N., Jr., and P. E. Irick, "The Pavement Serviceability-Performance Concept," Bulletin 250, Highway Research Board, January 1960.
5. Matlock, Hudson, W. R. Hudson, and Haliburton, "A Finite-Element Method of Solution for Linear-Elastic Beam-Columns," Research Report No. 56-1, Center for Highway Research, The University of Texas, Austin, 1960.
6. Hudson, W. R., "Concrete Pavement Load-Stresses at the AASHTO Road Test," Texas Highway Department, Departmental Research Report No. 62-2, 1962.
7. Packard, Robert G., "Design of Concrete Airport Pavement," Portland Cement Association, 1973.
8. "Design and Control of Concrete Mixtures," Eleventh Edition, Portland Cement Association, 1968.
9. "Thickness Design for Concrete Pavements," Portland Cement Association, 1966.
10. B. Frank McCullough, "Design Manual for Continuously Reinforced Concrete Pavement," United States Steel Corporation, Pittsburgh, Pennsylvania, August 1968.
11. Abou-Ayyash, Adnan, and W. R. Hudson, "Analysis of Bending Stiffness Variations at Cracks in Continuous Pavements," Research Report 56-22, Project 3-5-63-56, Center for Highway Research, The University of Texas at Austin, April 1972.

APPENDIX 1

DATA FOR LABORATORY SLAB MODEL L-5

TABLE A1.1. CRACKING AND DEFLECTION DATA FOR THE LABORATORY SLAB MODEL L-5 AND ITS COMPARISON WITH THE LABORATORY SLAB MODEL 177-2.

Observations	Slab Model L-5
Measured maximum deflection at 0.01-inch crack width level	0.05 in.
Measured maximum deflection at 0.04-inch crack width level	0.062 in.
Total crack length	207 in.
Thickness	4 in.
Level of void	No void

APPENDIX 2

COMPUTER OUTPUT FOR THE SLAB MODEL 177-2

APPENDIX 2. COMPUTER OUTPUT FOR THE SLAB MODEL 177-2

Input Data

To simulate the performance of the laboratory slab model through the SLAB 49 computer program, the following data were introduced in an effort to maintain as nearly as possible the physical conditions of the laboratory CRC slab.

Thickness	=	4 inches
Modulus of elasticity of concrete	=	4×10^6 psi
Percent steel reinforcement	=	0.55 percent
Steel reinforcement position	=	mid-depth
Poisson's ratio	=	0.25

Input variables are calculated as follows:

(1) Bending stiffness

$$D^x = D^y = \frac{Et^3}{12(1-\nu)^2}$$

where,

$$\begin{aligned} E &= 4 \times 10^6 \text{ psi} \\ \nu &= 0.25 \\ t &= 4 \text{ inches} \end{aligned}$$

Therefore,

$$D^x = D^y = \frac{4 \times 10^6 t^3}{12(1-0.25^2)}$$

For slab 177-2,

$$\begin{aligned} 1/4 D^x &= 1/4 \frac{4 \times 10^6 \times 4^3}{12(1-0.25^2)} \\ &= \underline{5,689 \times 10^6} \text{ lb} \cdot \text{in.}^2/\text{in.} \end{aligned}$$

(2) End Support

A pulling mechanism at two ends of the slab was used during the testing to simulate the horizontal forces in the slab. Also, two hold down beams with four bolt connectors, tightened to finger tip tightness on the test slab, was placed on both ends to simulate the continuity of the slab in real pavements. Large spring support value was used to model these two ends where,

$$S_{\text{end}} = \underline{1.5 \times 10^5} \text{ pci}$$

(3) Interior Support

A series of plate loading tests were performed on various thicknesses of rubber to obtain modulus of subgrade support value (NCHRP 1-15). The results of these tests indicated that a six-inch thick rubber mat has a modulus of subgrade reaction of 255 pci. Note that during the actual 177-slab test, the load was applied on the concrete slab and not directly on the rubber mat. Therefore, the K value of 255 pci used here is underestimating the real K value somewhat.

$$1/4 S_{\text{int}} = 1/4 (255 \times 3 \text{ in.} \times 2 \text{ in.}) = \underline{382.5} \text{ lb/in.}$$

(4) Twisting Stiffness

$$\begin{aligned} C^t &= \frac{Et^3}{12(1+\mu)} \\ &= \frac{4 \times 10^6 \times 4^3}{12(1+0.25)} \\ &= \underline{1.7067 \times 10^7} \text{ lb} \cdot \text{in.}^2/\text{in.} \end{aligned}$$

(5) Loads

A vertical load of 5,000 pounds was applied over a loading plate during the testing. The area of the plate is 72 square inches. Therefore,

$$\text{Load per sq. in.} = \frac{5000}{72} \text{ psi} = 69.44 \text{ psi}$$

$$\begin{aligned} \text{Load per increment} &= 69.44 \times 2'' \times 3'' \\ &= 416.67 \text{ lb,} \end{aligned}$$

$$\text{Load for 1/2 increment} = \underline{208.33} \text{ lb,}$$

(6) Voids

For slab 177-1,

$$\text{High void, area} = 27'' \times 26''$$

For slab 177-2 and 177-3,

$$\text{Low void, area} = 27'' \times 16''$$

(7) Crack Simulation

The bending stiffness, D^y , along the crack is reduced based on the moment curvature concept present in Ref 11. For,

$$\text{Steel percentage, } P = 0.55 \text{ percent}$$

$$\text{Conc. Comp. Strength, } f'_c = \left(\frac{E_c}{57,400} \right)^2 = 4856 \text{ psi}$$

From Ref 11, Fig 10, percentage reduction in bending stiffness is 89.5 percent. Therefore,

$$\text{Reduction in } D^y = 0.895 D^y$$

For slab 177-2,

$$\begin{aligned} \text{Reduction in } D^y &= -(2,276 \times 10^7 \times 0,895) \\ &= \underline{\underline{-2,036 \times 10^7}} \end{aligned}$$

Width along which to apply the stiffness reduction for,

$$\phi = \underline{.5 \text{ inch}}$$

$$A_s = \underline{.2 \text{ inch}^2}$$

$$\text{Perimeter, } P = 1.571 \text{ inches}$$

$$\text{Bond stress allowable, } u = \frac{3.4 \sqrt{f'_c}}{\phi} = \frac{3.4 \sqrt{4856}}{.5} = 473.86$$

$$L = 2 \frac{A_s f_s}{u p} = 2 \frac{(.2)(24,000)}{473.86 \times 1.571} = \underline{\underline{12.89''}}$$

where,

f_s = allowable steel tensile stress

p = bar perimeter

u = bond stress

A_s = bar area

Since increment length in y-direction is two inches long, the bending stiffness, D^y , reduced by 89.5 percent over six increments should be satisfactory.

Output Data

The most important data required to analyze the performance of the laboratory slab test results are deflections and stresses. The calculated deflection data along line A - A' (Fig A2.1) are compared with the measured deflection data in the laboratory slab (LVDT measurements).

The calculated stress level along line A - A' (Fig A2.1), and the maximum stress contours levels are compared with the distress development in the laboratory slab.

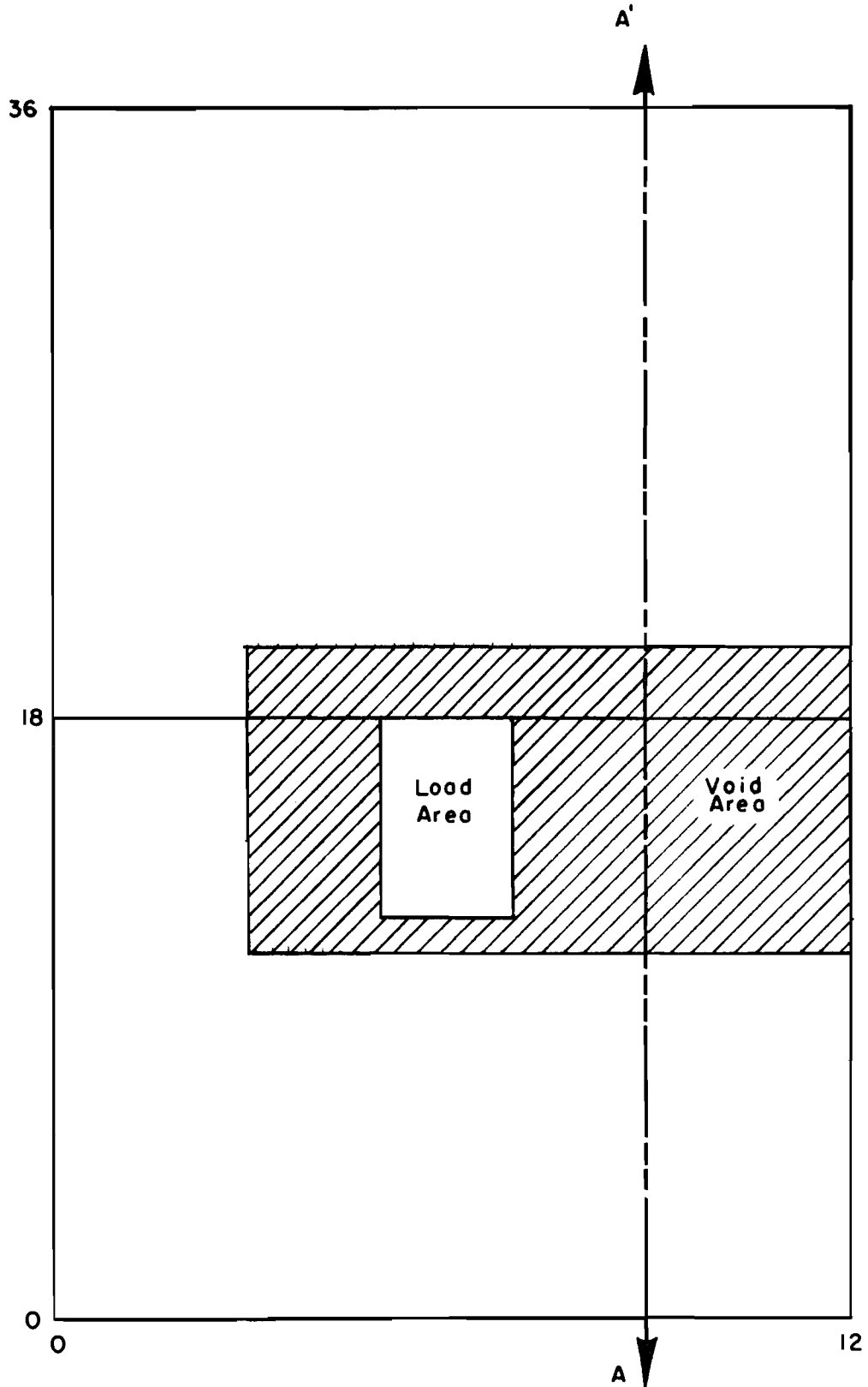


Fig A2.1 Plan view of line where deflections and stresses were predicted by the SLAB program.

PROGRAM SLAB 49 -DEVELOPMENT DECK- MATLOCK,PANAK, ENDRES REV DATE 13 JUL 71

```

. . . . .
;
; THIS PROGRAM IS BEING USED AT YOUR OWN RISK.
; CHANGES MAY OCCUR AFTER THE ABOVE REVISION DATE.
; PLEASE REPORT DIFFICULTIES TO THE ABOVE PEOPLE
; AT THE CENTER FOR HIGHWAY RESEARCH, UT AT AUSTIN.
;
. . . . .

```

SLAB 177-2, LOW VOID, THICK SLAB
VOID SIZE = 27 * 16 80.IN., THICKNESS = 4 IN.

PROB
1 FIRST CRACK, 89.5 PERCENT RED, FOR 6 STATIONS.

TABLE 1. CONTROL DATA

	TABLE NUMBER							
	2	3	4	5	6	7	8	9
KEEP FROM PRECEDING PROBLEM (1=YES)	0	0	0	0	0	0	0	0
NUM CARDS INPUT THIS PROBLEM	1	19	0	1	0	2	2	3
MULTIPLE LOAD OPTION	1							
STATICS CHECK OPTION	1							
PRIN STRESS OPTION	1							
PROFILE PLOT OPTION	0							
3-D PLOT OPTION	0							

TABLE 2. CONSTANTS

NUMBER OF INCREMENTS IN X DIRECTION	12
NUMBER OF INCREMENTS IN Y DIRECTION	36
INCREMENT LENGTH IN X DIRECTION	3.000E+00
INCREMENT LENGTH IN Y DIRECTION	2.000E+00
POISSONS RATIO	2.500E-01
SLAB THICKNESS	4.000E+00

TABLE 3. JOINT STIFFNESS AND LOAD DATA

FROM JOINT	THRU JOINT	DX	DY	FX	FY	Q	S
0	0 12 36	5.689E+06	5.689E+06	-0	-0	-0	2.250E+02
0	1 12 35	5.689E+06	5.689E+06	-0	-0	-0	2.250E+02
1	0 11 36	5.689E+06	5.689E+06	-0	-0	-0	2.250E+02
	1 11 35	5.689E+06	5.689E+06	-0	-0	-0	2.250E+02
	11 12 19	-0	-0	-0	-0	-0	-9.000E+02
0	0 12 2	-0	-0	-0	-0	-0	1.500E+05
0	34 12 36	-0	-0	-0	-0	-0	1.500E+05
0	15 12 15	-0	-1.018E+07	-0	-0	-0	-0
1	15 11 15	-0	-1.018E+07	-0	-0	-0	-0
0	16 12 16	-0	-1.018E+07	-0	-0	-0	-0

1	16	11	16	-P	-1.018E+07	-P	-0	-0	-0	-0
0	17	12	17	-Q	-1.018E+07	-0	-0	-0	-0	-0
1	17	11	17	-V	-1.018E+07	-V	-0	-0	-0	-0
0	18	12	18	-0	-1.018E+07	-0	-0	-0	-0	-0
	18	11	18	-0	-1.018E+07	-0	-0	-0	-0	-0
	19	12	19	-0	-1.018E+07	-0	-0	-0	-0	-0
1	19	11	19	-0	-1.018E+07	-V	-0	-0	-0	-0
0	20	12	20	-0	-1.018E+07	-0	-0	-0	-0	-0
1	20	11	20	-0	-1.018E+07	-0	-0	-0	-0	-0

TABLE 4. JOINT STIFFNESS AND LOAD DATA CONTD

FROM JOINT	THRU JOINT		RX	RY	TX	TY
		NONE				

TABLE 5. MESH STIFFNESS DATA

FROM MESH	THRU MESH	C	
1	1 12 36	1.707E+07	

TABLE 6. BAR STIFFNESS DATA

FROM BAR	THRU BAR		PX	PY	PBX	PHY
		NONE				

TABLE 7. MULTIPLE LOAD DATA

FROM JOINT	THRU JOINT		QM
5	12 7 17		2.083E+02
6	12 6 17		2.083E+02

TABLE 8. PROFILE OUTPUT AREAS

FROM JOINT	THRU JOINT	DEFL (1=YES)	X MOMENT (1=SLAB, 2=BEAM)	Y MOMENT	PRIN MOM OR STRESS (1=YES)
9	0 9 36	1	1	1	1
0	15 12 15	1	1	1	1

TABLE 9. PRINTED OUTPUT LIMITS

FROM Y STA	THRU Y STA	
		NONE

PROGRAM SLAB 49 -DEVELOPMENT DECK- MATLOCK,PANAK, ENDRES REV DATE 13 JUL 71

```

. . . . .
. THIS PROGRAM IS BEING USED AT YOUR OWN RISK.
. CHANGES MAY OCCUR AFTER THE ABOVE REVISION DATE.
. PLEASE REPORT DIFFICULTIES TO THE ABOVE PEOPLE
. AT THE CENTER FOR HIGHWAY RESEARCH, UT AT AUSTIN.
.
. . . . .
    
```

SLAB 177-2, LOW VOID, THICK SLAB
 VOID SIZE = 27 * 16 80,IN., THICKNESS = 4 IN.

PROB (CONTD)

1 FIRST CRACK, A9.5 PERCENT RED, FOR 6 STATIONS.

RFSULTS

SLAB X MOMENT AND X TWISTING MOMENT ACT IN THE X DIRECTION (ABOUT Y AXIS)
 Y TWISTING MOMENT = -X TWISTING MOMENT, COUNTERCLOCKWISE BETA ANGLES ARE
 POSITIVE FROM THE X AXIS TO THE DIRECTION OF THE LARGEST PRINCIPAL STRESS
 SLAB MOMENTS ARE PER UNIT WIDTH

X , Y	DEFL	SLAB X MOMENT	SLAB Y MOMENT	SLAB X TWISTING MOMENT	LARGEST PRINCIPAL SLAB STRESS	BETA X TO LARGEST STRESS	STATICS CHECK
0 36	1.680E-03	6.031E-12	5.702E-11	2.596E+01	9.736E+00	45.0	-4.384E-10
1 36	1.594E-03	3.304E+01	-1.140E-10	4.057E+01	2.262E+01	33.9	2.417E-09
2 36	1.537E-03	3.242E+01	1.097E-10	4.023E+01	2.234E+01	34.0	-1.536E-09
3 36	1.506E-03	2.387E+01	2.194E-11	3.025E+01	1.950E+01	36.3	4.484E-10
4 36	1.496E-03	1.470E+01	-1.315E-11	3.441E+01	1.595E+01	39.0	-1.255E-10
5 36	1.498E-03	7.385E+00	3.948E-11	2.910E+01	1.238E+01	41.4	2.419E-10
6 36	1.506E-03	2.669E+00	-7.456E-11	2.278E+01	9.059E+00	43.3	2.474E-10
7 36	1.517E-03	6.475E+01	2.632E-11	1.584E+01	6.063E+00	44.4	3.274E-10
8 36	1.528E-03	1.235E+00	7.018E-11	8.496E+00	3.426E+00	42.9	-9.250E-10
9 36	1.540E-03	4.190E+00	1.755E-11	7.492E+01	1.620E+00	9.8	1.234E-09
10 36	1.555E-03	8.661E+00	9.649E-11	-7.807E+00	4.972E+00	-30.5	2.638E-10
11 36	1.578E-03	1.153E+01	-3.068E-11	-1.853E+01	9.440E+00	-36.4	8.185E-12
12 36	1.611E-03	9.321E-12	2.083E-11	-1.993E+01	7.474E+00	-45.0	9.823E-11
0 35	2.848E-04	-1.651E-10	-6.927E+01	5.780E+01	-3.826E+01	-60.5	1.458E-09
1 35	1.691E-04	3.180E+01	-1.502E+02	8.640E+01	-6.926E+01	-68.2	-3.386E-09
2 35	8.266E-05	2.868E+01	-1.546E+02	8.037E+01	-6.932E+01	-69.4	3.170E-09
3 35	2.462E-05	1.307E+01	-1.588E+02	7.537E+01	-7.020E+01	-69.4	-1.982E-09
35	-1.116E-05	-3.743E+00	-1.631E+02	6.776E+01	-7.049E+01	-69.8	1.430E-09
35	-3.131E-05	-1.733E+01	-1.667E+02	5.753E+01	-6.987E+01	-71.2	-2.300E-10
6 35	-4.120E-05	-2.620E+01	-1.697E+02	4.539E+01	-6.856E+01	-73.8	-1.613E-09
7 35	-4.424E-05	-3.002E+01	-1.720E+02	3.206E+01	-6.707E+01	-77.8	2.460E-10
8 35	-4.181E-05	-2.875E+01	-1.739E+02	1.803E+01	-6.604E+01	-83.0	6.870E-10
9 35	-3.317E-05	-2.252E+01	-1.761E+02	3.349E+00	-6.607E+01	-88.8	-8.616E-10
10 35	-1.545E-05	-1.227E+01	-1.799E+02	-1.294E+01	-6.785E+01	85.6	-1.011E-09

11	35	1.606E-05	-1.637E+00	-1.873E+02	-3.493E+01	-7.262E+01	79.7	9.775E-10
12	35	6.664E-05	-6.025E-12	-9.859E+01	-3.987E+01	-4.226E+01	70.5	-2.002E-10
0	34	-1.137E-03	3.570E-11	-1.673E+02	5.239E+01	-6.838E+01	-74.0	-5.457E-11
	34	-1.286E-03	1.412E+00	-3.133E+02	8.655E+01	-1.258E+02	-75.6	-1.637E-11
	34	-1.402E-03	-7.295E+00	-3.143E+02	8.100E+01	-1.254E+02	-76.1	-2.154E-09
3	34	-1.487E-03	-2.199E+01	-3.199E+02	7.602E+01	-1.268E+02	-76.5	1.992E-10
4	34	-1.548E-03	-3.703E+01	-3.262E+02	6.851E+01	-1.281E+02	-77.3	-4.666E-10
5	34	-1.591E-03	-4.928E+01	-3.321E+02	5.842E+01	-1.289E+02	-78.8	3.647E-10
6	34	-1.619E-03	-5.743E+01	-3.370E+02	4.648E+01	-1.292E+02	-80.8	-4.366E-11
7	34	-1.636E-03	-6.104E+01	-3.411E+02	3.349E+01	-1.294E+02	-83.3	-1.275E-09
8	34	-1.643E-03	-5.987E+01	-3.447E+02	2.012E+01	-1.298E+02	-86.0	-1.537E-10
9	34	-1.638E-03	-5.372E+01	-3.489E+02	6.778E+00	-1.309E+02	-88.7	6.421E-10
10	34	-1.619E-03	-4.248E+01	-3.559E+02	-6.728E+00	-1.335E+02	88.8	-1.680E-09
11	34	-1.581E-03	-2.582E+01	-3.720E+02	-2.213E+01	-1.400E+02	86.4	-3.465E-10
12	34	-1.515E-03	3.683E-11	-2.105E+02	-2.281E+01	-7.984E+01	83.9	-8.722E-10
0	33	-2.621E-03	4.979E-11	-1.668E+02	4.169E+01	-6.625E+01	-76.7	-1.430E-10
1	33	-2.800E-03	-7.796E-01	-3.284E+02	8.257E+01	-1.305E+02	-76.6	-7.211E-10
2	33	-2.945E-03	-8.191E+00	-3.288E+02	8.078E+01	-1.302E+02	-76.6	1.565E-09
3	33	-3.058E-03	-1.978E+01	-3.307E+02	7.673E+01	-1.307E+02	-76.9	-2.431E-10
4	33	-3.145E-03	-3.175E+01	-3.347E+02	6.962E+01	-1.312E+02	-77.7	-2.760E-09
5	33	-3.210E-03	-4.170E+01	-3.391E+02	5.976E+01	-1.315E+02	-79.1	-1.394E-09
6	33	-3.257E-03	-4.851E+01	-3.433E+02	4.803E+01	-1.316E+02	-81.0	1.007E-09
7	33	-3.289E-03	-5.164E+01	-3.472E+02	3.541E+01	-1.318E+02	-83.3	6.666E-10
8	33	-3.305E-03	-5.072E+01	-3.512E+02	2.281E+01	-1.323E+02	-85.7	-1.824E-09
9	33	-3.306E-03	-4.539E+01	-3.562E+02	1.106E+01	-1.337E+02	-88.0	1.105E-09
10	33	-3.288E-03	-3.537E+01	-3.639E+02	8.850E+00	-1.364E+02	-89.8	-7.863E-10
11	33	-3.247E-03	-2.058E+01	-3.769E+02	-6.498E+00	-1.414E+02	89.0	-2.854E-09
12	33	-3.175E-03	1.501E-11	-1.983E+02	-3.382E+00	-7.438E+01	89.8	-1.404E-09
	32	-4.167E-03	-1.116E-10	-1.691E+02	4.081E+01	-6.692E+01	-77.1	-1.598E-09
1	32	-4.375E-03	-2.666E+00	-3.367E+02	8.107E+01	-1.332E+02	-77.1	-1.799E-09
2	32	-4.549E-03	-8.712E+00	-3.368E+02	8.021E+01	-1.333E+02	-77.0	-2.593E-09
3	32	-4.690E-03	-1.700E+01	-3.386E+02	7.689E+01	-1.335E+02	-77.2	1.483E-09
4	32	-4.803E-03	-2.604E+01	-3.416E+02	7.032E+01	-1.337E+02	-78.0	4.281E-09
5	32	-4.892E-03	-3.416E+01	-3.452E+02	6.086E+01	-1.338E+02	-79.3	5.910E-10
6	32	-4.958E-03	-3.968E+01	-3.488E+02	4.946E+01	-1.337E+02	-81.1	-8.183E-09
7	32	-5.004E-03	-4.249E+01	-3.524E+02	3.727E+01	-1.338E+02	-83.2	-3.671E-09
8	32	-5.031E-03	-4.214E+01	-3.561E+02	2.548E+01	-1.343E+02	-85.4	1.729E-09
9	32	-5.038E-03	-3.812E+01	-3.608E+02	1.516E+01	-1.356E+02	-87.3	-1.215E-09
10	32	-5.024E-03	-3.003E+01	-3.673E+02	7.263E+00	-1.378E+02	-88.8	8.098E-10
11	32	-4.983E-03	-1.766E+01	-3.766E+02	2.706E+00	-1.412E+02	-89.6	-5.415E-09
12	32	-4.910E-03	1.032E-10	-1.937E+02	1.273E+00	-7.262E+01	-89.6	4.766E-10
0	31	-5.777E-03	-2.638E-11	-1.709E+02	4.006E+01	-6.730E+01	-77.4	2.607E-10
1	31	-6.014E-03	-3.734E+00	-3.402E+02	8.028E+01	-1.344E+02	-77.2	-5.543E-09
2	31	-6.215E-03	-8.539E+00	-3.409E+02	7.995E+01	-1.347E+02	-77.2	5.438E-09
3	31	-6.385E-03	-1.458E+01	-3.428E+02	7.716E+01	-1.350E+02	-77.4	-2.778E-09
4	31	-6.524E-03	-2.079E+01	-3.456E+02	7.106E+01	-1.352E+02	-78.2	-2.822E-09
5	31	-6.636E-03	-2.629E+01	-3.489E+02	6.193E+01	-1.351E+02	-79.5	-6.304E-09
6	31	-6.722E-03	-3.056E+01	-3.521E+02	5.076E+01	-1.350E+02	-81.2	1.337E-08
7	31	-6.784E-03	-3.320E+01	-3.552E+02	3.889E+01	-1.350E+02	-83.2	-8.332E-10
8	31	-6.822E-03	-3.369E+01	-3.584E+02	2.773E+01	-1.353E+02	-85.2	-8.088E-09
9	31	-6.837E-03	-3.132E+01	-3.621E+02	1.850E+01	-1.362E+02	-86.8	1.632E-09
10	31	-6.826E-03	-2.541E+01	-3.671E+02	1.211E+01	-1.378E+02	-88.0	1.880E-09
11	31	-6.788E-03	-1.533E+01	-3.736E+02	9.071E+00	-1.402E+02	-88.6	1.883E-09
12	31	-6.717E-03	3.313E-10	-1.905E+02	4.746E+00	-7.148E+01	-88.6	-3.490E-09
0	30	-7.451E-03	-2.738E-10	-1.698E+02	3.922E+01	-6.690E+01	-77.6	2.544E-09
1	30	-7.715E-03	-4.090E+00	-3.389E+02	7.977E+01	-1.339E+02	-77.3	-3.740E-10
2	30	-7.946E-03	-7.551E+00	-3.400E+02	8.015E+01	-1.344E+02	-77.1	-4.832E-09

3	30	-8.143E-03	-1.102E+01	-3.424E+02	7.789E+01	-1.349E+02	-77.4	5.594E-09
4	30	-8.309E-03	-1.442E+01	-3.455E+02	7.214E+01	-1.352E+02	-78.2	9.385E-09
5	30	-8.444E-03	-1.765E+01	-3.489E+02	6.313E+01	-1.352E+02	-79.6	-1.131E-08
6	30	-8.550E-03	-2.068E+01	-3.520E+02	5.195E+01	-1.350E+02	-81.3	-2.098E-09
7	30	-8.628E-03	-2.334E+01	-3.546E+02	4.013E+01	-1.348E+02	-83.2	9.233E-09
	30	-8.678E-03	-2.488E+01	-3.569E+02	2.931E+01	-1.348E+02	-85.0	1.452E-09
9	30	-8.701E-03	-2.446E+01	-3.594E+02	2.085E+01	-1.353E+02	-86.5	-1.388E-09
10	30	-8.697E-03	-2.092E+01	-3.628E+02	1.561E+01	-1.363E+02	-87.4	-2.587E-09
11	30	-8.663E-03	-1.316E+01	-3.673E+02	1.383E+01	-1.379E+02	-87.8	-3.901E-09
12	30	-8.596E-03	-2.615E-11	-1.865E+02	7.659E+00	-7.005E+01	-87.7	-1.881E-09
0	29	-9.189E-03	2.367E-10	-1.662E+02	3.833E+01	-6.548E+01	-77.6	-4.632E-09
1	29	-9.481E-03	-3.872E+00	-3.318E+02	7.953E+01	-1.313E+02	-77.1	-1.116E-08
2	29	-9.739E-03	-5.707E+00	-3.335E+02	8.092E+01	-1.321E+02	-76.9	8.066E-09
3	29	-9.965E-03	-6.464E+00	-3.365E+02	7.928E+01	-1.330E+02	-77.2	-5.176E-09
4	29	-1.016E-02	-6.882E+00	-3.403E+02	7.376E+01	-1.335E+02	-78.1	-1.065E-08
5	29	-1.032E-02	-7.691E+00	-3.441E+02	6.461E+01	-1.335E+02	-79.5	5.857E-09
6	29	-1.044E-02	-9.455E+00	-3.472E+02	5.305E+01	-1.332E+02	-81.3	-3.145E-09
7	29	-1.054E-02	-1.220E+01	-3.493E+02	4.090E+01	-1.328E+02	-83.2	-4.256E-09
8	29	-1.060E-02	-1.519E+01	-3.506E+02	3.009E+01	-1.325E+02	-84.9	6.953E-09
9	29	-1.063E-02	-1.706E+01	-3.517E+02	2.212E+01	-1.324E+02	-86.2	-6.350E-09
10	29	-1.063E-02	-1.619E+01	-3.535E+02	1.786E+01	-1.329E+02	-87.0	2.452E-09
11	29	-1.061E-02	-1.096E+01	-3.564E+02	1.743E+01	-1.340E+02	-87.1	-6.315E-09
12	29	-1.054E-02	-1.796E-10	-1.805E+02	1.019E+01	-6.789E+01	-86.8	2.251E-09
0	28	-1.099E-02	2.854E-10	-1.592E+02	3.743E+01	-6.284E+01	-77.4	6.487E-10
1	28	-1.131E-02	-3.174E+00	-3.181E+02	7.964E+01	-1.264E+02	-76.6	7.859E-09
2	28	-1.160E-02	-2.982E+00	-3.203E+02	8.237E+01	-1.277E+02	-76.3	-1.660E-08
3	28	-1.185E-02	-6.697E+01	-3.243E+02	8.149E+01	-1.289E+02	-76.6	1.451E-08
4	28	-1.207E-02	2.257E+00	-3.290E+02	7.611E+01	-1.296E+02	-77.7	1.757E-09
	28	-1.225E-02	4.169E+00	-3.334E+02	6.650E+01	-1.298E+02	-79.2	-1.577E-08
6	28	-1.240E-02	3.774E+00	-3.366E+02	5.409E+01	-1.294E+02	-81.2	2.079E-08
7	28	-1.251E-02	7.261E-01	-3.381E+02	4.113E+01	-1.286E+02	-83.2	-6.936E-09
8	28	-1.259E-02	-4.069E+00	-3.383E+02	2.992E+01	-1.278E+02	-84.9	-5.170E-10
9	28	-1.263E-02	-8.720E+00	-3.388E+02	2.223E+01	-1.273E+02	-86.2	7.384E-09
10	28	-1.264E-02	-1.095E+01	-3.381E+02	1.892E+01	-1.272E+02	-86.7	1.254E-09
11	28	-1.262E-02	-8.608E+00	-3.396E+02	1.998E+01	-1.278E+02	-86.6	-7.772E-09
12	28	-1.256E-02	-3.158E-10	-1.715E+02	1.239E+01	-6.465E+01	-85.9	1.308E-09
0	27	-1.285E-02	1.101E-09	-1.483E+02	3.659E+01	-5.881E+01	-76.9	-1.289E-08
1	27	-1.320E-02	-2.062E+00	-2.966E+02	8.021E+01	-1.189E+02	-75.7	2.082E-10
2	27	-1.351E-02	6.440E-01	-2.996E+02	8.464E+01	-1.207E+02	-75.3	-5.697E-10
3	27	-1.379E-02	6.593E+00	-3.046E+02	8.470E+01	-1.223E+02	-75.7	-1.199E-08
4	27	-1.404E-02	1.348E+01	-3.104E+02	7.935E+01	-1.233E+02	-76.9	8.373E-09
5	27	-1.425E-02	1.861E+01	-3.156E+02	6.890E+01	-1.235E+02	-78.8	2.536E-09
6	27	-1.442E-02	1.977E+01	-3.189E+02	5.509E+01	-1.229E+02	-81.0	-3.932E-09
7	27	-1.455E-02	1.619E+01	-3.199E+02	4.073E+01	-1.218E+02	-83.2	6.461E-09
8	27	-1.464E-02	9.047E+00	-3.188E+02	2.870E+01	-1.205E+02	-85.0	9.340E-09
9	27	-1.469E-02	9.591E-01	-3.169E+02	2.107E+01	-1.194E+02	-86.2	-1.943E-08
10	27	-1.470E-02	-4.978E+00	-3.155E+02	1.873E+01	-1.187E+02	-86.6	-2.827E-09
11	27	-1.469E-02	-5.987E+00	-3.156E+02	2.149E+01	-1.189E+02	-86.0	1.292E-08
12	27	-1.464E-02	1.974E-10	-1.590E+02	1.424E+01	-6.008E+01	-84.9	-6.013E-09
0	26	-1.476E-02	-1.811E-09	-1.330E+02	3.585E+01	-5.327E+01	-75.8	1.173E-08
1	26	-1.514E-02	-6.073E+01	-2.664E+02	8.134E+01	-1.085E+02	-74.3	-2.674E-08
2	26	-1.548E-02	5.173E+00	-2.701E+02	8.784E+01	-1.109E+02	-73.7	1.066E-08
	26	-1.580E-02	1.554E+01	-2.762E+02	8.907E+01	-1.130E+02	-74.3	-1.445E-09
4	26	-1.608E-02	2.728E+01	-2.833E+02	8.369E+01	-1.142E+02	-75.8	-1.082E-08
5	26	-1.631E-02	3.639E+01	-2.895E+02	7.195E+01	-1.143E+02	-78.1	9.094E-09
6	26	-1.651E-02	3.941E+01	-2.931E+02	5.605E+01	-1.134E+02	-80.7	-1.556E-09
7	26	-1.665E-02	3.500E+01	-2.934E+02	3.958E+01	-1.118E+02	-83.2	-2.871E-09
8	26	-1.675E-02	2.475E+01	-2.909E+02	2.625E+01	-1.099E+02	-85.3	-6.631E-09

9	26	-1.681E-02	1.234E+01	-2.874E+02	1.851E+01	-1.082E+02	-86.5	-3.615E-09
10	26	-1.683E-02	1.918E+00	-2.843E+02	1.720E+01	-1.070E+02	-86.6	-2.337E-08
11	26	-1.682E-02	-3.019E+00	-2.829E+02	2.190E+01	-1.067E+02	-85.6	1.846E-08
12	26	-1.678E-02	8.904E-10	-1.421E+02	1.572E+01	-5.393E+01	-83.8	-7.868E-09
	25	-1.673E-02	6.405E+10	-1.128E+02	3.526E+01	-4.610E+01	-74.0	-6.989E-09
1	25	-1.713E-02	1.096E+00	-2.264E+02	8.311E+01	-9.508E+01	-71.9	1.200E-08
2	25	-1.751E-02	1.056E+01	-2.309E+02	9.210E+01	-9.824E+01	-71.3	1.533E-08
3	25	-1.785E-02	2.637E+01	-2.381E+02	9.479E+01	-1.007E+02	-72.2	1.500E-08
4	25	-1.816E-02	4.420E+01	-2.466E+02	8.931E+01	-1.019E+02	-74.2	2.879E-09
5	25	-1.843E-02	5.839E+01	-2.538E+02	7.580E+01	-1.017E+02	-77.1	-1.695E-08
6	25	-1.865E-02	6.374E+01	-2.577E+02	5.696E+01	-1.003E+02	-80.2	1.869E-09
7	25	-1.881E-02	5.806E+01	-2.572E+02	3.754E+01	-9.812E+01	-83.3	2.279E-08
8	25	-1.892E-02	4.366E+01	-2.533E+02	2.237E+01	-9.561E+01	-85.7	-2.540E+08
9	25	-1.898E-02	2.577E+01	-2.479E+02	1.430E+01	-9.325E+01	-87.0	2.419E-08
10	25	-1.901E-02	9.896E+00	-2.432E+02	1.425E+01	-9.149E+01	-86.8	-2.470E-09
11	25	-1.900E-02	3.571E-01	-2.404E+02	2.114E+01	-9.085E+01	-85.0	-2.396E-08
12	25	-1.898E-02	-7.890E-11	-1.203E+02	1.678E+01	-4.596E+01	-82.2	4.917E-09
	24	-1.874E-02	-4.377E-11	-8.739E+01	3.482E+01	-3.734E+01	-70.7	-4.732E-10
1	24	-1.916E-02	2.902E+00	-1.758E+02	8.551E+01	-7.880E+01	-68.1	1.383E-08
2	24	-1.957E-02	1.669E+01	-1.808E+02	9.748E+01	-8.279E+01	-67.7	-7.018E-09
3	24	-1.995E-02	3.920E+01	-1.890E+02	1.020E+02	-8.549E+01	-69.1	1.181E-08
4	24	-2.030E-02	6.480E+01	-1.988E+02	9.644E+01	-8.635E+01	-71.9	-1.578E-08
5	24	-2.060E-02	8.564E+01	-2.072E+02	8.060E+01	-8.546E+01	-75.6	2.545E-08
6	24	-2.084E-02	9.398E+01	-2.114E+02	5.779E+01	-8.323E+01	-79.6	-3.125E-08
7	24	-2.101E-02	8.642E+01	-2.100E+02	3.441E+01	-8.022E+01	-83.5	-1.440E-08
8	24	-2.113E-02	6.641E+01	-2.043E+02	1.685E+01	-7.701E+01	-86.5	1.348E-08
9	24	-2.120E-02	4.152E+01	-1.972E+02	8.545E+00	-7.405E+01	-88.0	-8.133E-09
10	24	-2.123E-02	1.907E+01	-1.909E+02	9.793E+00	-7.177E+01	-87.3	1.440E-09
11	24	-2.123E-02	4.185E+00	-1.869E+02	1.916E+01	-7.081E+01	-84.3	-2.040E-08
12	24	-2.121E-02	-1.751E-11	-9.295E+01	1.737E+01	-3.603E+01	-79.8	-3.537E-10
	23	-2.078E-02	-3.333E-10	-5.637E+01	3.450E+01	-2.728E+01	-64.6	8.051E-09
1	23	-2.123E-02	4.602E+00	-1.138E+02	8.846E+01	-6.039E+01	-61.9	-5.163E-08
2	23	-2.167E-02	2.331E+01	-1.189E+02	1.040E+02	-6.515E+01	-62.2	6.231E-09
3	23	-2.209E-02	5.410E+01	-1.278E+02	1.108E+02	-6.757E+01	-64.7	-1.877E-08
4	23	-2.248E-02	8.963E+01	-1.384E+02	1.053E+02	-6.734E+01	-68.6	4.776E-08
5	23	-2.281E-02	1.193E+02	-1.478E+02	8.650E+01	-6.502E+01	-73.5	-4.890E-08
6	23	-2.307E-02	1.317E+02	-1.523E+02	5.852E+01	-6.144E+01	-70.8	2.932E-08
7	23	-2.326E-02	1.213E+02	-1.498E+02	2.997E+01	-5.740E+01	-83.8	-5.501E-09
8	23	-2.339E-02	9.358E+01	-1.424E+02	9.452E+00	-5.354E+01	-87.7	-1.111E-08
9	23	-2.346E-02	5.979E+01	-1.337E+02	9.044E-01	-5.015E+01	-89.7	-2.162E-09
10	23	-2.349E-02	2.947E+01	-1.264E+02	3.835E+00	-4.742E+01	-88.6	-8.676E-09
11	23	-2.350E-02	8.505E+00	-1.214E+02	1.594E+01	-4.626E+01	-83.1	1.823E-08
12	23	-2.349E-02	2.605E-09	-5.966E+01	1.745E+01	-2.415E+01	-74.8	-2.125E-08
	22	-2.284E-02	2.842E-14	-1.960E+01	3.422E+01	-1.702E+01	-53.0	-2.696E-09
1	22	-2.332E-02	5.901E+00	-3.994E+01	9.177E+01	-4.185E+01	-52.0	-3.481E-08
2	22	-2.380E-02	3.004E+01	-4.456E+01	1.114E+02	-4.678E+01	-54.3	-8.072E-09
3	22	-2.426E-02	7.099E+01	-5.322E+01	1.212E+02	5.440E+01	31.4	-2.728E-08
4	22	-2.468E-02	1.192E+02	-6.393E+01	1.158E+02	6.574E+01	25.8	1.308E-08
5	22	-2.505E-02	1.608E+02	-7.371E+01	9.362E+01	7.261E+01	19.3	-2.733E-08
6	22	-2.534E-02	1.787E+02	-7.811E+01	5.907E+01	7.187E+01	12.4	-1.007E-08
7	22	-2.555E-02	1.640E+02	-7.456E+01	2.397E+01	6.239E+01	5.7	-8.068E-09
8	22	-2.568E-02	1.257E+02	-6.577E+01	3.103E-02	4.713E+01	0	-1.606E-08
9	22	-2.575E-02	8.061E+01	-5.620E+01	-8.505E+00	3.043E+01	-3.5	1.835E-08
10	22	-2.578E-02	4.108E+01	-4.844E+01	-3.488E+00	-1.821E+01	87.8	-1.665E-08
11	22	-2.579E-02	1.339E+01	-4.320E+01	1.154E+01	-1.705E+01	-70.9	-5.100E-09
12	22	-2.578E-02	6.142E-11	-2.008E+01	1.697E+01	-1.116E+01	-60.3	7.880E-09
	21	-2.491E-02	1.412E-09	2.299E+01	3.418E+01	1.783E+01	54.3	-2.745E-09

1	21	-2,542E-02	6,423E+00	4,581E+01	9,517E+01	4,624E+01	50,8	-8,455E-09
2	21	-2,593E-02	3,626E+01	4,245E+01	1,195E+02	5,960E+01	45,7	-1,111E-08
3	21	-2,644E-02	8,969E+01	3,539E+01	1,328E+02	7,428E+01	39,2	2,424E-08
4	21	-2,691E-02	1,539E+02	2,648E+01	1,280E+02	8,743E+01	31,8	-3,759E-08
5	21	-2,731E-02	2,118E+02	1,792E+01	1,019E+02	9,580E+01	23,2	1,830E-08
	21	-2,763E-02	2,375E+02	1,429E+01	5,935E+01	9,460E+01	14,0	6,243E-10
7	21	-2,785E-02	2,162E+02	1,854E+01	1,631E+01	8,156E+01	4,7	2,738E-08
8	21	-2,798E-02	1,631E+02	2,754E+01	-1,135E+01	6,150E+01	-4,8	-4,914E-09
9	21	-2,845E-02	1,038E+02	3,657E+01	-1,942E+01	4,089E+01	-15,0	-4,933E-09
10	21	-2,807E-02	5,377E+01	4,358E+01	-1,185E+01	2,309E+01	-33,4	-2,339E-09
11	21	-2,808E-02	1,902E+01	4,827E+01	6,201E+00	1,857E+01	78,5	1,599E-09
12	21	-2,809E-02	-5,088E-10	2,583E+01	1,562E+01	1,244E+01	64,8	7,081E-09
0	20	-2,697E-02	1,831E-10	7,145E+01	3,386E+01	3,186E+01	68,3	3,803E-09
1	20	-2,751E-02	3,956E+00	1,428E+02	1,000E+02	7,318E+01	62,4	-1,033E-08
2	20	-2,806E-02	4,155E+01	1,414E+02	1,326E+02	8,742E+01	55,3	2,827E-08
3	20	-2,861E-02	1,144E+02	1,383E+02	1,522E+02	1,046E+02	47,2	3,256E-09
4	20	-2,913E-02	2,034E+02	1,345E+02	1,485E+02	1,205E+02	38,5	3,454E-08
5	20	-2,958E-02	2,882E+02	1,310E+02	1,153E+02	1,309E+02	27,9	-3,064E-09
6	20	-2,993E-02	3,274E+02	1,302E+02	5,668E+01	1,285E+02	14,9	2,966E-08
7	20	-3,016E-02	2,941E+02	1,335E+02	-2,257E+00	1,103E+02	-0,8	-3,828E-09
8	20	-3,029E-02	2,159E+02	1,392E+02	-3,652E+01	8,645E+01	-21,8	1,719E-08
9	20	-3,035E-02	1,346E+02	1,452E+02	-4,271E+01	6,860E+01	-48,5	-1,054E-09
10	20	-3,037E-02	6,912E+01	1,500E+02	-2,943E+01	5,985E+01	-72,0	3,520E-08
11	20	-3,037E-02	2,496E+01	1,533E+02	-4,787E+00	5,756E+01	-87,9	-2,177E-08
12	20	-3,038E-02	-8,412E-10	7,750E+01	1,287E+01	2,984E+01	80,8	1,209E-08
0	19	-2,879E-02	1,360E-09	1,274E+02	3,178E+01	5,056E+01	76,8	-6,517E-09
1	19	-2,936E-02	-3,834E+00	2,560E+02	1,012E+02	1,090E+02	71,6	2,483E-09
2	19	-2,995E-02	3,899E+01	2,574E+02	1,424E+02	1,229E+02	63,7	1,617E-09
	19	-3,056E-02	1,337E+02	2,588E+02	1,706E+02	1,418E+02	55,1	1,622E-08
	19	-3,114E-02	2,502E+02	2,587E+02	1,717E+02	1,598E+02	45,7	-1,211E-08
5	19	-3,165E-02	3,718E+02	2,576E+02	1,306E+02	1,715E+02	33,2	1,252E-09
6	19	-3,203E-02	4,317E+02	2,582E+02	4,800E+01	1,666E+02	14,5	2,088E-08
7	19	-3,226E-02	3,786E+02	2,627E+02	-3,479E+01	1,456E+02	-15,5	-5,267E-09
8	19	-3,238E-02	2,649E+02	2,691E+02	-7,652E+01	1,288E+02	-45,8	1,260E-08
9	19	-3,241E-02	1,586E+02	2,745E+02	-7,752E+01	1,175E+02	-63,4	-1,539E-08
10	19	-3,241E-02	7,856E+01	2,786E+02	-5,532E+01	1,098E+02	-75,5	7,165E-09
11	19	-3,240E-02	2,729E+01	2,817E+02	-2,186E+01	1,063E+02	-85,1	-7,535E-09
12	19	-3,241E-02	-2,237E-09	1,420E+02	7,247E+00	5,340E+01	87,1	5,173E-09
0	18	-3,018E-02	-1,114E-09	1,849E+02	2,639E+01	7,073E+01	82,0	8,820E-09
1	18	-3,078E-02	-1,517E+01	3,727E+02	9,117E+01	1,474E+02	77,4	-2,122E-08
2	18	-3,142E-02	3,147E+01	3,774E+02	1,359E+02	1,591E+02	70,9	4,350E-08
3	18	-3,208E-02	1,451E+02	3,832E+02	1,715E+02	1,773E+02	62,4	-1,284E-08
4	18	-3,272E-02	2,936E+02	3,878E+02	1,825E+02	1,985E+02	52,2	-2,121E-09
5	18	-3,329E-02	4,711E+02	3,902E+02	1,400E+02	2,162E+02	36,9	1,219E-08
6	18	-3,371E-02	5,667E+02	3,925E+02	3,362E+01	2,149E+02	10,5	-1,924E-08
7	18	-3,394E-02	4,787E+02	3,975E+02	-7,291E+01	1,956E+02	-30,4	4,221E-08
8	18	-3,402E-02	3,104E+02	4,024E+02	-1,160E+02	1,804E+02	-55,8	-2,285E-08
9	18	-3,402E-02	1,744E+02	4,049E+02	-1,068E+02	1,676E+02	-68,6	2,593E-08
10	18	-3,399E-02	7,990E+01	4,063E+02	-7,578E+01	1,586E+02	-77,5	5,533E-09
11	18	-3,396E-02	2,363E+01	4,075E+02	-3,663E+01	1,541E+02	-84,6	-7,460E-09
12	18	-3,397E-02	-1,432E-09	2,045E+02	2,627E-01	7,670E+01	89,9	2,764E-09
0	17	-3,095E-02	3,325E-09	2,373E+02	1,680E+01	8,944E+01	86,0	-2,820E-08
	17	-3,157E-02	-2,850E+01	4,799E+02	6,550E+01	1,831E+02	82,8	3,981E-08
2	17	-3,224E-02	1,973E+01	4,900E+02	1,040E+02	1,924E+02	78,1	-3,787E-08
3	17	-3,296E-02	1,471E+02	5,050E+02	1,364E+02	2,067E+02	71,3	1,523E-08
4	17	-3,367E-02	3,256E+02	5,238E+02	1,492E+02	2,264E+02	61,8	-3,869E-09
5	17	-3,430E-02	5,850E+02	5,460E+02	1,126E+02	2,549E+02	40,1	-4,166E+02
6	17	-3,476E-02	7,420E+02	5,602E+02	1,472E+01	2,787E+02	4,6	-8,332E+02

7	17	-3,497E-02	5,931E+02	5,550E+02	-8,309E+01	2,472E+02	-38,5	-4,166E+02
8	17	-3,500E-02	3,438E+02	5,416E+02	-1,195E+02	2,242E+02	-64,8	1,614E-08
9	17	-3,495E-02	1,796E+02	5,316E+02	-1,072E+02	2,106E+02	-74,3	-1,648E-08
10	17	-3,488E-02	7,378E+01	5,248E+02	-7,653E+01	2,015E+02	-80,6	6,127E-09
11	17	-3,484E-02	1,527E+01	5,214E+02	-4,036E+01	1,967E+02	-85,5	-8,715E-09
12	17	-3,484E-02	-2,138E-09	2,606E+02	-4,213E+00	9,774E+01	-89,1	1,078E-09
0	16	-3,092E-02	-2,037E-10	2,734E+02	2,860E+00	1,025E+02	89,4	1,971E-09
1	16	-3,155E-02	-3,824E+01	5,540E+02	2,257E+01	2,081E+02	87,8	-3,979E-09
2	16	-3,225E-02	1,166E+01	5,682E+02	4,301E+01	2,143E+02	85,6	1,058E-08
3	16	-3,300E-02	1,496E+02	5,894E+02	6,048E+01	2,241E+02	82,3	-3,013E-09
4	16	-3,375E-02	3,522E+02	6,150E+02	6,672E+01	2,366E+02	76,5	-1,638E-09
5	16	-3,442E-02	6,615E+02	6,424E+02	4,536E+01	2,619E+02	39,1	-4,166E+02
6	16	-3,489E-02	8,518E+02	6,589E+02	-8,272E+00	3,195E+02	-2,5	-8,332E+02
7	16	-3,509E-02	6,696E+02	6,531E+02	-6,141E+01	2,712E+02	-41,2	-4,166E+02
8	16	-3,509E-02	3,706E+02	6,362E+02	-8,135E+01	2,472E+02	-74,3	9,454E-09
9	16	-3,500E-02	1,830E+02	6,219E+02	-7,303E+01	2,373E+02	-80,8	1,051E-08
10	16	-3,490E-02	6,773E+01	6,093E+02	-5,323E+01	2,304E+02	-84,4	2,509E-09
11	16	-3,484E-02	7,622E+00	6,026E+02	-3,040E+01	2,266E+02	-87,1	8,791E-09
12	16	-3,483E-02	1,848E-09	3,405E+02	-5,455E+00	1,127E+02	-89,0	-3,997E-09
0	15	-2,998E-02	9,773E-10	2,838E+02	-1,597E+01	1,068E+02	-86,8	-4,550E-09
1	15	-3,060E-02	-4,844E+01	5,772E+02	-3,805E+01	2,173E+02	-86,5	1,393E-08
2	15	-3,130E-02	1,069E+01	5,975E+02	-4,792E+01	2,255E+02	-85,4	1,198E-08
3	15	-3,206E-02	1,521E+02	6,278E+02	-5,377E+01	2,377E+02	-83,6	1,283E-08
4	15	-3,281E-02	3,645E+02	6,646E+02	-5,309E+01	2,526E+02	-80,3	8,876E-09
5	15	-3,349E-02	6,959E+02	7,028E+02	-4,638E+01	2,797E+02	-47,1	-4,166E+02
6	15	-3,396E-02	9,008E+02	7,247E+02	-3,579E+01	3,404E+02	-11,1	-8,332E+02
7	15	-3,415E-02	7,033E+02	7,156E+02	-2,440E+01	2,755E+02	-52,1	-4,166E+02
8	15	-3,412E-02	3,814E+02	6,901E+02	-1,516E+01	2,591E+02	-87,2	2,395E-08
	15	-3,402E-02	1,834E+02	6,659E+02	-9,873E+00	2,498E+02	-88,8	5,159E-09
10	15	-3,390E-02	6,444E+01	6,478E+02	-8,350E+00	2,430E+02	-89,2	8,545E-10
11	15	-3,383E-02	3,743E+00	6,373E+02	-8,634E+00	2,390E+02	-89,2	-1,162E-08
12	15	-3,381E-02	-1,159E-09	3,172E+02	-2,860E+00	1,190E+02	-89,5	7,275E-09
0	14	-2,808E-02	-1,141E-09	2,532E+02	-2,876E+01	9,616E+01	-83,6	1,035E-08
1	14	-2,868E-02	-1,755E+01	5,252E+02	-7,907E+01	2,012E+02	-81,9	-3,105E-08
2	14	-2,935E-02	3,103E+01	5,564E+02	-1,073E+02	2,165E+02	-78,9	-2,231E-08
3	14	-3,007E-02	1,581E+02	6,058E+02	-1,277E+02	2,390E+02	-75,2	-1,272E-08
4	14	-3,078E-02	3,485E+02	6,719E+02	-1,304E+02	2,692E+02	-70,6	5,692E-09
5	14	-3,141E-02	6,480E+02	7,640E+02	-1,051E+02	3,098E+02	-59,4	-4,166E+02
6	14	-3,185E-02	8,341E+02	8,214E+02	-5,247E+01	3,302E+02	-41,6	-8,332E+02
7	14	-3,203E-02	6,541E+02	7,781E+02	-9,957E+01	2,918E+02	89,5	-4,166E+02
8	14	-3,201E-02	3,624E+02	7,008E+02	2,908E+01	2,637E+02	85,1	9,536E-09
9	14	-3,192E-02	1,839E+02	6,511E+02	3,175E+01	2,450E+02	86,1	-2,779E-08
10	14	-3,181E-02	7,555E+01	6,212E+02	2,054E+01	2,333E+02	87,8	2,376E-08
11	14	-3,174E-02	1,772E+01	6,074E+02	4,317E+00	2,278E+02	89,6	-1,583E-10
12	14	-3,173E-02	9,995E-10	3,047E+02	-3,542E+00	1,143E+02	-89,3	-1,111E-08
0	13	-2,608E-02	2,842E-09	2,223E+02	-3,326E+01	8,520E+01	-81,7	-2,521E-08
1	13	-2,666E-02	-9,219E+00	4,640E+02	-9,066E+01	1,803E+02	-79,5	3,085E-08
2	13	-2,730E-02	3,887E+01	4,990E+02	-1,188E+02	1,980E+02	-76,3	-1,515E-08
3	13	-2,797E-02	1,570E+02	5,550E+02	-1,404E+02	2,240E+02	-72,4	1,707E-08
4	13	-2,863E-02	3,312E+02	6,315E+02	-1,450E+02	2,588E+02	-68,0	-2,056E-08
5	13	-2,922E-02	6,057E+02	7,412E+02	-1,177E+02	3,035E+02	-60,0	-4,166E+02
	13	-2,963E-02	7,767E+02	8,097E+02	-5,595E+01	3,193E+02	-53,2	-8,332E+02
	13	-2,980E-02	6,104E+02	7,550E+02	6,583E+00	2,835E+02	87,4	-4,166E+02
8	13	-2,979E-02	3,424E+02	6,618E+02	3,626E+01	2,497E+02	83,6	-4,796E-08
9	13	-2,971E-02	1,741E+02	6,034E+02	3,620E+01	2,274E+02	85,2	1,408E-08
10	13	-2,961E-02	7,646E+01	5,699E+02	2,197E+01	2,141E+02	87,5	-4,876E-08
11	13	-2,955E-02	2,008E+01	5,554E+02	2,269E+00	2,083E+02	89,8	5,963E-09
12	13	-2,953E-02	1,070E-09	2,795E+02	-8,733E+00	1,049E+02	-88,2	-1,948E-08

0	12	-2,400E-02	9,736E-10	1,879E+02	-3,793E+01	7,323E+01	-79,0	-1,084E-08
1	12	-2,456E-02	-2,925E+00	3,925E+02	-1,016E+02	1,564E+02	-76,4	-4,809E-09
2	12	-2,515E-02	4,396E+01	4,244E+02	-1,312E+02	1,745E+02	-72,7	-1,023E-08
3	12	-2,577E-02	1,515E+02	4,747E+02	-1,552E+02	2,014E+02	-68,1	-2,274E-08
	12	-2,638E-02	3,050E+02	5,409E+02	-1,636E+02	2,342E+02	-62,9	2,886E-08
5	12	-2,691E-02	5,360E+02	6,364E+02	-1,351E+02	2,739E+02	-55,2	-4,166E+02
6	12	-2,729E-02	6,772E+02	6,971E+02	-5,949E+01	2,803E+02	-49,7	-8,332E+02
7	12	-2,746E-02	5,395E+02	6,503E+02	1,665E+01	2,448E+02	81,6	-4,166E+02
8	12	-2,746E-02	3,133E+02	5,699E+02	4,700E+01	2,168E+02	79,9	-2,606E-09
9	12	-2,739E-02	1,679E+02	5,212E+02	4,191E+01	1,973E+02	83,3	9,981E-09
10	12	-2,731E-02	7,440E+01	4,929E+02	2,358E+01	1,853E+02	86,8	2,833E-08
11	12	-2,725E-02	2,080E+01	4,609E+02	-2,873E+01	1,803E+02	-90,0	-3,242E-08
12	12	-2,723E-02	7,717E-10	2,426E+02	-1,283E+01	9,123E+01	-87,0	-2,941E+09
0	11	-2,185E-02	-4,914E-10	1,496E+02	-4,132E+01	6,011E+01	-75,5	4,735E-09
1	11	-2,237E-02	2,247E+00	3,116E+02	-1,099E+02	1,300E+02	-72,3	-2,161E-08
2	11	-2,293E-02	4,696E+01	3,355E+02	-1,403E+02	1,472E+02	-67,9	1,792E-08
3	11	-2,349E-02	1,420E+02	3,709E+02	-1,643E+02	1,713E+02	-62,4	1,348E-09
4	11	-2,404E-02	2,727E+02	4,088E+02	-1,719E+02	1,971E+02	-55,8	-4,608E-08
5	11	-2,452E-02	4,304E+02	4,413E+02	-1,414E+02	2,180E+02	-45,3	-1,600E-09
6	11	-2,485E-02	5,292E+02	4,576E+02	-6,278E+01	2,121E+02	-30,2	1,636E-08
7	11	-2,501E-02	4,406E+02	4,535E+02	1,629E+01	1,742E+02	55,8	-3,018E-08
8	11	-2,504E-02	2,785E+02	4,339E+02	4,797E+01	1,678E+02	74,2	3,215E-08
9	11	-2,499E-02	1,538E+02	4,108E+02	4,262E+01	1,566E+02	80,8	-4,995E-08
10	11	-2,492E-02	6,961E+01	3,936E+02	2,291E+01	1,482E+02	86,0	1,290E-08
11	11	-2,486E-02	2,005E+01	3,859E+02	-3,604E+00	1,447E+02	-89,4	-1,083E-08
12	11	-2,484E-02	6,139E-11	1,951E+02	-1,687E+01	7,370E+01	-85,1	-2,329E-09
0	10	-1,965E-02	4,911E-10	1,085E+02	-4,340E+01	4,640E+01	-70,7	-1,075E-08
	10	-2,014E-02	6,292E+00	2,247E+02	-1,145E+02	1,026E+02	-66,8	1,831E-08
	10	-2,064E-02	4,753E+01	2,388E+02	-1,436E+02	1,184E+02	-61,8	-2,086E-08
3	10	-2,115E-02	1,268E+02	2,559E+02	-1,646E+02	1,381E+02	-55,7	-1,247E-08
4	10	-2,164E-02	2,328E+02	2,711E+02	-1,669E+02	1,575E+02	-48,3	-4,729E-09
5	10	-2,206E-02	3,497E+02	2,778E+02	-1,348E+02	1,700E+02	-37,5	1,760E-08
6	10	-2,235E-02	4,076E+02	2,805E+02	-6,556E+01	1,633E+02	-22,9	-3,006E-09
7	10	-2,251E-02	3,507E+02	2,873E+02	4,061E+00	1,316E+02	3,6	7,839E-10
8	10	-2,255E-02	2,359E+02	2,903E+02	3,715E+01	1,159E+02	63,1	-1,521E-08
9	10	-2,251E-02	1,342E+02	2,853E+02	3,677E+01	1,102E+02	77,0	1,441E-08
10	10	-2,246E-02	6,115E+01	2,785E+02	1,928E+01	1,051E+02	85,0	-2,408E-08
11	10	-2,240E-02	1,726E+01	2,746E+02	-7,122E+00	1,031E+02	-88,4	1,628E-08
12	10	-2,237E-02	3,683E-10	1,378E+02	-1,934E+01	5,268E+01	-82,2	-1,444E-08
0	9	-1,740E-02	3,860E-10	6,611E+01	-4,434E+01	3,314E+01	-63,3	5,040E-10
1	9	-1,785E-02	8,856E+00	1,359E+02	-1,157E+02	7,663E+01	-59,4	-8,436E-09
2	9	-1,832E-02	4,523E+01	1,422E+02	-1,420E+02	9,142E+01	-54,4	-1,655E-08
3	9	-1,877E-02	1,095E+02	1,477E+02	-1,589E+02	1,082E+02	-48,4	2,061E-08
4	9	-1,920E-02	1,920E+02	1,496E+02	-1,567E+02	1,233E+02	-41,2	-1,937E-08
5	9	-1,956E-02	2,737E+02	1,460E+02	-1,256E+02	1,315E+02	-31,5	-3,055E-08
6	9	-1,982E-02	3,109E+02	1,445E+02	-6,767E+01	1,256E+02	-19,6	7,062E-09
7	9	-1,996E-02	2,734E+02	1,526E+02	-9,336E+00	1,028E+02	-4,4	-2,116E-08
8	9	-2,001E-02	1,923E+02	1,626E+02	2,293E+01	7,680E+01	28,5	-3,788E-09
9	9	-1,999E-02	1,124E+02	1,669E+02	2,725E+01	6,681E+01	67,5	2,543E-09
10	9	-1,994E-02	5,165E+01	1,670E+02	1,363E+01	6,320E+01	83,3	-1,122E-08
11	9	-1,989E-02	1,440E+01	1,662E+02	-1,048E+01	6,258E+01	-86,1	-3,328E-08
12	9	-1,985E-02	-2,053E-09	8,337E+01	-2,020E+01	3,300E+01	-77,1	1,239E-08
0	8	-1,513E-02	-2,544E-10	2,393E+01	-4,444E+01	2,175E+01	-52,5	-7,408E-09
1	8	-1,555E-02	9,889E+00	4,873E+01	-1,144E+02	5,450E+01	-49,8	3,058E-09
2	8	-1,596E-02	4,050E+01	4,976E+01	-1,375E+02	6,851E+01	-46,0	2,025E-08
3	8	-1,637E-02	9,091E+01	4,849E+01	-1,504E+02	8,310E+01	-41,0	-9,497E-09
4	8	-1,674E-02	1,527E+02	4,372E+01	-1,454E+02	9,505E+01	-34,7	-2,755E-09

5	8	-1,705E-02	2,092E+02	3,646E+01	-1,169E+02	1,006E+02	-26,8	2,044E-08
6	8	-1,727E-02	2,329E+02	3,351E+01	-6,910E+01	9,544E+01	-17,4	-3,799E-08
7	8	-1,741E-02	2,074E+02	4,008E+01	-2,076E+01	7,872E+01	-7,0	3,432E-08
8	8	-1,745E-02	1,500E+02	5,072E+01	9,280E+00	5,658E+01	5,3	4,928E-09
9	8	-1,744E-02	8,911E+01	5,832E+01	1,687E+01	3,621E+01	23,8	-2,799E-09
1	8	-1,740E-02	4,074E+01	6,173E+01	7,274E+00	2,400E+01	72,6	-6,234E-09
11	8	-1,735E-02	1,082E+01	6,259E+01	-1,369E+01	2,475E+01	-76,1	-2,806E-09
12	8	-1,730E-02	6,140E-10	3,146E+01	-2,078E+01	1,567E+01	-63,6	-5,645E-09
0	7	-1,285E-02	-1,751E-11	-1,697E+01	-4,404E+01	-2,000E+01	50,5	7,916E-09
1	7	-1,323E-02	9,614E+00	-3,479E+01	-1,118E+02	-4,746E+01	50,6	-2,254E-08
2	7	-1,360E-02	3,402E+01	-3,676E+01	-1,318E+02	-5,168E+01	52,5	1,332E-08
3	7	-1,396E-02	7,179E+01	-4,144E+01	-1,415E+02	6,284E+01	-34,1	-6,741E-09
4	7	-1,428E-02	1,161E+02	-4,898E+01	-1,350E+02	7,192E+01	-29,3	1,707E-08
5	7	-1,454E-02	1,542E+02	-5,720E+01	-1,096E+02	7,529E+01	-23,0	-1,291E-08
6	7	-1,473E-02	1,688E+02	-6,077E+01	-6,987E+01	7,066E+01	-15,7	1,983E-08
7	7	-1,485E-02	1,507E+02	-5,636E+01	-2,953E+01	5,808E+01	-8,0	-1,842E-08
8	7	-1,489E-02	1,101E+02	-4,761E+01	-2,118E+00	4,130E+01	-8	5,991E-09
9	7	-1,489E-02	6,507E+01	-4,012E+01	7,512E+00	2,460E+01	4,1	9,472E-09
10	7	-1,485E-02	2,847E+01	-3,617E+01	1,490E+00	-1,357E+01	-88,7	2,704E-09
11	7	-1,480E-02	6,306E+00	-3,529E+01	-1,620E+01	-1,532E+01	71,0	-1,351E-08
12	7	-1,474E-02	-1,228E-10	-1,792E+01	-2,096E+01	-1,191E+01	56,6	-7,531E-09
0	6	-1,058E-02	8,071E-10	-5,597E+01	-4,341E+01	-2,986E+01	61,4	-1,382E-08
1	6	-1,093E-02	8,395E+00	-1,135E+02	-1,087E+02	-6,646E+01	59,6	9,600E-09
2	6	-1,125E-02	2,649E+01	-1,168E+02	-1,261E+02	-7,131E+01	59,8	-1,273E-08
3	6	-1,156E-02	5,285E+01	-1,227E+02	-1,334E+02	-7,297E+01	61,7	3,211E-08
4	6	-1,183E-02	8,260E+01	-1,310E+02	-1,262E+02	-7,106E+01	65,1	-1,389E-08
5	6	-1,205E-02	1,069E+02	-1,391E+02	-1,035E+02	-6,634E+01	70,0	-6,317E-09
6	6	-1,221E-02	1,149E+02	-1,432E+02	-7,004E+01	-6,037E+01	75,8	-1,841E-09
7	6	-1,231E-02	1,015E+02	-1,410E+02	-3,575E+01	-5,480E+01	81,8	-4,944E-10
8	6	-1,235E-02	7,287E+01	-1,349E+02	-1,071E+01	-5,000E+01	87,1	4,848E-09
9	6	-1,234E-02	4,083E+01	-1,294E+02	2,549E-01	-4,851E+01	-89,9	5,450E-09
10	6	-1,231E-02	1,504E+01	-1,268E+02	-2,695E+00	-4,757E+01	88,9	-1,625E-08
11	6	-1,225E-02	8,144E-01	-1,275E+02	-1,729E+01	-4,867E+01	82,5	-1,146E-09
12	6	-1,218E-02	-2,718E-10	-6,494E+01	-2,050E+01	-2,657E+01	73,9	2,349E-09
0	5	-8,329E-03	-9,641E-11	-9,291E+01	-4,260E+01	-4,111E+01	68,7	4,300E-09
1	5	-8,639E-03	6,646E+00	-1,871E+02	-1,060E+02	-8,768E+01	66,2	-6,097E-09
2	5	-8,927E-03	1,846E+01	-1,903E+02	-1,213E+02	-9,220E+01	65,4	-4,914E-09
3	5	-9,186E-03	3,441E+01	-1,963E+02	-1,266E+02	-9,458E+01	66,2	-5,334E-10
4	5	-9,411E-03	5,187E+01	-2,045E+02	-1,190E+02	-9,421E+01	68,6	-3,593E-09
5	5	-9,591E-03	6,533E+01	-2,125E+02	-9,860E+01	-9,146E+01	72,3	5,405E-09
6	5	-9,722E-03	6,826E+01	-2,170E+02	-6,964E+01	-8,743E+01	77,0	2,042E-10
7	5	-9,802E-03	5,783E+01	-2,168E+02	-3,972E+01	-8,342E+01	81,9	-2,561E-10
8	5	-9,833E-03	3,797E+01	-2,136E+02	-1,648E+01	-8,050E+01	86,3	-6,070E-09
9	5	-9,827E-03	1,652E+01	-2,107E+02	-4,366E+00	-7,904E+01	88,9	4,145E-09
10	5	-9,791E-03	5,379E-01	-2,109E+02	-4,479E+00	-7,911E+01	88,8	8,628E-10
11	5	-9,733E-03	-5,673E+00	-2,147E+02	-1,612E+01	-8,099E+01	85,6	-1,247E-08
12	5	-9,654E-03	1,137E-13	-1,102E+02	-1,910E+01	-4,253E+01	80,4	-2,216E-10
0	4	-6,112E-03	-2,763E-10	-1,202E+02	-4,249E+01	-5,288E+01	73,2	8,356E-10
1	4	-6,389E-03	4,768E+00	-2,555E+02	-1,043E+02	-1,096E+02	70,6	-4,872E-09
2	4	-6,636E-03	1,026E+01	-2,575E+02	-1,177E+02	-1,132E+02	69,3	1,176E-08
3	4	-6,852E-03	1,652E+01	-2,633E+02	-1,213E+02	-1,157E+02	69,5	-1,680E-08
4	4	-7,033E-03	2,334E+01	-2,715E+02	-1,132E+02	-1,162E+02	71,2	5,138E-09
5	4	-7,176E-03	2,798E+01	-2,796E+02	-9,448E+01	-1,149E+02	74,2	-4,221E-09
6	4	-7,277E-03	2,674E+01	-2,849E+02	-6,872E+01	-1,123E+02	78,1	6,180E-09
7	4	-7,337E-03	1,812E+01	-2,865E+02	-4,183E+01	-1,095E+02	82,3	-9,269E-09
8	4	-7,359E-03	4,731E+00	-2,857E+02	-1,969E+01	-1,076E+02	86,1	3,299E-09
9	4	-7,349E-03	-8,104E+00	-2,855E+02	-6,198E+00	-1,071E+02	88,7	-4,253E-09
10	4	-7,312E-03	-1,522E+01	-2,890E+02	-3,178E+00	-1,084E+02	89,3	5,507E-09

11	4	-7.252E-03	-1.379E+01	-2.980E+02	-1.153E+01	-1.119E+02	87.7	-4.716E-09
12	4	-7.165E-03	-4.798E+11	-1.551E+02	-1.628E+01	-5.880E+01	84.1	-4.316E-10
0	3	-3.943E-03	-3.245E-10	-1.636E+02	-4.311E+01	-6.536E+01	76.1	4.586E-09
	3	-4.186E-03	2.951E+00	-3.182E+02	-1.050E+02	-1.311E+02	73.4	-8.800E-09
	3	-4.394E-03	1.885E+00	-3.181E+02	-1.155E+02	-1.333E+02	72.1	6.722E-10
3	3	-4.567E-03	-1.094E+00	-3.245E+02	-1.171E+02	-1.359E+02	72.1	-1.532E-09
4	3	-4.707E-03	-3.719E+00	-3.338E+02	-1.004E+02	-1.373E+02	73.3	1.969E-10
5	3	-4.813E-03	-6.515E+00	-3.428E+02	-9.078E+01	-1.371E+02	75.8	-8.809E-10
6	3	-4.886E-03	-1.136E+01	-3.492E+02	-6.729E+01	-1.358E+02	79.1	3.177E-09
7	3	-4.927E-03	-1.901E+01	-3.521E+02	-4.250E+01	-1.341E+02	82.8	-1.389E-09
8	3	-4.938E-03	-2.767E+01	-3.530E+02	-2.085E+01	-1.329E+02	86.3	-1.791E-09
9	3	-4.924E-03	-3.364E+01	-3.547E+02	-5.497E+00	-1.330E+02	89.0	-6.970E-10
10	3	-4.887E-03	-3.296E+01	-3.612E+02	1.765E+00	-1.355E+02	-89.7	1.831E-10
11	3	-4.826E-03	-2.269E+01	-3.777E+02	-1.116E+00	-1.416E+02	89.8	-2.586E-09
12	3	-4.734E-03	2.019E-10	-2.030E+02	-1.086E+01	-7.634E+01	86.9	-3.959E-10
0	2	-1.835E-03	-1.091E-11	-2.051E+02	-6.069E+01	-8.313E+01	74.7	-1.382E-10
1	2	-2.043E-03	9.256E-02	-3.710E+02	-1.116E+02	-1.507E+02	74.5	-2.014E-09
2	2	-2.211E-03	-7.219E+00	-3.711E+02	-1.141E+02	-1.515E+02	74.0	6.930E-10
3	2	-2.344E-03	-1.884E+01	-3.811E+02	-1.129E+02	-1.550E+02	74.0	2.128E-10
4	2	-2.444E-03	-2.996E+01	-3.934E+02	-1.038E+02	-1.579E+02	75.1	3.010E-09
5	2	-2.515E-03	-3.923E+01	-4.044E+02	-8.708E+01	-1.590E+02	77.3	-4.031E-09
6	2	-2.560E-03	-4.733E+01	-4.121E+02	-6.541E+01	-1.588E+02	80.1	1.375E-09
7	2	-2.582E-03	-5.465E+01	-4.161E+02	-4.222E+01	-1.579E+02	83.4	4.129E-10
8	2	-2.583E-03	-6.003E+01	-4.175E+02	-2.088E+01	-1.570E+02	86.7	-1.724E-09
9	2	-2.565E-03	-6.092E+01	-4.192E+02	-3.250E+00	-1.572E+02	89.5	1.326E-09
10	2	-2.528E-03	-5.431E+01	-4.261E+02	1.005E+01	-1.599E+02	-84.5	-8.549E-11
11	2	-2.470E-03	-3.673E+01	-4.494E+02	2.124E+01	-1.690E+02	-87.1	-1.874E-09
12	2	-2.380E-03	-2.497E-10	-2.635E+02	1.880E+01	-9.933E+01	-85.9	1.721E-09
1	1	1.953E-04	-7.549E-11	-9.028E+01	-7.342E+01	-4.925E+01	60.8	5.600E-10
1	1	3.021E-05	3.949E+01	-1.884E+02	-1.141E+02	-8.841E+01	67.5	-1.111E-09
2	1	-9.838E-05	3.738E+01	-1.932E+02	-1.124E+02	-8.959E+01	67.9	9.193E-10
3	1	-1.908E-04	2.168E+01	-2.005E+02	-1.097E+02	-9.209E+01	67.7	-2.228E-10
4	1	-2.530E-04	5.277E+00	-2.086E+02	-1.003E+02	-9.312E+01	68.4	-3.709E-09
5	1	-2.909E-04	-8.044E+00	-2.156E+02	-8.430E+01	-9.209E+01	70.4	3.585E-09
6	1	-3.005E-04	-1.805E+01	-2.203E+02	-6.398E+01	-8.958E+01	73.8	2.703E-10
7	1	-3.124E-04	-2.501E+01	-2.227E+02	-4.187E+01	-8.669E+01	78.5	7.910E-10
8	1	-3.024E-04	-2.828E+01	-2.233E+02	-2.047E+01	-8.454E+01	84.1	-1.424E-09
9	1	-2.808E-04	-2.642E+01	-2.240E+02	-1.012E+00	-8.400E+01	-89.7	-1.155E-09
10	1	-2.467E-04	-1.843E+01	-2.277E+02	1.758E+01	-8.594E+01	-85.2	1.817E-09
11	1	-1.964E-04	-6.512E+00	-2.392E+02	4.167E+01	-9.242E+01	-80.1	-1.377E-09
12	1	-1.236E-04	-2.160E-11	-1.308E+02	4.795E+01	-5.495E+01	-71.9	1.244E-10
0	0	2.192E-03	2.138E-11	-1.316E-11	-3.389E+01	1.271E+01	-45.0	-3.547E-10
1	0	2.066E-03	4.317E+01	3.075E-11	-5.416E+01	2.996E+01	-34.1	9.259E-10
2	0	1.977E-03	4.310E+01	-4.320E-12	-5.600E+01	3.058E+01	-34.5	2.510E-10
3	0	1.924E-03	3.346E+01	-1.313E-11	-5.502E+01	2.784E+01	-36.5	2.892E-10
4	0	1.899E-03	2.332E+01	1.756E-11	-5.026E+01	2.372E+01	-38.5	8.004E-11
5	0	1.893E-03	1.523E+01	8.333E-11	-4.226E+01	1.896E+01	-39.9	2.892E-10
6	0	1.901E-03	9.554E+00	8.782E-12	-3.210E+01	1.396E+01	-40.8	2.256E-10
7	0	1.916E-03	6.141E+00	1.009E-10	-2.106E+01	9.131E+00	-40.9	2.674E-10
8	0	1.937E-03	5.074E+00	4.391E-12	-1.016E+01	4.877E+00	-38.0	7.731E-10
9	0	1.962E-03	6.617E+00	-1.316E-11	1.294E-01	2.482E+00	1.1	8.276E-10
10	0	1.993E-03	1.044E+01	-8.768E-12	1.036E+01	6.308E+00	31.6	5.821E-11
11	0	2.033E-03	1.334E+01	1.755E-11	2.306E+01	1.150E+01	36.9	4.202E-10
12	0	2.083E-03	-2.632E-11	-6.579E-12	2.529E+01	-9.484E+00	-45.0	2.383E-10

STATICS CHECK.

SUMMATION OF REACTIONS = 4.999E+03

MAXIMUM STATICS CHECK ERROR AT STA 6 12 = -8.332E+02

PROGRAM SLAB 49 -DEVELOPMENT DECK- MATLOCK,PANAK, FNDRES REV DATE 13 JUL 71 I-

```

. . . . .
. THIS PROGRAM IS BEING USED AT YOUR OWN RISK.
. CHANGES MAY OCCUR AFTER THE ABOVE REVISION DATE.
. PLEASE REPORT DIFFICULTIES TO THE ABOVE PEOPLE
. AT THE CENTER FOR HIGHWAY RESEARCH, UT AT AUSTIN.
.
. . . . .

```

SLAB 177-2, LOW VOID, THICK SLAB
VOID SIZE = 27 * 16 SQ.IN., THICKNESS = 4 IN.

PROR (CONTO)

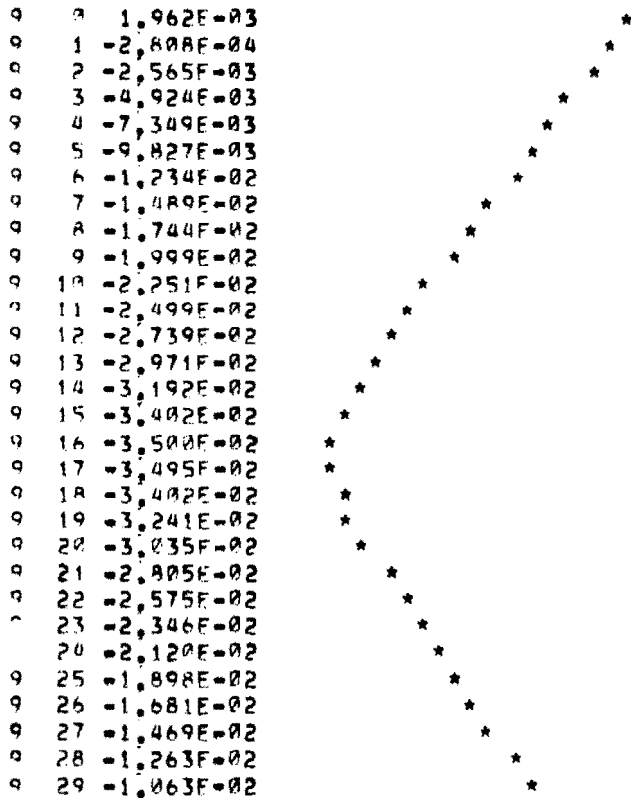
1 FIRST CRACK, 89.5 PERCENT RED, FOR 6 STATIONS.

PROFILE OUTPUT AREAS

X MOMENTS ACT IN X DIRECTION (ABOUT Y AXIS)
THE PLOTTED RESULTS INDICATE THE RELATIVE VALUE EACH HAS WITHIN THAT LIST

DEFLECTIONS BETWEEN (9 , 0) AND (9 , 36)

, Y DEFLECTION



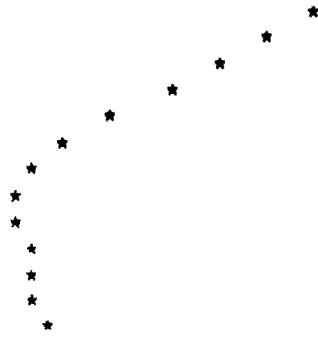
9 30 =8,701E-03
 9 31 =6,837E-03
 9 32 =5,038E-03
 9 33 =3,306E-03
 9 34 =1,638E-03
 9 35 =-3,317E-05
 9 36 =1,540E-03



DEFLECTIONS BETWEEN (0 , 15) AND (12 , 15)

X , Y DEFLECTION

0 15 =2,998E-02
 1 15 =-3,060E-02
 2 15 =-3,130E-02
 3 15 =-3,206E-02
 4 15 =-3,281E-02
 5 15 =-3,349E-02
 6 15 =-3,396E-02
 7 15 =-3,415E-02
 8 15 =-3,412E-02
 9 15 =-3,402E-02
 10 15 =-3,390E-02
 11 15 =-3,383E-02
 12 15 =-3,381E-02



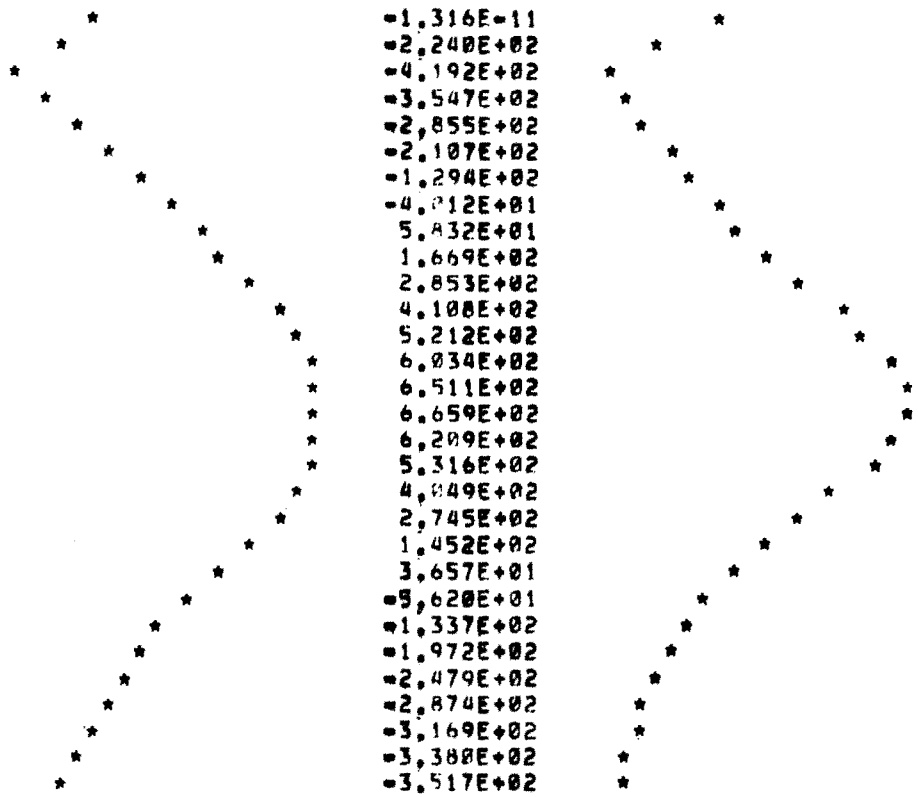
SLAB X AND SLAB Y MOMENT BETWEEN (9 , 0) AND (9 , 36)

X , Y SLAB X MOM

9 0 6,617E+00
 9 1 -2,642E+01
 9 2 =6,092E+01
 9 3 =-3,364E+01
 9 4 =-8,184E+00
 9 5 1,652E+01
 9 6 4,083E+01
 9 7 6,507E+01
 9 8 8,911E+01
 9 9 1,124E+02
 9 10 1,342E+02
 9 11 1,538E+02
 9 12 1,679E+02
 9 13 1,781E+02
 9 14 1,839E+02
 9 15 1,834E+02
 9 16 1,830E+02
 9 17 1,796E+02
 9 18 1,744E+02
 9 19 1,586E+02
 9 20 1,346E+02
 9 21 1,038E+02
 9 22 8,061E+01
 9 23 5,979E+01
 9 24 4,152E+01
 9 25 2,577E+01
 9 26 1,234E+01
 9 27 9,591E+00
 9 28 =8,720E+00
 9 29 =-1,706E+01

SLAB Y MOM

=-1,316E-11
 =2,240E+02
 =4,192E+02
 =3,547E+02
 =2,855E+02
 =2,107E+02
 =1,294E+02
 =4,012E+01
 5,832E+01
 1,669E+02
 2,853E+02
 4,108E+02
 5,212E+02
 6,034E+02
 6,511E+02
 6,659E+02
 6,209E+02
 5,316E+02
 4,049E+02
 2,745E+02
 1,452E+02
 3,657E+01
 =5,620E+01
 =1,337E+02
 =1,972E+02
 =2,479E+02
 =2,874E+02
 =3,169E+02
 =3,380E+02
 =3,517E+02



9	30	-2.406E+01	*		-3.594E+02	*
9	31	-3.132E+01	*		-3.621E+02	*
9	32	-3.812E+01	*		-3.604E+02	*
9	33	-4.539E+01	*		-3.562E+02	*
9	34	-5.372E+01	*		-3.489E+02	*
	35	-2.252E+01	*		-1.761E+02	*
9	36	4.190E+00	*		1.755E+11	*

SLAB X AND SLAB Y MOMENT BETWEEN (0 , 15) AND (12 , 15)

X , Y	SLAB X MOM		SLAB Y MOM	
0 15	9.773E+10	*	2.838E+02	*
1 15	-4.044E+01	*	5.772E+02	*
2 15	1.069E+01	*	5.975E+02	*
3 15	1.521E+02	*	6.278E+02	*
4 15	3.645E+02	*	6.646E+02	*
5 15	6.959E+02	*	7.028E+02	*
6 15	9.000E+02	*	7.247E+02	*
7 15	7.033E+02	*	7.156E+02	*
8 15	3.814E+02	*	6.901E+02	*
9 15	1.834E+02	*	6.659E+02	*
10 15	6.444E+01	*	6.478E+02	*
11 15	3.743E+00	*	6.373E+02	*
12 15	-1.159E+09	*	3.172E+02	*

PRINCIPAL STRESS BETWEEN (9 , 0) AND (9 , 36)

X , Y	PRIN STRESS	
9 0	2.482E+00	*
9 1	-8.400E+01	*
9 2	-1.572E+02	*
9 3	-1.330E+02	*
9 4	-1.071E+02	*
9 5	-7.904E+01	*
9 6	-4.851E+01	*
9 7	2.460E+01	*
9 8	3.621E+01	*
9 9	6.681E+01	*
9 10	1.102E+02	*
9 11	1.566E+02	*
9 12	1.973E+02	*
9 13	2.274E+02	*
9 14	2.450E+02	*
9 15	2.498E+02	*
9 16	2.373E+02	*
9 17	2.106E+02	*
9 18	1.676E+02	*
9 19	1.175E+02	*
9 20	6.860E+01	*
9 21	4.089E+01	*
9 22	3.043E+01	*
9 23	-5.015E+01	*
9 24	-7.405E+01	*
9 25	-9.325E+01	*
9 26	-1.082E+02	*
9 27	-1.194E+02	*
9 28	-1.273E+02	*
9 29	-1.324E+02	*

9	30	=1,353E+02	*
9	31	=1,362E+02	*
9	32	=1,356E+02	*
9	33	=1,337E+02	*
9	34	=1,309E+02	*
	35	=6,607E+01	*
9	36	1,620E+00	*

PRINCIPAL STRESS BETWEEN (0 , 15) AND (12 , 15)

X , Y PRIN STRESS

0	15	1,068E+02	*
1	15	2,173E+02	*
2	15	2,255E+02	*
3	15	2,377E+02	*
4	15	2,526E+02	*
5	15	2,797E+02	*
6	15	3,404E+02	*
7	15	2,755E+02	*
8	15	2,591E+02	*
9	15	2,498E+02	*
10	15	2,430E+02	*
11	15	2,390E+02	*
12	15	1,197E+02	*

TIME FOR THIS PROBLEM = 0 MINUTES 21.230 SECONDS

ELAPSED TIME = 0 MINUTES 33.312 SECONDS

PROGRAM SLAB 49 -DEVELOPMENT DECK- MATLOCK,PANAK, ENDRES REV DATE 13 JUL 71 I-

```

. . . . .
. THIS PROGRAM IS BEING USED AT YOUR OWN RISK. .
. CHANGES MAY OCCUR AFTER THE ABOVE REVISION DATE. .
. PLEASE REPORT DIFFICULTIES TO THE ABOVE PEOPLE .
. AT THE CENTER FOR HIGHWAY RESEARCH, UT AT AUSTIN. .
. . . . .

```

SLAB 177-2, LOW VOID, THICK SLAB
VOID SIZE = 27 * 16 SQ.IN., THICKNESS = 4 IN.

ELAPSED TIME = 0 MINUTES 33.328 SECONDS

KEEP RUN TIME RECORDS FOR FUTURE ESTIMATES OF PARENT AND OFFSPRING RUN TIMES

THE AUTHORS

Enrique Jimenez received his Bachelor Degree in Civil Engineering at the Universidad Nacional Autonoma de Mexico, in 1965. During the following years he was employed by the Public Works Federal Agency and the Federal Pay Tool Roads and Bridges as a Civil Engineer at various levels of responsibility. Resident and Superintendent were his initial levels on the construction of roads and bridges (1965 - 1967), General Supervisor in the Construction of Airports (1967 - 1973) as well as Consultant in the Bituminous Materials, area for the Industrial Department in Federal Pay Tool Roads and Bridges. In January 1974, he entered the Graduate School of The Univeristy of Texas at Austin and was employed by the Center for Highway Research as a Research Engineer Assistant. In December 1975, he recieved his Master's Degree in Civil Engineering from The University of Texas at Austin.

B. Frank McCullough is a Professor of Civil Engineering at The University of Texas at Austin. He has strong interests in pavements and pavement design and has developed design methods for continuously reinforced concrete pavements currently used by the State Department of Highways and Public Transportation, U. S. Steel Corporation, and others. He has also developed overlay design methods now being used by the FAA, U. S. Air Force, and the FHWA. During the nine years with the State Department of Highways and Public Transportation, he was active in a variety of research and design activities. He has authored over 100 publications which have appeared in national journals.



W. Ronald Hudson is a Professor of Civil Engineering at The University of Texas at Austin. He has had a wide variety of experience as a research engineer with the State Department of Highways and Public Transportation and the Center for Highway Research at The University of Texas at Austin and was Assistant Chief of the Rigid Pavement Research Branch of the AASHO Road Test. He is the author of



numerous publications and was the recipient of the 1967 ASCE J. James R. Croes Medal. He is presently concerned with research in the areas of (1) analysis and design of pavement management systems, (2) measurement of pavement roughness performance, (3) slab analysis and design, and (4) tensile strength of stabilized subbase materials.